**ALGERIAN DEMOCRATIC AND POPULAR REPUBLIC**
**MINISTRY OF HIGHER EDUCATION AND SCIENTIFIC RESEARCH**

**UNIVERSITY BLIDA 1**
**Faculty of Technology**
**Department of mechanics**

## THESIS OF DOCTORATE (LMD)

In mechanical engineering

Speciality: Energetics

# ENERGY VALORISATION OF SOLID AGRI-FOOD IN ALGERIA

By

**HAMAIDI Badr Eddine**

In front of the jury composed of:

| | | | |
|---|---|---|---|
| Y. BENKHEDDA | Prof | University BLIDA1 | President |
| D. SEMMAR | Prof | University BLIDA1 | Examinator |
| M. ALLICHE | Prof | Université YF MEDEA | Examinator |
| B. BOUMEDDANE | Prof | University BLIDA1 | Supervisor |
| A. BENAROUS | Prof | University BLIDA1 | Co-Supervisor |

Blida, Juin 2025

# ملخص

تستكشف هذه الدراسة إمكانية استخدام نفايات النخيل، التي تُعدّ من الموارد الحيوية الوفيرة في الجزائر، كمادة أولية مستدامة لعمليات التغويز وإنتاج الميثانول. تبدأ الدراسة بتحديد أهم موارد الكتلة الحيوية في الجزائر، مع التركيز على أهمية المخلفات الزراعية في تطبيقات الطاقة المتجددة. ومن بين هذه الموارد، تم اختيار نفايات النخيل من منطقة بسكرة كعينة تمثيلية نظرًا لتوافرها الكبير وإمكانياتها العالية في التثمين.

تعتمد المنهجية المتبعة على الجمع بين البيانات التجريبية المستخلصة من الأدبيات العلمية والنمذجة المتقدمة للعمليات باستخدام برنامج .Aspen Plus يتيح هذا الإطار الشامل للنمذجة تحليل المعايير التشغيلية الرئيسية، مثل نسبة البخار إلى الكتلة الحيوية ودرجة حرارة التغويز، من أجل تحسين عمليات التغويز وتخليق الميثانول. وقد تم التأكد من دقة النموذج من خلال التحقق الصارم عبر مقارنة نتائجه بالبيانات التجريبية المنشورة في الدراسات السابقة.

تشير النتائج لهذه الدراسة إلى أن الظروف المثلى لتغويز نفايات نخيل التمر بالبخار تتحقق عند نسبة بخار إلى كتلة حيوية تبلغ 0.9 ودرجة حرارة تغويز قدرها 800 درجة مئوية. تحت هذه الظروف، يتكون غاز الإصطناع الناتج من 58.38٪ هيدروجين ($H_2$) و24.21٪ أول أكسيد الكربون(CO) .
كما تكشف الدراسة أن الظروف المثلى لتصنيع الميثانول تتطلب العمل عند ضغط قدره 50 بار ودرجة حرارة تبلغ 220 درجة مئوية، مما يؤدي إلى قدرة إنتاج ميثانول تبلغ 368.98 كغ/ساعة.

تُبرز هذه الدراسة الإمكانات الكبيرة لاستخدام موارد الكتلة الحيوية في الجزائر لإنتاج الطاقة المستدامة، بما يتماشى مع أهداف مشروع ."REFFECT AFRICA" ومن خلال دمج تحسين العمليات بالنمذجة مع التطبيقات العملية، تُسهم النتائج في تطوير تقنيات الطاقة المتجددة وتعزيز التنمية المستدامة في المنطقة.

**الكلمات المفتاحية:**

نفايات نخيل، تغويز بالبخار، غاز الاصطناع، الميثانول، محاكاة باستخدام Aspen Plus

# Abstract

This research explores the potential of utilizing date palm waste, an abundant biomass resource in Algeria, as a sustainable feedstock for gasification and methanol production. The study begins by identifying the most prominent biomass resources in Algeria, emphasizing the importance of agricultural residues for renewable energy applications. Among these, date palm waste from the Biskra region was selected as a representative sample due to its significant availability and high potential for valorisation.

The methodological approach combines experimental data from the literature with advanced process simulation using Aspen Plus software. This comprehensive modelling framework facilitates the analysis of key operating parameters, such as the steam-to-biomass ratio and gasification temperature, to optimize the gasification process and subsequent methanol synthesis. The model's reliability is confirmed through rigorous validation against experimental results reported in prior studies.

Key findings from this study indicate that the optimal conditions for steam gasification of date palm waste are achieved at a steam to biomass ratio of 0.9 and a gasification temperature of 800 °C. Under these conditions, the resulting syngas composition comprises 58.38% hydrogen (H2) and 24.21% carbon monoxide (CO). Additionally, the study reveals that the ideal conditions for methanol synthesis involve operating at a pressure of 50 bar and a temperature of 220 ◦C, resulting in a methanol Production capacity of 368.98 kg/h.

This study underscores the potential of leveraging Algeria's biomass resources for sustainable energy production, aligning with the goals of the “REFFECT AFRICA” project. By integrating simulation-based optimization with practical applications, the findings contribute to advancing renewable energy technologies and promoting sustainable development in the region.



**Key Word:**

Date palm waste, Steam gasification, Syngas, Methanol, Aspen Plus simulation



# Résumé

Cette recherche explore le potentiel d'utilisation des déchets de palmier dattier, une biomasse abondante en Algérie, comme matière première durable pour la gazéification et la production

de méthanol. L'étude débute par l'identification des principales ressources de biomasse en Algérie, en mettant en évidence l'importance des résidus agricoles dans les applications d'énergie renouvelable. Parmi ces ressources, les déchets de palmier dattier de la région de Biskra ont été sélectionnés comme échantillon représentatif en raison de leur disponibilité significative et de leur fort potentiel de valorisation.

L'approche méthodologique combine des données expérimentales issues de la littérature avec une simulation avancée des processus à l'aide du logiciel Aspen Plus. Ce cadre de modélisation complet permet d'analyser les paramètres opérationnels clés, tels que le rapport vapeur/biomasse et la température de gazéification, afin d'optimiser le processus de gazéification et la synthèse de méthanol. La fiabilité du modèle est confirmée par une validation rigoureuse basée sur les résultats expérimentaux rapportés dans des études antérieures.

Les résultats de cette étude indiquent que les conditions optimales pour la gazéification à la vapeur des déchets de palmier dattier sont obtenues avec un rapport vapeur/biomasse de 0,9 et une température de gazéification de 800 °C. Dans ces conditions, la composition du gaz de synthèse obtenu comprend 58,38 % d'hydrogène ($H_2$) et 24,21 % de monoxyde de carbone (CO). Par ailleurs, l'étude révèle que les conditions idéales pour la synthèse du méthanol correspondent à une pression de fonctionnement de 50 bar et une température de 220 °C, aboutissant à une capacité de production de méthanol de 368,98 kg/h.

Cette étude met en lumière le potentiel de valorisation des ressources de biomasse en Algérie pour la production d'énergie durable, en cohérence avec les objectifs du projet « REFFECT AFRICA ». En intégrant l'optimisation par simulation et des applications pratiques, les résultats contribuent à l'avancement des technologies d'énergie renouvelable et à la promotion du développement durable dans la région.

**Mots clés :**

Déchets de palmier, Gazéification à la vapeur, Gaz de synthèse, Méthanol Aspen Plus simulation.

# Acknowledgment

I would like to express my deepest gratitude to my supervisor, Professor BOUMEDDANE Boussad, for his invaluable guidance, encouragement, and unwavering support throughout the course of my research. His insightful advice and constructive feedback have been instrumental in shaping the direction and quality of this work. I am truly honoured to have had the opportunity to learn under his mentorship.

I am also profoundly grateful to my co-supervisor, Professor BENAROUS Abdallah, for his dedication, expertise, and thoughtful input. His meticulous attention to detail and commitment to excellence have greatly contributed to the success of this project. His guidance has not only enhanced my research but has also inspired me to push beyond my limits.

I would like to extend my sincere thanks to the President of the Jury, Professor BENKHEDA Younes, professor at University Blida1 I extend my heartfelt thanks to the jury members, Professor SEMMAR Djaffer, professor at University Blida 1 and Professor ALLICHE Mounir, Professor at Yahya Fares Medea University.

To my parents my wife and all my family, words cannot fully express my gratitude for your unconditional love, encouragement, and belief in me. You have been my constant source of strength and motivation throughout this journey.

# Table of Contents

# List of Figures

# List of Tables

# Symbols and abbreviations

**Acronyms**

| | |
|---|---|
| ANN | Artificial neural network |
| AR | As-received |
| BFB | bubbling fluidized bed |
| CFD | Computational fluid dynamics |
| CHP | Combined heat and power |
| CRF | Char Reactivity Factor |
| DPW | Date palm waste |
| ER | Equivalence ratio |
| FBR | Fixed-bed reactor |
| FC | Fixed carbon |
| GHG | Green house gas |
| HF | Heat of formation |
| HHV | Higher Heating Value |
| HR | The heat of reaction |
| LCA | Life Cycle Assessment |
| LHV | Lower Heating Value |
| MSW | Municipal solid waste |
| MT | Million metric tons |
| NC | Non-conventional |
| PR-PM | Peng-Robinson equation of state with Boston-Mathias alpha function |
| S/B | Steam to biomass ratio |
| VM | Volatile matter |

**Symbols**

| | |
|---|---|
| a | Number of atoms |
| A | $Pre-exponential\ factor$ [ $s^{-1}\ atm^{-1}$ ] |
| Cp | Heat capacity $J/Kg.K$ |
| $E_a$ | Activation energy $(J/mol)$ |
| G | Gibbs free energy $(J)$ |

| | |
|---|---|
| K | Apparent reaction constant ($s^{-1}$) |
| m | Masse ($Kg$) |
| n | Stochiometric number |
| r | Reaction rate ($s^{-1}$) |
| R | Gas constant ($8.314\ J/K\ mol$) |
| t | Time ($s$) |
| T | Temperature ($K$) |
| y | Molar fraction [%] |

**Subscript**

| | |
|---|---|
| d | dry |
| f | formation |
| i | initial |
| $i$ | species |
| p | pyrolysis |
| t | total |

# Introduction

## General context

Access to reliable electricity remains one of the most pressing challenges across Africa, where many regions continue to face severe energy poverty. Over 600 million people lack access to electricity, hampering economic development, education, and healthcare services. This energy deficit exacerbates social inequalities and slows progress toward sustainable development. While some urban areas benefit from centralized power grids, rural and remote communities often rely on expensive and polluting diesel generators or have no electricity at all. Addressing this challenge requires innovative, sustainable, and accessible energy solutions that are adaptable to the continent's diverse conditions.

Among the promising alternatives, renewable energy sources offer a path toward achieving energy independence while mitigating environmental impacts. Biomass, in particular, holds significant potential as a renewable energy resource due to its widespread availability and ability to transform agricultural and organic waste into energy. Unlike solar or wind energy, which depend on climatic conditions, biomass provides a more stable and continuous energy supply, making it an attractive option for regions with high agricultural activity.

Africa's agricultural sector is a powerhouse of biomass resources, with millions of tons of agricultural residues generated annually. These residues, often considered waste, represent a largely untapped source of energy. Utilizing biomass not only addresses energy challenges but also promotes environmental sustainability by reducing waste accumulation and greenhouse gas emissions. Successful biomass-to-energy projects in countries like Kenya and Ghana have demonstrated the feasibility of this approach, paving the way for further exploration across the continent.

In Algeria, biomass potential is equally significant, particularly given the country’s large agricultural output. Algeria produces vast amounts of agricultural residues, including olive, wheat, and date palm waste. However, only a small fraction of this potential is currently utilized. For example, the estimated recoverable biomass potential in Algeria is 3.7 million tons of oil equivalent (Mtoe) annually, representing just 10% of the total biomass resource. This underutilization highlights the need for improved waste management and valorisation strategies to unlock the energy potential of agricultural residues.

Among these biomass resources, date palm waste stands out as particularly abundant and promising. Algeria, one of the world’s largest producers of dates, generates approximately 2000

tons of date palm waste daily, particularly concentrated in regions like Biskra. Despite its abundance, this resource remains underexploited, often discarded or burned, which contributes to environmental pollution. However, date palm residues possess favorable physicochemical properties for energy recovery through processes such as gasification, making them an ideal candidate for renewable energy initiatives.

This thesis aims to explore the potential of date palm waste as a sustainable biomass feedstock for energy production. By focusing on steam gasification, the research investigates the optimal conditions for converting date palm waste into syngas—a versatile energy carrier composed of hydrogen, carbon monoxide, and methane. Additionally, the study integrates gasification with methanol synthesis, providing a complete pathway from agricultural waste to high-value energy products.

The research aligns with the objectives of the REFFECT AFRICA project, which seeks to promote energy independence and environmental sustainability by leveraging biomass waste from agriculture and the food industry. Through bibliographic analysis, detailed modelling, and experimental validation, this work contributes to advancing knowledge on biomass gasification, offering a sustainable solution to address energy challenges in Algeria and beyond.

# Chapter 1 Biomass and energy

## 1.1 Introduction

The pursuit of sustainable and renewable energy sources has brought biomass back into focus, a prominence it lost during the industrial revolution when coal was discovered. Currently, biomass contributes modestly, accounting for 10% of the world's primary energy mix [1] However, with increasing concerns about global warming and sustainability, this share is likely to grow. Biomass is commonly used for energy through direct combustion, followed by gasification, carbonization, and pyrolysis. There's a rising interest in producing transportation fuel from biomass through methods like pyrolysis, trans-esterification, fermentation, and gasification-based synthesis.

Carbonization, a technique for producing charcoal from biomass, has ancient roots in India and China (around 4000 BCE) for extracting iron from iron ore. Charcoal is still utilized globally as a smokeless fuel and for water or gas filtration. Torrefaction, a relatively new biomass conversion option (derived from the French word "roasting"), is similar to carbonization but has notable differences. It's gaining attention, particularly for co-firing biomass in coal-fired power plants and potentially replacing coke in metallurgy.

Gasification represents a chemical process that transforms carbonaceous materials, such as biomass, into practical and convenient gaseous fuels or chemical feedstock. Related processes include pyrolysis, partial oxidation, and hydrogenation. In contrast, combustion also changes carbonaceous materials into product gases, but notable distinctions exist. Notably, the product gas resulting from combustion lacks useful heating value, whereas the product gas from gasification possesses this valuable property. Gasification encapsulates energy within chemical bonds in the product, whereas combustion releases it. Gasification occurs in reducing (oxygen-deficient) environments, necessitating heat, while combustion unfolds in an oxidizing environment, releasing heat.

The process now includes liquids or even gases to generate more valuable fuels. For instance, the partial oxidation of methane gas is extensively employed in the production of synthetic gas, known as syngas, constituting a blend of $H_2$ and CO.

## 1.2 Biomass and its products

Biomass encompasses organic materials derived from living or recently living plants or animals [2]. Although a universally accepted definition is challenging to pinpoint, the one adopted by the United Nations Framework Convention on Climate Change [3] is pertinent:

"[A] *non-fossilized and biodegradable organic material originating from plants, animals, and micro-organisms. This shall also include products, by-products, residues, and waste from agriculture, forestry, and related industries as well as the non-fossilized and biodegradable organic fractions of industrial and municipal wastes."*

Biomass is sourced from botanical (plant species) or biological (animal waste or carcass) origins, or a combination of both. It specifically includes living and recently deceased biological species that can be utilized as fuel or in chemical production. Notably, biomass excludes organic materials transformed into fossil fuels like coal or petroleum over geological timescales. Common biomass sources encompass:

- Agricultural: Food grain, bagasse (crushed sugarcane), corn stalks, straw, seed hulls, nutshells, and manure from cattle, poultry, and hogs.
- Forest: Trees, wood waste, wood or bark, sawdust (SW), timber slash, and mill scrap.
- Municipal: Sewage sludge, refuse-derived fuel (RDF), food waste, waste paper, and yard clippings.
- Energy Crops: Poplars, willows, switchgrass, alfalfa, prairie bluestem, corn, soybean, canola, and other plant oils.
- Biological: Animal waste, aquatic species, and biological waste.

Botanical biomass is generated through the conversion of carbon dioxide (CO2) from the atmosphere into carbohydrates, facilitated by the sun's energy in the presence of chlorophyll and water. Biological species, in turn, grow by consuming botanical or other biological entities.

Plants harness solar energy through a process known as photosynthesis (Figure 1.1). In the presence of sunlight with specific wavelengths, green plants break down water to obtain electrons and protons, utilizing them to convert CO2 into glucose (depicted as CHmOn), with the release of O2 as a byproduct. This process can be represented by the equation [4]

$$Living\ plant + co_2 + H_2O + Sunlight \xrightarrow{Chlorophyll} (CH_mO_n) + O_2 - 480Kj/mol \qquad (1.1)$$

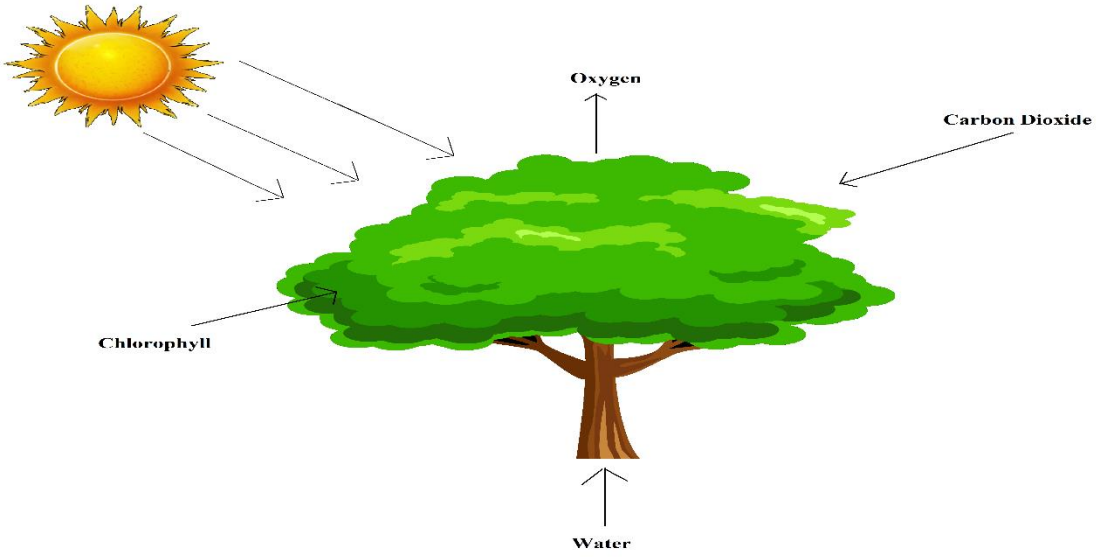


Figure 1.1 Biomass grows by absorbing solar energy, carbon dioxide, and water through photosynthesis.

### *1.2.1 Type of biomass*

Biomass is derived from a diverse array of sources, as outlined in Table 1.1. The European Committee for Standardization has established two standards for the classification and specification (ISO 17225) [5] and quality assurance (EN 15234) [6] of biomass. These standards categorize biomass into four main groups based on their origin:

- Woody biomass
- Herbaceous biomass
- Fruit biomass
- Blend and mixtures

Table 1.1 Type of biomass [7]

| | | |
|---|---|---|
| A. Virgin Biomass | A.1 Terrestrial biomass | Forest biomass<br>ii. Grasses<br>iii. Energy crops<br>iv. Cultivated crops |
| | A.2 Aquatic biomass | i. Algae<br>ii. Water plant |
| B. Waste biomass | B.1 Municipal waste | i. MSW<br>ii. Biosolids, sewage |

| | | |
|---|---|---|
| | | iii. Landfill gas |
| | B.2 Agricultural solid waste | i. Livestock and manures<br>ii. Agricultural crop residue |
| | B.3 Forestry residues | i. Bark, leaves, floor residues |
| | B.4 Industrial wastes | i. Demolition wood, sawdust<br>ii. Waste oil/fat |

Table 1.1 categorizes various biomass types into two main classifications: virgin and waste, which can be further divided into the following broad groups:

1. Virgin biomass:
    - Wood, plants, and leaves (lignocellulose)
    - Crops and vegetables (carbohydrates)
2. Waste biomass:
    - Solid and liquid wastes (municipal solid waste (MSW))
    - Sewage, animal, and human wastes
    - Gases derived from landfilling (mainly methane)
    - Agricultural wastes

### *1.2.1.a Lignocellulosic biomass*

A significant portion of biomass is comprised of lignocellulose, and this type is worth exploring in greater detail. Lignocellulosic material constitutes the non-starch, fibrous component of plant materials, with cellulose, hemicellulose, and lignin as its three primary constituents. Unlike carbohydrates or starch, lignocellulose is not easily digestible by humans. For instance, while we can consume rice, a carbohydrate, we cannot digest the husk or straw, which consists of lignocellulose. Importantly, lignocellulosic biomass is not part of the human food chain, ensuring that its utilization for biogas or bio-oil production does not pose a threat to the world's food supply.

The trunk and leaves of tree plants constitute the most substantial group of accessible biomass. These are categorized as lignocellulosic, given that their primary constituents are cellulose, hemicellulose, and lignin. Table 1.2 provides the percentage of these components in various plants.

Table 1.2 Composition of Some Lignocellulose Biomass [8,9]

| Plant | Lignin (%) | Cellulose (%) | Hemicellulose (%) |
|---|---|---|---|
| Deciduous plants | 18 - 25 | 40_44 | 15_35 |
| Coniferous plants | 25 - 35 | 40_44 | 20_32 |
| Straws | 30 - 43 | 22 - 35 | 15 - 23 |
| Herbs | 25 - 40 | 35 - 50 | 10 – 30 |

### *1.2.2 Constituents of biomass cells:*

The polymeric composition of cell walls and other elements within biomass exhibits considerable variation, but fundamentally consists of three major polymers: cellulose, hemicellulose, and lignin.

#### *1.2.2.a Cellulose*

Cellulose, the most prevalent organic compound on Earth, serves as the principal structural component of cell walls in biomass. Its quantity ranges from 90% (by weight) in cotton to around 33% for most other plants. Represented by the generic formula $(C_6H_{10}O_5)_n$. [10]

#### *1.2.2.b Hemicellulose*

Hemicellulose is an additional constituent found in the cell walls of plants. In contrast to cellulose, which possesses a crystalline and robust structure resistant to hydrolysis, hemicellulose exhibits a random, amorphous structure with limited strength. It comprises a group of carbohydrates with a branched chain structure and a lower degree of polymerization (DP<100–200), represented by the generic formula $(C_5H_8O_4)_n$. [11]

#### *1.2.2.c Lignin*

Lignin is a biopolymer belonging to the family of macromolecules, specifically a polyphenolic polymer and one of the main components of wood along with cellulose and hemicellulose. Lignin is found in vascular plants and certain algae. Its function is to provide rigidity, water impermeability, and high resistance to decomposition. This material is not biologically convertible into biofuel; however, after decomposition, it serves as an energy source in conversion processes.

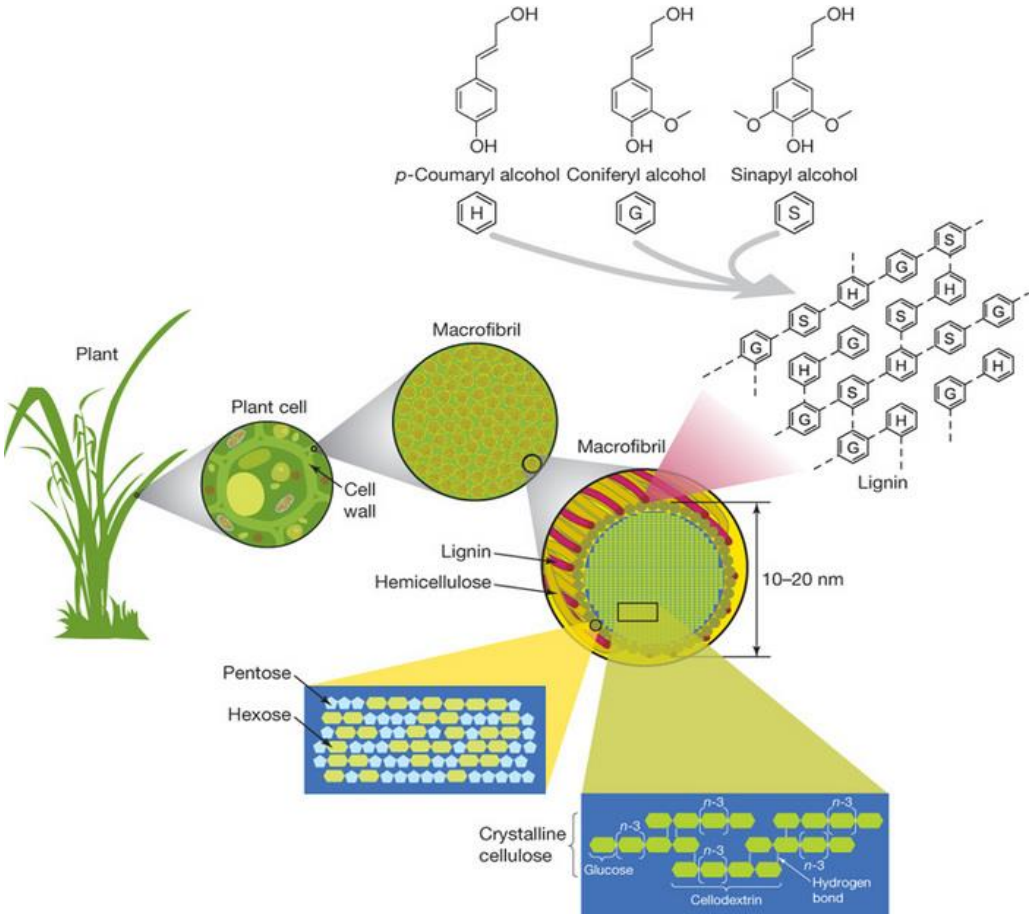


Figure 1.2 Structure of lignocellulose [12]

## 1.3 Properties of biomass

The following sections describe some important thermophysical properties of biomass that are relevant to gasification.

### *1.3.1 Physical properties*

Certain physical properties of biomass play a crucial role in influencing its pyrolysis and gasification behaviour. For instance, permeability is a significant factor in pyrolysis. Higher permeability allows pyrolysis gases to be captured in the pores, prolonging their residence time in the reaction zone. This extended residence time increases the potential for secondary cracking, leading to the production of char.

In wood, the pores are generally oriented longitudinally. Consequently, the thermal conductivity and diffusivity in the longitudinal direction differ from those in the lateral direction. This anisotropic behaviour of wood can impact its thermochemical conversion. Processes like torrefaction, involving biomass densification, can mitigate this anisotropic behaviour, consequently altering the permeability of biomass.

### *1.3.1.a Densities*

Density is an important design parameter for any biomass conversion system. For a granular biomass, we can define four characteristic densities: true, apparent, bulk, and biomass (growth).

A. True density

True density is the weight per unit volume occupied by the solid constituent of biomass. Total weight is divided by actual volume of the solid content to give its true density.

$$\rho_{true} = \frac{total\ mass\ of\ Biomass}{solid\ volume\ in\ biomass}$$

The cell walls represent the primary solid component of biomass. In the case of typical wood, the density of the cell wall is generally around 1530 kg/m³, and this value remains relatively constant for most wood cells [13]. Determining the true density of biomass is as challenging as measuring its true solid volume. This can be assessed using a pycnometer or estimated through the ultimate analysis and the true density of its constituent elements.

B. Apparent density

Apparent density is derived from the apparent or external volume of the biomass, encompassing its pore volume or cell cavities. In the case of regularly shaped biomass, mechanical tools like micrometers can measure different sides of a particle to determine its apparent volume. An alternative method is using volume displacement in water. Apparent density takes into account the internal pores of a biomass particle but does not consider the interstitial volume between biomass particles when packed together [14].

$$\rho_{apparent} = \frac{total\ mass\ of\ biomass}{apparent\ volume\ of\ biomass\ including\ solids\ and\ internal\ pores}$$

The pore volume of a biomass, expressed as a fraction of its total volume, is referred to as its porosity, denoted as Ap. These characteristic holds significance in understanding the biomass structure.

Apparent density is most commonly used for design calculations because it is the easiest to measure, and it gives the actual volume occupied by a particle in a system.

C. Bulk density

Bulk density is based on the overall space occupied by an amount or a group of biomass particles [14]:

$$\rho_{bulk} = \frac{total\ total\ mass\ of\ biomass\ particles\ or\ stackmass\ of\ biomass}{bulk\ volume\ occupied\ by\ biomass\ particles\ or\ stack}$$

Bulk volume includes interstitial volume between the particles, and as such it depends on how the biomass is packed. For example, after pouring the biomass particles into a vessel, if the vessel is tapped, the volume occupied by the particles settles to a lower value. The interstitial volume expressed as a function of the total packed volume is known as bulk porosity, Ab. To determine the biomass bulk density, we can use standards like the American Society for Testing of Materials (ASTM) E-873-06.

D. Biomass (growth) density

The term biomass (growth) density is used in bioresource industries to express how much biomass is available per unit area of land. It is defined as the total amount of above-ground living organic matter in trees expressed as oven-dry tons per unit area (e.g., tons per hectare) and includes all organic materials: leaves, twigs, branches, main bole, bark, and trees.

### *1.3.2 Thermodynamic properties*

Gasification is a thermochemical conversion process, so the thermodynamic properties of a biomass heavily influence its gasification. This section describes three important thermodynamic properties: thermal conductivity, specific heat, and heat of formation of biomass.

#### *1.3.2.a Thermal conductivity*

Biomass particles undergo heat conduction along and across their fibres, significantly impacting their pyrolysis behaviour. Consequently, the thermal conductivity of biomass becomes a crucial parameter in this context, and it is known to change with density and moisture content. MacLean (1941), based on a substantial number of samples, developed the following correlations, as reported by [15]

$$K_{eff}\left(\frac{W}{m.k}\right) = \gamma(0.2 + 0.004m_d) + 0.0238 \qquad for\ m_d > 40\% \qquad (1.2)$$

$$K_{eff}\left(\frac{W}{m.k}\right) = \gamma(0.2 + 0.0055m_d) + 0.0238 \qquad for\ m_d < 40\% \qquad (1.3)$$

Where $\gamma$ is the specific gravity of the fuel and it represents a dimensionless quantity that expresses the density of the biomass relative to the density of water. $m_d$ is the moisture percentage of the biomass on a dry basis (db).

### *1.3.2.b Specific heat*

Specific heat is a vital thermodynamic property of biomass, often necessary for thermodynamic calculations, serving as an indicator of the heat capacity of a substance. The specific heat of biomass is influenced by both moisture and temperature. The specific heat undergoes significant changes with temperature and, to some extent, depends on the type and source of biomass [16].

### *1.3.2.c Heat of Formation*

Heat of formation, also referred to as enthalpy of formation, denotes the enthalpy change occurring when 1 mol of a compound is formed at standard state (25°C, 1 atm) from its constituent elements in their standard state. For instance, hydrogen and oxygen are stable in their elemental form, resulting in a zero enthalpy of formation. However, when they combine to form steam, energy is released, amounting to 241.5 kJ per mole.

$$H_2(gas) + 0.5O_2(gas) = H_2O\ (gas) - 245\,\frac{Kj}{mol} \qquad (1.4)$$

The heat of formation of steam is thus -241.5 kJ/mol (g). This amount of energy is taken out of the system and is therefore given a negative (-) sign in the equation to indicate an exothermic reaction .

### *1.3.2.d Heat of combustion (reaction)*

The heat of reaction (HR) is the amount of heat released or absorbed in a chemical reaction with no change in temperature. In the context of combustion reactions, HR is called heat of combustion, $\Delta H_{comb}$, which can be calculated from the heat of formation (HF) as :

$$CH_4 + 2O_2 \rightarrow 2H_2O + CO_2 \qquad (1.5)$$

For example:

$$\Delta H_{comb} = 2\Delta H_{H_2O} + \Delta H_{CO_2} - \Delta H_{CH_4} - 2\Delta H_{O_2} \qquad (1.6)$$

### *1.3.2.e Heating value*

The heating value of biomass is the quantity of energy released when biomass undergoes complete combustion in sufficient oxygen. This property holds immense significance in the realm of energy conversion. In comparison to most fossil fuels, biomass exhibits a relatively low heating value, particularly on a volume basis. This is attributed to its low density and its nature as a high-oxygen-containing fuel [17].

### *1.3.2.f Ignition temperature*

Ignition temperature is a critical property for any fuel as it signifies the point at which the combustion reaction becomes self-sustaining. In a typical gasifier, a certain level of combustion is essential to supply the necessary energy for drying, pyrolysis, and ultimately for the endothermic gasification reaction [14]. The ignition temperature is generally lower for higher volatile matter content fuel. Because biomass particles have a higher volatile matter content than coal, they have a significantly lower ignition temperature, Table 1.3 gives.

Table 1.3 Ignition Temperatures of Some Fuels

| Fuel | Ignition Temperature (°C) | Volatile matter in Fuel (dry ash-free (%) | Reference |
|---|---|---|---|
| Wheat straw | 220 | 72 | [18] |
| Poplar wood | 235 | 75 | [18] |
| Eucalyptus | 285 | 64 | [18] |
| Olive pit | 220 | 75 | [19] |

### *1.3.3 Composition of biomass*

Biomass is composed of many complex organic compounds, moisture (M), and a minor amount of inorganic impurities referred to as ash (ASH). The organic compounds primarily consist of four elements: carbon (C), hydrogen (H), oxygen (O), and nitrogen (N). Biomass, such as municipal solid waste (MSW) and animal waste, may also contain trace amounts of chlorine (Cl) and sulfur (S).

The thermal design of a biomass utilization system, whether it's a gasifier or a combustor, requires knowledge of the fuel's composition and energy content. In the context of thermal conversion, such as combustion, the following two types of compositions are commonly used:

1 Ultimate or Elemental Composition

2 Proximate Composition

### *1.3.3.a Ultimate analysis*

Here, the composition of the hydrocarbon fuel is expressed in terms of its basic elements except for its moisture, M, and inorganic constituents, ASH. A typical ultimate analysis is:

$$C + H + O + N + S + ASH + M = 100\% \quad (1.7)$$

Table 1.4 Comparison of ultimate analysis (dry basis) of Some Biomass and its comparison with other fossil fuels[20]

| Biomass | C (%) | H (%) | N (%) | S (%) | O (%) | Ash (%) | HHV (kJ/kg) |
|---|---|---|---|---|---|---|---|
| Maple | 50.6 | 6.0 | 0.3 | 0 | 41.7 | 1.4 | 19,958 |
| Redwood | 53.5 | 5.9 | 0.1 | 0 | 40.3 | 0.2 | 21,028 |
| Straw-rice | 39.2 | 5.1 | 0.6 | 0.1 | 35.8 | 19.2 | 15,213 |
| Husk-rice | 38.5 | 5.7 | 0.5 | 39.8 | 0 | 15.5 | 15,376 |
| MSW | 47.6 | 6.0 | 1.2 | 0.3 | 32.9 | 12.0 | 19,879 |
| Animal waste | 42.7 | 5.5 | 2.4 | 0.3 | 31.3 | 17.8 | 17,167 |
| PRB coal | 65.8 | 4.88 | 0.86 | 1.0 | 16.2 | 11.2 | 26,436 |
| Petcoke | 82 | 0.5 | 0.7 | 0.8 | 10.0 | 6.0 | 28,377 |

### *1.3.3.b Proximate analysis*

Proximate analysis gives the composition of the biomass in terms of gross components such as moisture (M), volatile matter (VM), ash (ASH), and fixed carbon (FC) [21].

I. Volatile Matter (Vm): The volatile matter of a fuel is the condensable and noncondensable vapor released when the fuel is heated. Its amount depends on the rate of heating and the temperature to which it is heated.

II. ASH: is the inorganic solid residue left after the fuel is completely burned. Its primary ingredients are silica, aluminum, iron, and calcium; small amounts of magnesium, titanium, sodium, and potassium may also be present.

III. Moisture: This is defined as the percentage of moisture in a biomass sample under examination when it is heated just over the boiling point of water (105°C) [22] . The total moisture content of some biomass can be as high as 90% (db. Moisture drains much of the deliverable energy from a gasification plant, as the energy used in evaporation is not recovered. This important input parameter for design must be known for assessment of the cost of transportation or energy penalty in drying the biomass.

IV. Fixed Carbon (FC): Represents the solid carbon in the biomass that remains in the char in the pyrolysis process after devolatilization. With coal, FC includes elemental carbon in the original fuel plus any carbonaceous residue formed while heating, in the determination of VM and it is determined from the following equation:

$$FC = 1 - Moisture - VM - ASH \quad (1.8)$$

### *1.3.3.c Bases of expressing biomass composition*

The composition of a fuel is often expressed on different bases depending on the situation. The following four bases of analysis are commonly used:

a) As-received
b) Air-dry
c) Total dry
d) Dry and ash-free.

A comparison of these bases is shown in Figure 1.3:

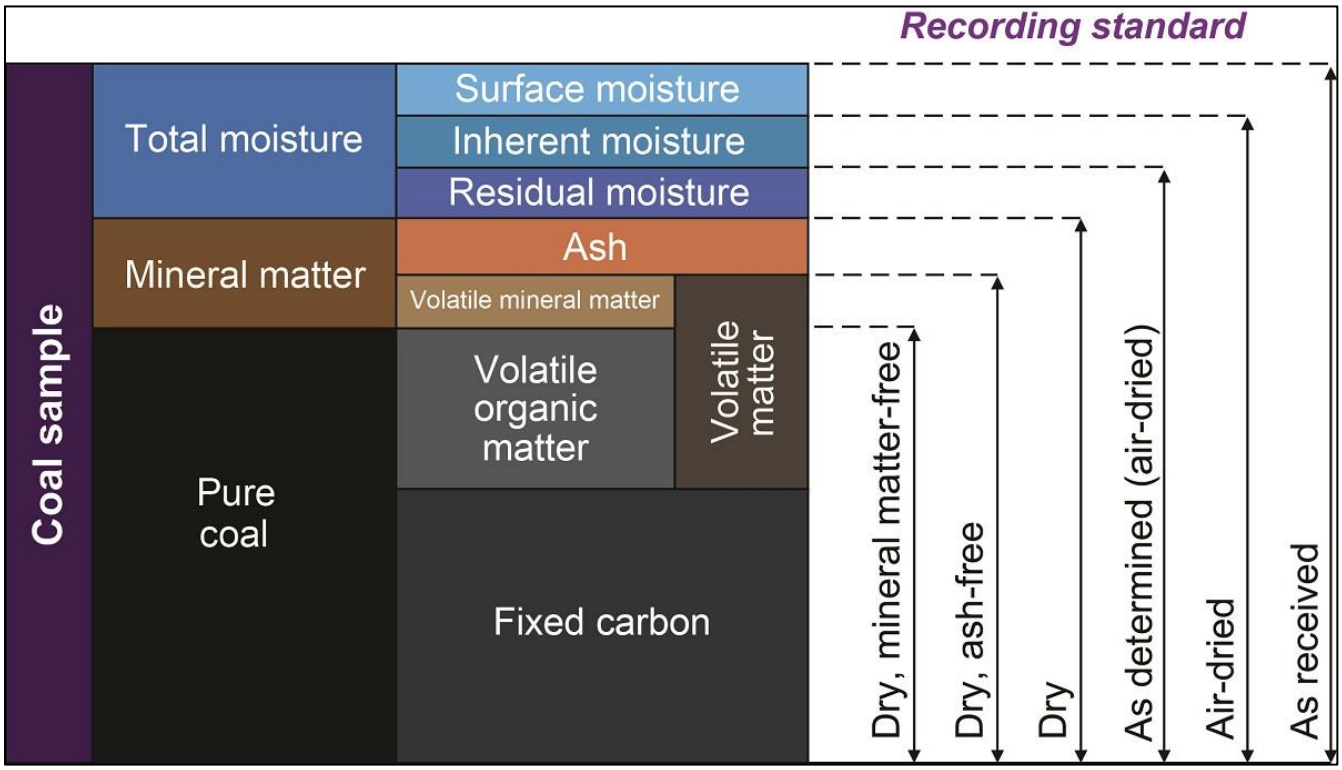


Figure 1.3 Different recording standards are used for different measurements of coal components [23].

a) As received

When using the as-received (ar) basis, the results of ultimate and proximate analyses may be written as follows:

$$Ultimate\ Analysis:\ C + H + O + N + S + ASH + M = 100\% \quad (1.9)$$

$$Proximate\ Analysis:\ VM + FC + M + ASH = 100\% \quad (1.10)$$

where VM, FC, M, and ASH represent the weight percentages of volatile atter, fixed carbon, moisture, and ash, respectively, measured by proximate analysis, and C, H, O, N, and S represent the weight percentages of carbon, hydrogen, oxygen, nitrogen, and sulfur, respectively, as measured by ultimat analysis. The ash and moisture content of the fuel is the same in both analyses. “As received” can be converted into other bases.

b) Air dried

When the fuel is dried in air, its surface moisture is removed while its inherent moisture is retained. So, to express the constituent on an air-dry (ad) basis, the amount is divided by the total mass less the surface moisture. For example, the carbon percentage on the “ad” basis is calculated as:

$$C_{ad} = \frac{100C}{100 - M_a} \quad (1.11)$$

where $M_a$ is the mass of surface moisture removed from 100 kg of moist fuel after drying in air. Other constituents of the fuel can be expressed similarly.

c) Dry basis

Fuel composition on the “ad” basis is a practical parameter and is easy to measure, but to express it on a totally moisture-free (total Dry) basis, we must make allowance for surface as well as inherent moisture, Mi. This gives the carbon percentage on a total dry basis, $C_{td}$:

$$C_{td} = \frac{100C}{100 - M_i} \quad (1.12)$$

where M is the total moisture in the fuel.

d) Dry ash free basis

Ash is another component that at times is eliminated along with moisture. This gives the fuel composition on a daf basis. Following the aforementioned examples, the carbon percentage on a "daf" basis, $C_{daf}$ can be found:

$$C_{daf} = \frac{100C}{100 - M - ASH} \quad (1.13)$$

Where $(100 - M - ASH)$ is the mass of biomass without Moisture and ASH. The percentage of all constituents on any basis totals 100.

***1.3.3.d Heating value of the biomass***

The heat value, or amount of heat available in a fuel (kJ/kg), is one of the most important characteristics of a fuel because it indicates the total amount of energy that is available in the fuel. The heat value in a given fuel type is mostly a function of the fuel's chemical composition. The heat value can be expressed in one of two ways: the higher heating value or the lower heating value[24].

a) Higher Heating Value (HHV)

It is defined as the heat released per unit mass or volume of fuel (initially at 25°C) once combustion occurs, and the products cool back to a temperature of 25°C. This measure incorporates the latent heat of water vaporization. HHV, also known as gross calorific value, is commonly used in North America to express the thermal efficiency of a system. Thus, understanding the HHV of the designated fuel is essential for system design. Refer to Table 1.4 for the HHV values of various biomass types.

b) Lower Heating Value (LHV)

The lower heating value (LHV), also referred to as the net calorific value, is defined as the heat released when a specified quantity is fully combusted, minus the heat of vaporization of the water in the combustion product. The relationship between higher heating value (HHV) and LHV is expressed by :

$$LHV = HHV - h_g\left(\frac{9H}{100} - \frac{M}{100}\right) \quad (1.14)$$

where LHV, HHV, H, and M represent lower heating value, higher heating value, hydrogen percentage, and moisture percentage, respectively, on an "ar" basis. Here, hg denotes the latent

heat of steam in the same units as HHV. The latent heat of vaporization when the reference temperature is 100°C is 2260 kJ/kg. Numerous European countries define the efficiency of a thermal system in terms of LHV [14].

Table 1.5 delineates the two types of harvested biomass, categorized as food and nonfood, along with the potential conversion products associated with them. This distinction is crucial because the large-scale commercial production of transport fuel (ethanol) from cereals, though

relatively straightforward and established, raises concerns. Using food crops for energy production, particularly cereals, may pose sustainability challenges as it redirects these resources from the traditional grain market to the energy market, carrying economic, social, and political implications. Consequently, endeavours are underway to increase ethanol production from non-food sources like cellulosic materials, aiming to ensure that our pursuit of additional energy does not strain the world's food supply.

Table 1.5 Sources of Biomass [14]

| | | |
|---|---|---|
| Farm products | Corn, sugarcane, sugar beet, wheat, etc. | Products ethanol |
| | Rapeseed, soybean, palm sunflower seed, Jatropha, etc. | Produces biodiesel |
| Lignocellulosic materials | Straw or cereal plants, husk, wood, scrap, slash, etc. | Can produce ethanol, bioliquid, and gas |

### *1.3.4 Biomass products:*

Three types of primary fuels could be produced from biomass and are as follows:

1. Liquid fuels (ethanol, biodiesel, methanol, vegetable oil, and pyrolysis oil).
2. Gaseous fuels (biogas (CH4, CO2), producer gas (CO, H2, CH4, CO2, H2), syngas (CO, H2), substitute natural gas (CH4).
3. Solid fuels (charcoal, torrefied biomass, biocoke, biochar).

#### *1.3.4.a Chemicals industries*

In theory, the majority of chemicals derived from petroleum or natural gas can also be produced from biomass. Chemical production from biomass primarily occurs through two principal platforms: sugar-based and syngas-based. The sugar-based platform utilizes sugars such as glucose, fructose, xylose, arabinose, lactose, sucrose, and starch. On the other hand, the syngas-based platform involves the use of carbon monoxide (CO) and hydrogen (H2).

### *1.3.4.b Energy industries*

Biomass likely served as the initial on-demand energy source harnessed by humans. The prominence of biomass as a primary energy source significantly varies based on geographical and socioeconomic factors. For instance, it constitutes a substantial 90% of the primary energy source in Nepal, while it accounts for only a minimal 0.1% in Middle Eastern countries. A more effective and contemporary commercial utilization of biomass involves its use in generating steam for processing heat and electricity generation. Heat and electricity are two forms of primary energy derived from biomass. The use of biomass for efficient energy production is presently on the rise in developed countries because of its carbon-neutral feature [25].

### *1.3.4.c Transport industries*

Diesel and gasoline derived from crude petroleum are extensively employed in modern transportation industries. Biomass presents a sustainable option to replace these fossil fuel-based transport alternatives with carbon-neutral options. Ethanol, primarily sourced from sugarcane and corn, is utilized in gasoline engines (spark-ignition), while biodiesel, derived from vegetable oils like rapeseed, is employed in diesel engines (compression-ignition). Through gasification and anaerobic digestion, methane gas can be generated from biomass. This methane can either be directly used in certain spark-ignition engines for transportation or converted into gasoline through methanol.

**Biomass conversion**

The considerable bulk, low energy density, and impractical form of biomass pose significant obstacles to a swift shift from fossil fuels to biomass fuels. Unlike gas or liquid fuels, biomass is challenging to handle, store, and transport. This challenge underscores the importance of converting solid biomass into liquid and gaseous fuels, which boast higher energy density and are more manageable and storable. Achieving this conversion typically involves one of two main routes (as illustrated in Figure 1.4): biochemical conversion (fermentation) and thermochemical conversion (pyrolysis, gasification).

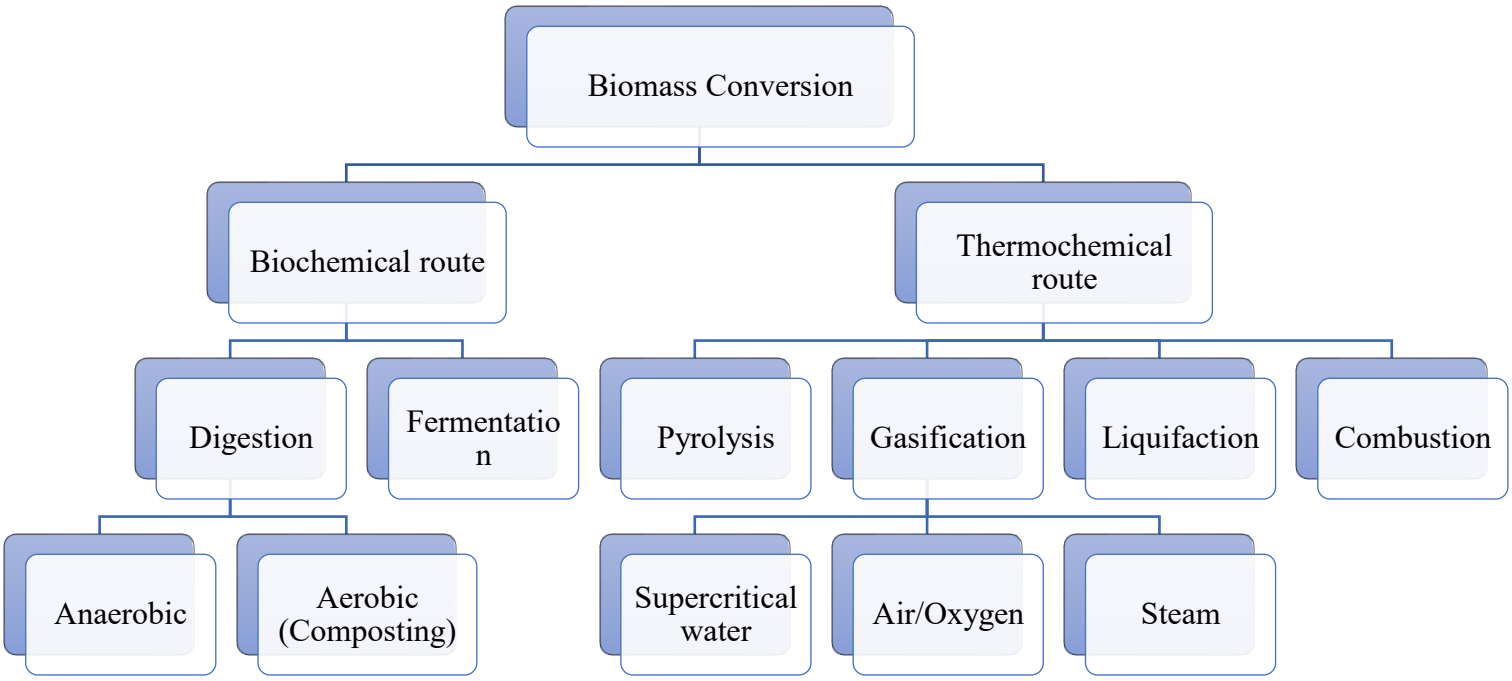


Figure 1.4 Different options for conversion of biomass into fuel gases or chemicals.

### *1.3.5 Biochemical conversion*

Biochemical conversion processes harness the enzymatic activities of bacteria and other microorganisms to break down biomass This process is much slower than thermochemical conversion process but does not require much external energy. The three principal routes for biochemical conversion are as follows[26]:

1. Digestion (anaerobic and aerobic)
2. Fermentation
3. Enzymatic or acid hydrolysis.

Anaerobic digestion primarily yields methane and carbon dioxide, along with a solid residue, as its main products. Notably, bacteria extract oxygen from the biomass rather than the surrounding air during this process.

On the other hand, aerobic digestion, also known as composting, is another biochemical breakdown of biomass. It occurs in the presence of oxygen, utilizing various types of microorganisms that draw oxygen from the air. The outcome includes carbon dioxide, heat, and a solid digestate. In the fermentation pathway, an organic substrate of biomass is chemically changed by the action of enzymes, which is secreted by different microorganisms such as yeasts. Fermentation is a widely adopted technology in different countries to produce ethanol ($C_2H_5OH$) on a large-scale from sugar crops such as sugarcane and sugar beet, as well as starch crops such as maize and wheat[27].

### *1.3.6 Thermochemical conversion*

The thermochemical process entails the application of heat and chemicals to extract products from biomass. This process comprises two key stages: the initial stage involves converting biomass into gas and subsequently transforming it into hydrocarbons. The second stage encompasses the direct liquefaction of biomass through high-pressure liquefaction, high-temperature pyrolysis, or supercritical extraction. The specific method of conversion depends on the type and quantity of biomass, as well as the desired energy product [28].

Moreover, thermochemical processes can be categorized into:

a) Combustion
b) Carbonization/torrefaction
c) Pyrolysis
d) Gasification
e) Liquefaction.

Each of these processes serves distinct purposes in the overall utilization of biomass for energy production. In the thermochemical route (Figure 1.5), the biomass is first converted into syngas, which is then converted into ethanol through synthesis or some other means.

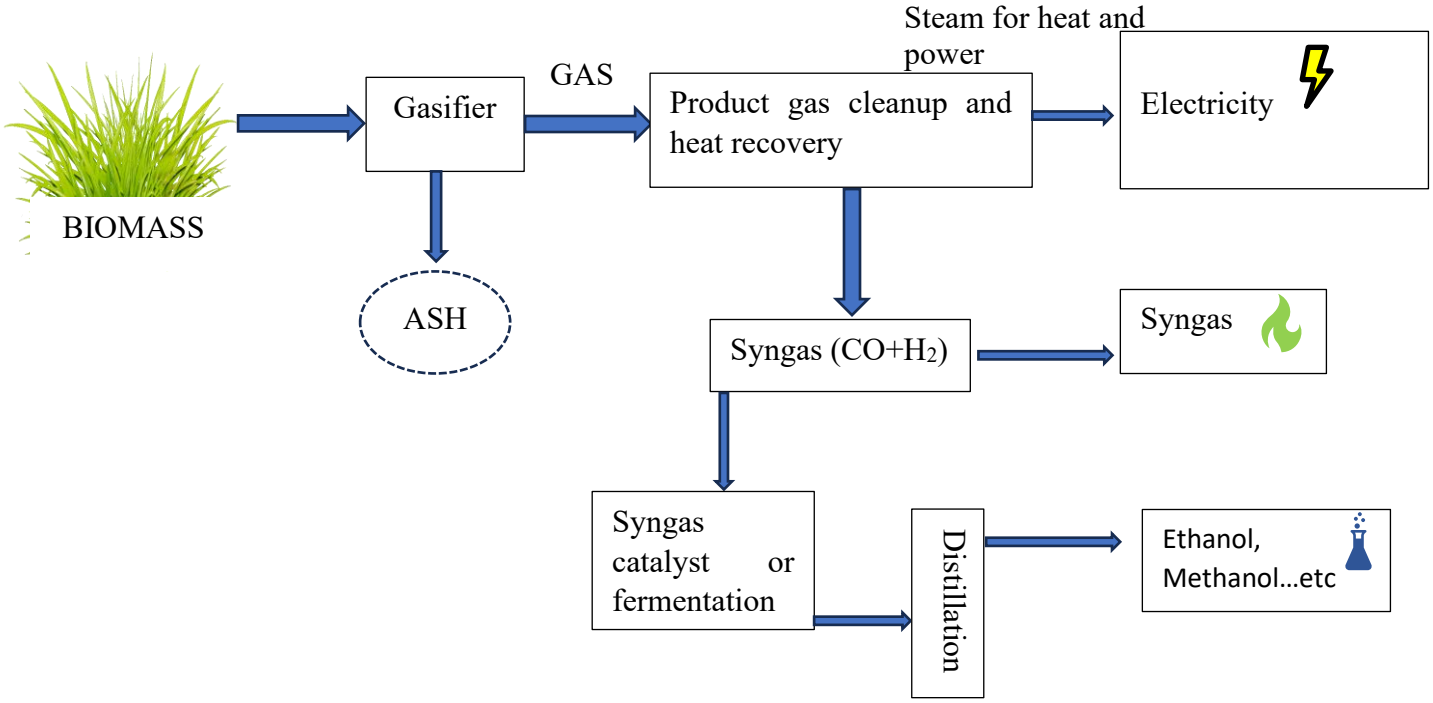


Figure 1.5 Thermochemical route for production of energy, gas, ethanol, Methanol… Etc.

### *1.3.6.a Combustion*

It is the conventional process of combusting biomass in the presence of air to convert chemical energy into heat, mechanical, or electrical energy. This method finds applications in various industrial and commercial sectors, including steam turbines, turbo-generators, stoves, boilers, furnaces, and more [28].

### *1.3.6.b Pyrolysis*

Unlike combustion, pyrolysis occurs in the complete absence of oxygen, except in cases where partial combustion is permitted to supply the required thermal energy for the process. This thermal process breaks down biomass into gas, liquid, and solid components by rapidly heating biomass to temperatures above 300°C-400°C. In pyrolysis, large hydrocarbon molecules of biomass are broken down into smaller molecules. Fast pyrolysis primarily yields liquid fuel, known as bio-oil, while slow pyrolysis produces some gas and solid charcoal, an ancient fuel used for heating and metal extraction before the discovery of coal. Pyrolysis holds promise for converting waste biomass into valuable liquid fuels. Importantly, unlike combustion, pyrolysis is not an exothermic process [29]

### *1.3.6.c Torrefaction*

Torrefaction is being explored as an efficient means to utilize biomass as a clean and convenient solid fuel. In this process, biomass is gradually heated to temperatures between 200°C to 300°C with minimal or no contact with oxygen. Torrefaction brings about changes in the chemical structure of biomass hydrocarbons, increasing carbon content while decreasing oxygen. This process also boosts the energy density of biomass and makes it hygroscopic. These characteristics enhance the commercial value of wood for energy production and transportation [14].

### *1.3.6.d Gasification*

Gasification is the process of converting fossil or non-fossil fuels (solid, liquid, or gaseous) into useful gases and chemicals. This transformation requires a medium for the reaction, which can be gas or supercritical water (distinct from ordinary water at subcritical conditions). Gaseous mediums include air, oxygen, subcritical steam, or a combination of these.

Currently, gasification of fossil fuels is more prevalent than that of non-fossil fuels like biomass for the production of synthetic gases. The process essentially converts a potential fuel from one form to another. There are several key motivations for such a transformation, including:

- To increase the heating value of the fuel by rejecting noncombustible
- components like nitrogen and water.
- To strip the fuel gas of sulfur such that it is not released into the atmosphere
- when the gas is burnt.
- To increase the H/C mass ratio in the fuel.
- To reduce the oxygen content of the fuel.

### *1.3.6.e Liquefaction*

The liquefaction of solid biomass into liquid fuel can be achieved through pyrolysis, gasification, and a hydrothermal process. In the hydrothermal process, biomass is transformed into an oily liquid by exposing it to water at elevated temperatures (300–350°C) and high pressure (12–20 MPa) for a specific duration. Other methods, such as the supercritical water process also exist for the direct liquefaction of biomass. Benhrendt et al. [30] provided a comprehensive review of these various processes.

## 1.4 Motivation for biomass conversion

The conversion of biomass, particularly into heat and light, has been ingrained in human civilization since ancient times. The discovery of fire from wood marked a pivotal point in the scientific development of the human race, distinguishing it from other creatures. Over time, the use of biomass declined with the availability of more energy-dense and convenient fossil fuels like coal and oil. However, there has been a recent resurgence of interest in converting biomass into gas or liquid. This renewed interest is primarily driven by three key factors:

1 Renewability benefits.
2 Environmental benefits.
3 Sociopolitical benefits.

A brief description of these benefits is provided in the following sections.

### *1.4.1 Renewability benefits*

Fossil fuels such as coal, oil, and gas are practical and convenient sources of energy, effectively meeting society's energy demands. However, a significant drawback exists: fossil fuel resources are finite and non-renewable. In contrast, biomass is renewable as it grows. A crop harvested this year can regrow next year, and a tree cut today may fully regrow within a decade through fresh growth. Unlike fossil fuels, biomass is not likely to be depleted with consumption. This characteristic renders its use sustainable, contributing to the increasing interest in biomass for energy production.

While there are concerns about cutting trees for energy supply, it's essential to recognize that a tree stops absorbing CO2 once it stops growing or dies. If left on the forest floor, it can release CO2 through natural degradation or in a forest fire. Moreover, a dead tree might release more harmful CH4 if it decomposes in water. Using a tree as fuel provides carbon-neutral energy, avoiding methane gas release from decomposed deadwood. Although careless use of trees for energy could pose environmental risks, managed utilization with fresh planting following cutting, as practiced by some pulp industries, can sustain its use for energy in an environmentally friendly manner. Energy plantation with fast-growing plants like Switchgrass and Miscanthus is also being explored as fuel for new energy projects, given their very short growing periods measured in months.

### *1.4.2 Environmental benefits*

With the growing evidence of global warming, there is a heightened awareness of the urgent need to reduce human-made greenhouse gas (GHG) emissions. Additionally, the emission of other air pollutants such as NO, SO2, and Hg is no longer acceptable. From elementary schools to corporate boardrooms, the environment has become a major focal point, serving as a significant driver for the utilization of biomass in energy production.

Biomass holds a special appeal in this context because, as explained below, it makes no net contribution of carbon dioxide to the atmosphere. Many countries have implemented regulations to make biomass economically viable. For instance, if biomass replaces fossil fuel in a power plant, that plant could earn credits for CO2 reduction equivalent to what the fossil fuel was emitting. These credits can be sold on the market, providing additional revenue in countries where such trades are practiced.

When biomass is burned, it releases CO2 recently absorbed from the atmosphere, not millions of years ago, as is the case with fossil fuels. The net addition of CO2 to the atmosphere through biomass combustion is considered zero, rendering biomass a carbon-neutral fuel. While some argue that CO2 is emitted during biomass harvesting, transporting, and processing, similar indirect emissions occur with fossil fuels in mining, transporting, and preparing them. A life cycle analysis comparing CO2 release from all direct and indirect actions shows biomass as a clear winner over fossil fuels. Even disregarding the carbon-neutral aspect, the carbon intensity of biomass (39.6–50.4 g/kWhe) is significantly lower than that of fossil fuels like coal due to its low carbon-to-hydrogen ratio [31]. Gasification-based power plants emit slightly less CO2 on a unit heat release basis compared to combustion power plants. For instance, an integrated gasification combined cycle (IGCC) plant emits 745 g/kWh, while a combustion-based subcritical pulverized coal (PC) plant emits 770 g/kWh [32]. The concentration of CO2 in the flue gas from an IGCC plant makes it easier to sequester compared to a conventional PC plant, where CO2 is diluted with nitrogen. Table 1.6 provides a comparison of CO2 emissions from different electricity-generation technologies.

Table 1.6 Comparison of emissions and water use for electricity generation from coal using two technologies [33]

| | PC Combustion | Gasification (IGCC) |
|---|---|---|
| CO2 (kg/1000 MWh) | 0.77 | 0.68 |
| Water use (L/1000 MWh) | 4.62 | 2.84 |
| SO2 emission (kg/MWh) | 0.68 | 0.045 |
| NOx emission (kg/MWh) | 0.61 | 0.082 |
| Total solids (kg/100 MWh) | 0.98 | 0.34 |

### *1.4.3 Sociopolitical benefits*

The sociopolitical benefits of employing biomass are significant. Firstly, biomass is a locally cultivated resource. To be economically feasible, biomass-based power plants rely on biomass from a limited radius around the facility. This fosters the development of associated industries for biomass cultivation, collection, and transportation. Some experts suggest that a biomass fuel plant could generate up to 20 times more local employment compared to a coal- or oil-based plant [34] Consequently, the biomass industry positively influences the local economy.

Another crucial aspect of biomass-based energy, fuel, or chemicals is the reduction of dependence on imported fossil fuels, providing a country with added energy independence. Given the volatile nature of the global political landscape, the supply and price of fossil fuels can undergo drastic changes rapidly, leading to a significant increase in feedstock prices. In contrast, locally grown biomass is relatively immune to such uncertainties.

## 1.5 Commercial attraction

Gasification is a valuable method for converting various types of fuels, including waste and low-cost options like biomass, coal, and petcoke, into high-value chemicals such as methanol. Industries and businesses, particularly in the energy sector, find biomass particularly attractive. Here are some reasons why [35]:

1. The cost of cleaning flue gas downstream of a gasification plant is typically lower compared to that of a coal-fired plant.
2. Gasifier plants offer polygeneration capabilities, providing steam for processes, electricity for the grid, and gas for synthesis, along with producing elemental sulfur as a by-product for high-sulfur fuel.

3. Integrated Gasification Combined Cycle (IGCC) plants can achieve higher overall efficiency (38-41%) for power generation compared to combustion-based Rankin cycle plants with a steam turbine.
4. IGCC plants can capture and store CO2 (Carbon Capture and Storage, CCS) at about half the cost of traditional pulverized coal (PC) plants. Other gasification applications, such as producing transport fuel or chemicals, may have even lower CCS costs.
5. Process plants that typically use natural gas as feedstock can switch to locally available biomass or organic waste, reducing reliance on imported natural gas, which is prone to supply and price fluctuations.
6. Gasification-based power plants boast much lower total water consumption compared to conventional power plants , and they can be engineered to recycle their process water. This efficiency in water usage makes gasification technology a staple in zero-emission plants.
7. Furthermore, gasification plants emit significantly fewer major air pollutants like sulfur dioxide (SO2), nitrogen oxides (NOx), and particulates.
8. Moreover, an IGCC plant produces lower CO2 emissions per megawatt-hour (MWh) compared to a combustion-based steam power plant.

## 1.6 Description of some biomass conversion processes

The following section presents a brief description of reactions that take place in different thermal conversion processes of biomass.

### *1.6.1 Torrefaction*

Torrefaction is a thermal treatment process carried out in an inert atmosphere at temperatures ranging from 200 to 300 °C. Its primary purpose is to alter the chemical properties of biomass. This process is endothermic, which means it absorbs energy to initiate and maintain the transformation [36].

$$C_nH_mO_p + heat \rightarrow char + CO + CO_2 + H_2O + condensable\ vapors \qquad 1.15$$

### *1.6.2 Gasification*

Gasification involves converting solid or liquid feedstock into a convenient gaseous fuel or chemical feedstock that can be used for energy generation or the production of valuable chemicals. While gasification and combustion are closely related thermochemical processes, they differ fundamentally.

In gasification, energy is stored in the chemical bonds of the product gas, whereas combustion releases energy by breaking these bonds. During gasification, hydrogen is added to and carbon is stripped away from the hydrocarbon feedstock, resulting in gases with a higher hydrogen-to-carbon (H/C) ratio. Conversely, combustion oxidizes hydrogen and carbon into water and carbon dioxide, respectively. A typical biomass gasification process may involve the following steps [37]:

- Drying
- Pyrolysis
- Combustion
- Gasification

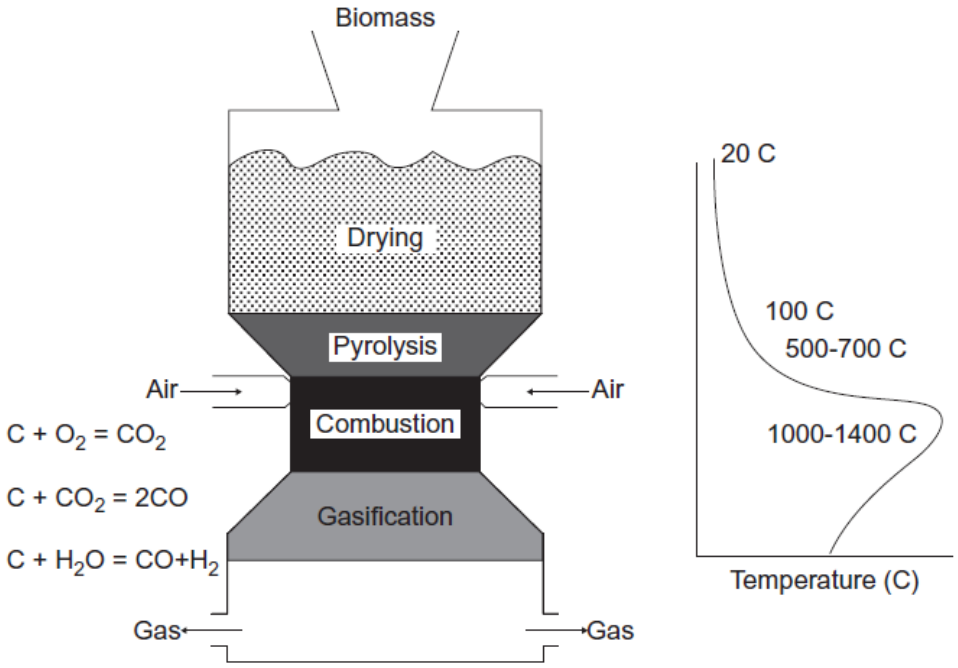


Figure 1.6 Gasification reactions in a downdraft gasifier [29]

Table below lists some of the important chemical reactions taking place in a gasifier.

Table 1.7 Typical gasification reactions at 25 °C

| Type of reaction | Title | Reaction | Reference |
|---|---|---|---|
| Carbon reactions | R1 (Boudouard) | $C+CO_2 \leftrightarrow 2CO$ +172 kJ/mol | [38] |
| | R2 (water-gas or steam) | $C+H_2O \leftrightarrow CO+H_2$+131 kJ/mol | [29,39] |
| | R3 (hydrogasification) | $C+2H_2 \leftrightarrow CH_4$ -74.8 kJ/mol | [29,39] |
| | R4 | $C+0.5O_2 \leftrightarrow CO$ -111 kJ/mol | [29] |
| Oxidation reactions | R5 | $C+O_2 \leftrightarrow CO_2$ -394 kJ/mol | [38] |
| | R6 | $CO+0.5O_2 \leftrightarrow CO_2$ -284 kJ/mol | [29] |
| Shift reaction | R7 | $CO+H_2O \leftrightarrow CO_2+H_2$ -41 kJ/mol | [38–40] |
| Methanation reactions | R8 | $2CO+2H_2 \leftrightarrow CH_4+CO_2$ -247 kJ/mol | [29] |
| | R9 | $CO+3H_2 \leftrightarrow CH_4+H_2O$ -206 kJ/mol | [14] |
| Steam-reforming reactions | R10 | $CH_4+H_2O \leftrightarrow CO+3H_2$ +206 kJ/mol | [29] |
| | R11 | $CH_4+0.5O_2 \leftrightarrow CO+2H_2$ -36 kJ/mol | [29] |

Before delving into the process steps of gasification, it's essential to discuss the gasifying medium. Biomass gasification necessitates a gasifying medium to produce synthesis gas. The main gasifying agents utilized for gasification are oxygen, steam, and air. While oxygen is commonly employed, it's mainly used for combustion or partial gasification within the gasifier.

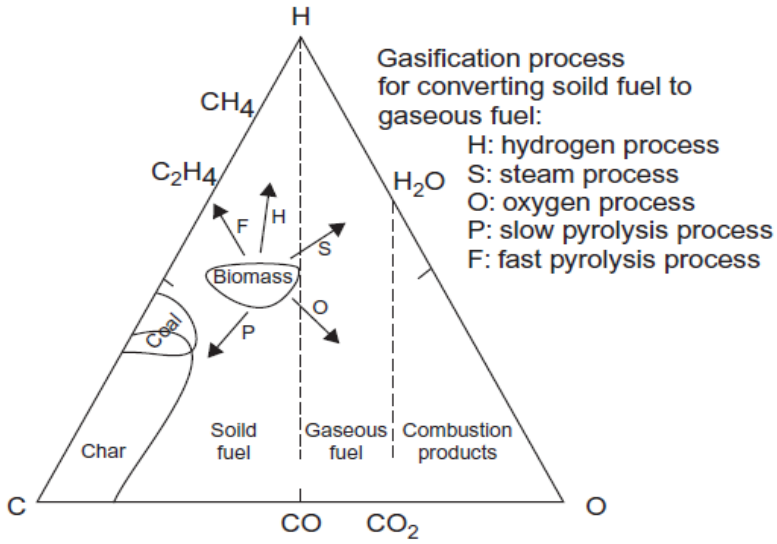


Figure 1.7 Ternary diagram

It can be introduced either in its pure form or via air. The heating value and composition of the gas produced in a gasifier greatly depend on the type and quantity of the gasifying agent utilized.

Ternary diagram (refer to **Fig.1.7**) depicting carbon, hydrogen, and oxygen showcases the conversion pathways leading to the formation of various products in a gasifier.

When oxygen serves as the gasifying agent, the conversion pathway shifts towards the oxygen corner of the diagram. The resulting products include carbon monoxide (CO) for lower oxygen levels and carbon dioxide (CO2) for higher oxygen levels. If the oxygen quantity surpasses a certain stoichiometric amount, the process transitions from gasification to combustion, yielding "flue gas" instead of "fuel gas," which contains no residual heating value. Moving towards the oxygen corner during gasification leads to a decrease in hydrogen content and an increase in carbon-based compounds like CO and CO2 in the product gas.

In contrast, if steam is utilized as the gasification agent, the process moves upwards towards the hydrogen corner in Fig.1.7. Consequently, the product gas contains a higher proportion of hydrogen per unit of carbon, resulting in an elevated H/C ratio.

The choice of gasifying agent also impacts the heating value of the product gas. For instance, if air is used instead of oxygen, the nitrogen present in it dilutes the product gas, reducing its heating value [41].

According to Table 1.8, oxygen gasification yields the highest heating value, followed by steam and air gasification. Air, functioning as the gasification medium, produces a product gas with the lowest heating value primarily due to the dilution effect of nitrogen.

Table 1.8 Differente gasifying medium

| Gasifying medium | Heating value (MJ/kg biomass) | Reference |
|---|---|---|
| Oxygen | 15-17 | [40] |
| Air | 4-8 | [42] |
| Steam | 18 | [39] |

### *1.6.2.a Drying*

During this stage, moisture in the biomass evaporates without undergoing any chemical breakdown, and this highly heat-absorbing step occurs within a temperature range of 100 to 120°C. A lower moisture content in the biomass allows for higher temperatures in the reduction phase, resulting in more efficient conversion of coal into synthesis gas. However, excessive

dryness in the biomass is undesirable for gasification because moisture content affects the hydrogen-to-carbon ratio in the syngas, thereby impacting its heating value. To ensure effective gasification, the moisture content in the biomass should not exceed 25%. Additionally, reducing the particle size decreases the time required for heat conduction and moisture diffusion within the particle, with the drying process being almost instantaneous in fluidized bed or entrained bed gasifiers [43].

### *1.6.2.b Pyrolysis*

During pyrolysis, the larger hydrocarbon molecules found in biomass are decomposed into initial outcome that consists of condensable gases and solid char. These condensable gases can further decompose into noncondensable gases like carbon monoxide (CO), carbon dioxide ($CO_2$), hydrogen ($H_2$), and methane ($CH_4$), as well as liquid and char (see Figure 1.8). This decomposition process involves a combination of gas-phase homogeneous reactions and gas-solid-phase heterogeneous thermal reactions. In gas-phase reactions, the condensable vapor undergoes cracking to form smaller molecules of noncondensable permanent gases such as CO and CO2.char [7].

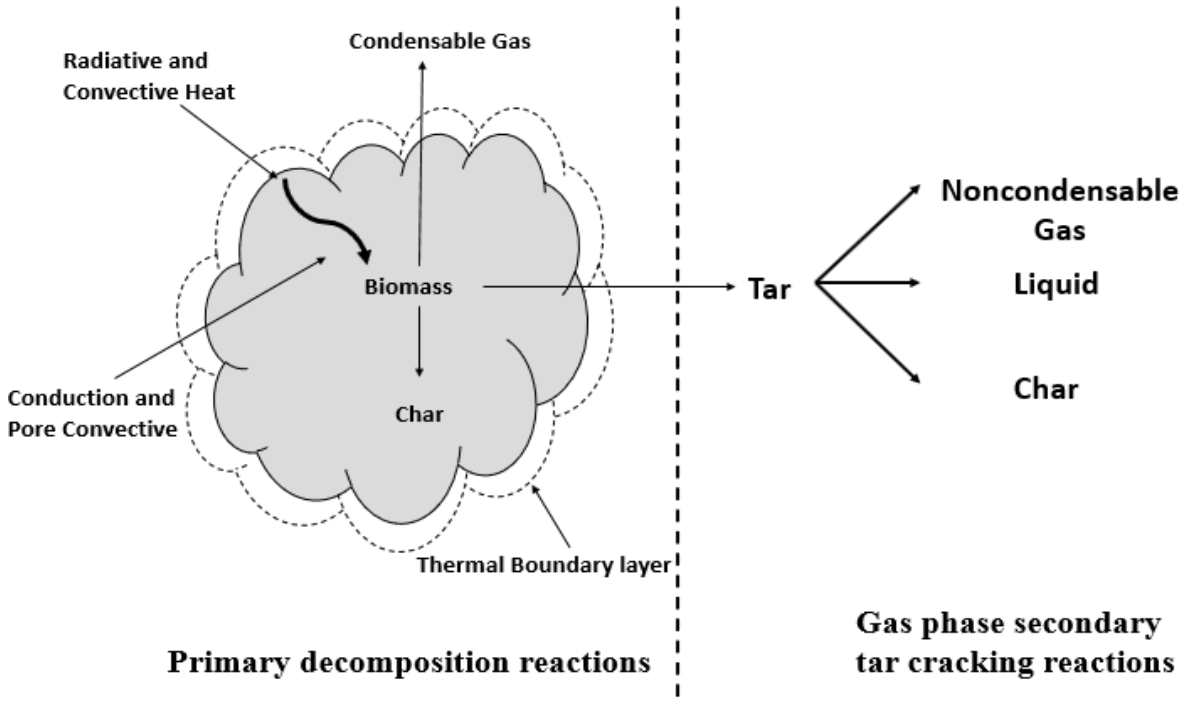


Figure 1.8 Pyrolysis process in a biomass particle .

Typically, pyrolysis takes place within a high temperature range of 600–900°C, with low heating rates and extended residence times to yield a hydrogen-enriched syngas efficiently. The operational conditions of pyrolysis can be classified into three stages: slow pyrolysis, fast pyrolysis, and flash pyrolysis [44].

$$C_nH_mO_p + heat \rightarrow \sum_{Liquid} C_aH_bO_c + \sum_{Gas} C_xH_yO_z + \sum_{Solid} C \qquad (1.16)$$

### *1.6.3 Combustion of carbon*

In the following discussion, we'll consider simple carbon as the starting material and present the chemical reaction to demonstrate the conversion process. In the reaction equations, a positive sign on the right side ($+Q\ kJ/kmol$) indicates that heat is absorbed during the reaction, while a negative sign ($-Q\ kJ/kmol$) signifies heat release.

When 1 kilomole of carbon undergoes complete combustion in sufficient air or oxygen, it generates 394 (MJ) of heat and produces carbon dioxide. This process represents a combustion reaction (R5).

$$C+O_2 \rightarrow CO_2 \qquad -393,770 \text{ kJ/kmol} \qquad (1.17)$$

#### *1.6.3.a Gasification (Reduction)*

Looking at the science behind it, gasification is the process of turning the char produced during pyrolysis into synthesis gas at high temperatures with the help of an oxidizing agent. Ideally, all the volatile substances created during pyrolysis turn into carbon dioxide and water vapor. This happens through two different reactions in the reduction zone.

- Boudouard reaction (R1 Table 1.7)

$$C+CO_2 \leftrightarrow 2CO \qquad \Delta H = 172 \text{ kJ/mol} \qquad (1.18)$$

- Water gas reaction

$$C+H_2O \leftrightarrow CO+H_2 \qquad \Delta H = 131 \text{ kJ/mol} \qquad (1.19)$$

However, in practice, the volatile substances from pyrolysis are not fully oxidized. Their existence in the reduction zone adds to the number of competing reactions, including a heterogeneous reaction:

- Hydrogasification reaction (R3 Table 1.7)

$$C+2H_2 \leftrightarrow CH_4 \qquad \Delta H = -74.8 \text{ kJ/mol} \qquad (1.20)$$

Additionally, there are two homogeneous reactions occur among the gasification products.

- Shift reaction ( R7 Table 1.7)

$$CO+H_2O \leftrightarrow CO_2+H_2 \qquad \Delta H = -41 \text{ kJ/mol} \qquad (1.21)$$

- Steam reforming reaction (R10 Table 1.7)

$$CH_4+H_2O \leftrightarrow CO+3H_2 \qquad \Delta H = 206 \text{ kJ/mol} \qquad (1.22)$$

## 1.7 Gasification processes in reactors

Gasification reactions in reactors vary depending on the type of gas-solid contacting reactors employed. The following sections provide a brief overview of this process as it unfolds in some primary reactor types.

### *1.7.1 Fixed/Moving-bed reactor*

In gasifiers like entrained-flow and fluidized-bed types, the gasifying medium carries the fuel particles through the reactor. However, in fixed-bed gasifiers, the fuel sits on a grate and moves downward as a plug. These gasifiers are also known as moving bed due to this movement. They are attractive because they can be made inexpensively in small sizes. Many small-scale moving-bed biomass gasifiers are used globally for this reason [45].

Fixed-bed or moving-bed gasifiers can be categorized into three main types:

1. Updraft gasifier.
2. Downdraft gasifier.
3. Crossdraft. gasifier.

Their characteristics are compared in Table1.9 below:

Table 1.9 Characteristics of fixed-bed gasifiers [46]

| **Fuel (wood)** | **Updraft gasifier** | **Downdraft gasifier** | **Crossdraft. Gasifier** |
|---|---|---|---|
| Moisture wet basis (%) | 60 max | 25 max | 10-20 |
| Dry-ash basis (%) | 25 max | 6 max | 0.5-1.0 |
| Ash melting temperature (°C) | >1000 | >1250 | |
| Size (mm) | 5-100 | 20-100 | 5-20 |
| Gas exit temperature (°C) | 200-400 | 700-900 | 1250 |
| Tar (g/N $m^3$) | 30-150 | 0.015-3.0 | 0.01-0.1 |
| Gas LHV (MJ/N $m^3$) | 5-6 | 4.5-5.0 | 4.0-4.5 |

### *1.7.1.a Updraft gasifiers*

An updraft gasifier is one of the oldest and simplest designs used for gasification. In this design (see Figure 1.9), the gasification medium, which can be air, oxygen, or steam, moves upward while the bed of fuel moves downward. This creates a counter-current flow of gas and solids. The gas produced exits from near the top of the gasifier. The gasifying medium enters the bed through a grate or distributor, where it encounters the hot bed of ash. The ash then falls through the grate, which is often designed to move, such as rotating or reciprocating, especially in larger units, to help with ash removal.

Updraft gasifiers are suitable for biomass with high ash content (up to 25%) and high moisture content (up to 60%). They are also suitable for fuels with low volatility, like charcoal. Updraft gasification is particularly suitable for direct firing applications, where the produced gas is burned in a furnace or boiler without needing cleaning or cooling. In this process, the tar produced doesn't require cleaning.

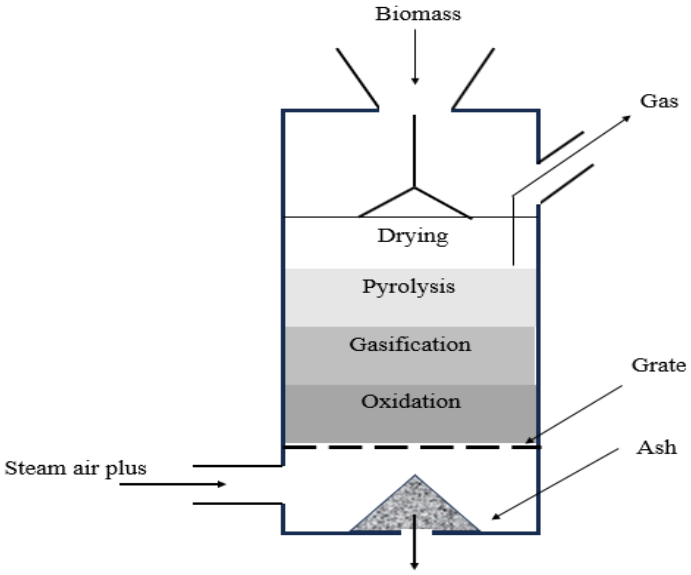


Figure 1.9 Schematic of an updraft gasifier [47]

### *1.7.1.b Downdraft gasifiers*

A downdraft gasifier operates as a co-current reactor where air enters the gasifier from a specific height below the top. The gas produced flows downward, hence the name "downdraft," and exits from the lower section of the gasifier through a bed of hot ash. This configuration ensures that the gas passes through a high-temperature zone of hot ash, which promotes the cracking of tar present in the product gas.

In a downdraft gasifier, air enters from nozzles positioned around the gasifier's periphery (Figure 1.11) and moves downward. It encounters pyrolyzed char particles, creating a combustion zone with temperatures typically around 1200 to 1400°C (see figure 1.12). The gas then continues to descend through the bed of hot char particles, where gasification occurs. The ash produced is carried out with the gas and is collected at the bottom of the reactor.

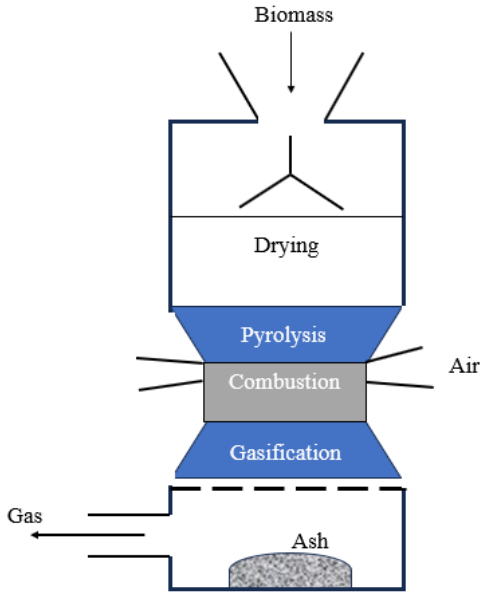


Figure 1.10 Schematic of a throated-type downdraft gasifier [7].

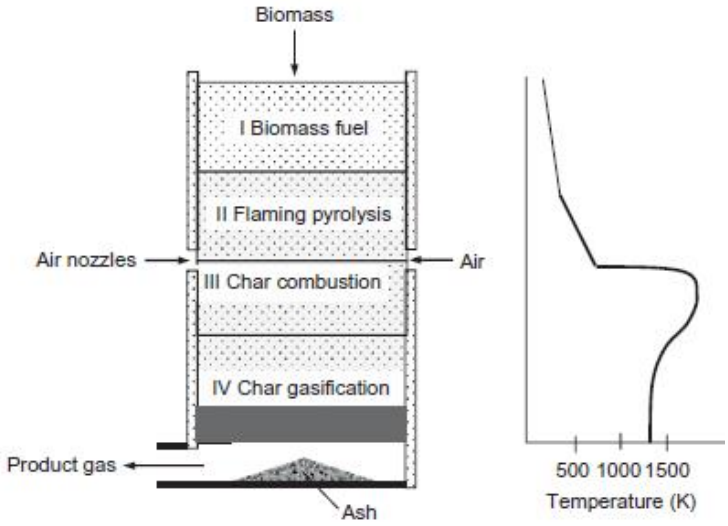


Figure 1.11 Schematic of the operation of a throatless downdraft gasifier. Temperature gradient along the height shown at the right [29].

Downdraft gasifiers are particularly suitable for applications with internal-combustion engines that require cleaner gas. The suction from the engine draws air through the fuel bed, producing gas as a result. The low tar content (typically 0.015 to 3 g/Nm$^3$) in the product gas makes them advantageous for use with internal-combustion engines. Additionally, downdraft gasifiers

require a shorter time (approximately 20 to 30 minutes) to ignite and reach operating temperature compared to updraft gasifiers.

### *1.7.1.c Crossdraft gasifier*

A Crossdraft gasifier operates as a cocurrent moving-bed reactor where fuel is introduced from the top and air is injected through a nozzle located at the side of the gasifier. This type of gasifier is primarily utilized for gasifying charcoal with very low ash content. Unlike downdraft and updraft gasifiers, the product gas is released from the sidewall opposite to where the air enters for gasification, hence it's also known as a Sidedraft gasifier.

High-velocity air enters the gasifier through a nozzle positioned at a certain height above the grate (figure 1.13). Excess oxygen in front of the nozzles aids in the combustion (oxidation) of part of the char, generating a zone with very high temperatures (above 1500 degrees Celsius). The remaining char is then gasified to carbon monoxide downstream in the subsequent zone. The product gas exits from the opposite side of the gasifier. Heat from the combustion zone is conducted around the pyrolysis zone, allowing the fresh biomass to undergo pyrolysis as it pases through.

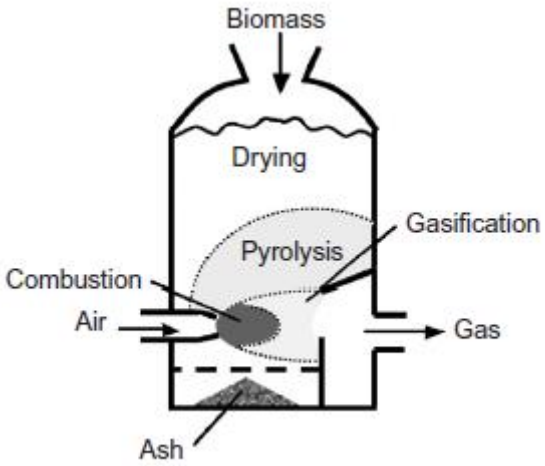


Figure 1.12 Schematic of a Crossdraft gasifier[14].

Crossdraft gasifiers are commonly used in small-scale biomass units. One of their key characteristics is a relatively small reaction zone with low thermal capacity, resulting in faster response times compared to other moving-bed types. Moreover, the start-up time is much shorter (about 5 to 10 minutes) compared to downdraft and updraft units. These features enable

a crossdraft gasifier to effectively respond to load changes when directly powering an engine. Due to its low tar production (typically 0.01 to 0.1 g/Nm$^3$), a crossdraft gasifier requires a relatively simple gas-cleaning system.

### *1.7.2 Fluidized-bed gasifiers*

Fluidized-bed gasifiers are recognized for their exceptional mixing and consistent temperature distribution. In these gasifiers, a bed of granular solids, known as bed materials, is maintained in a semi-suspended state (fluidized state) by the passage of the gasifying medium through them at specific velocities. The superior mixing of gas and solids, coupled with the substantial thermal capacity of the bed, makes fluidized-bed gasifiers less sensitive to variations in fuel quality. Additionally, the uniform temperature distribution reduces the likelihood of fuel agglomeration.

The fluidized-bed design is particularly beneficial for biomass gasification. The production of tar in fluidized-bed gasifiers falls between that of updraft and downdraft, typically averaging around 10 g/Nm$^3$. There are two main types of fluidized-bed gasifiers: bubbling and circulating.

#### *1.7.2.a Bubbling fluidized-bed gasifier*

The bubbling fluidized-bed gasifier, pioneered by Fritz Winkler in 1921, stands as one of the earliest commercial applications of fluidized beds. It has been widely employed for coal gasification for many years (see Figure 1.14), and it has become a favoured option for biomass gasification. Numerous designs of bubbling fluidized-bed gasifiers are operational, catering to various needs and conditions. Due to their suitability for medium-sized units (up to 25 MW$_{th}$), many biomass gasifiers operate on the bubbling fluidized-bed principle.

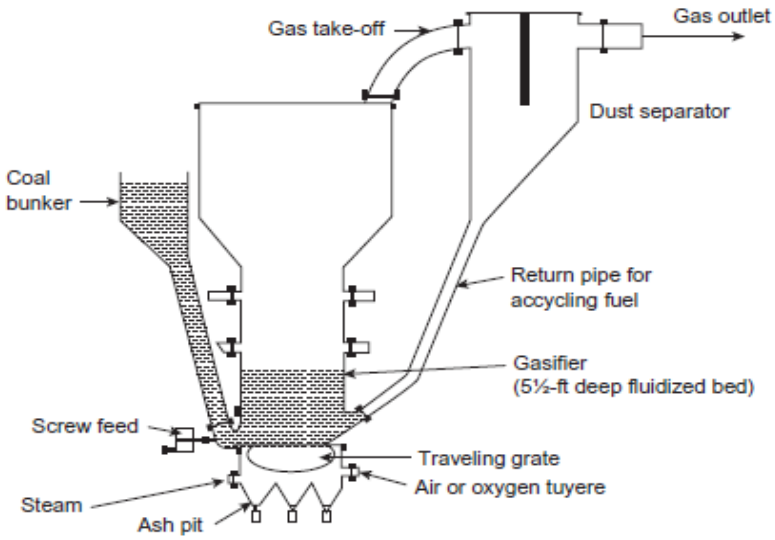


Figure 1.13 A schematic of the original Winkler bubbling fluidized-bed gasifier [48]

Bubbling-bed gasifiers can be classified based on operating conditions into low-temperature and high-temperature types and can function at either atmospheric or elevated pressures. In this common type of fluidized bed, biomass, crushed to less than 10 mm, is introduced into a bed of hot materials. These materials are fluidized with steam, air, oxygen, or their combination, depending on the chosen gasification medium. Any ash produced from the fuel or associated inorganic materials is easily drained from the bottom of the bed[48].

To prevent ash fusion and agglomeration, the bed temperature is typically kept below 980°C for coal and below 900°C for biomass. The gasifying medium may be supplied in two stages: the first stage maintains the fluidized bed at the desired temperature, while the second stage, added above the bed, converts any entrained unreacted char particles and hydrocarbons into useful gas.

### *1.7.2.b Circulating fluidized-bed gasifier*

A circulating fluidized-bed (CFB) gasifier holds particular promise for biomass gasification due to its ability to provide a prolonged gas residence time. This type of gasifier is especially well-suited for fuels with high volatile content. A typical CFB reactor consists of a riser, a cyclone, and a solid recycle device (as depicted in Figure 1.14), where the riser serves as the gasifier reactor.

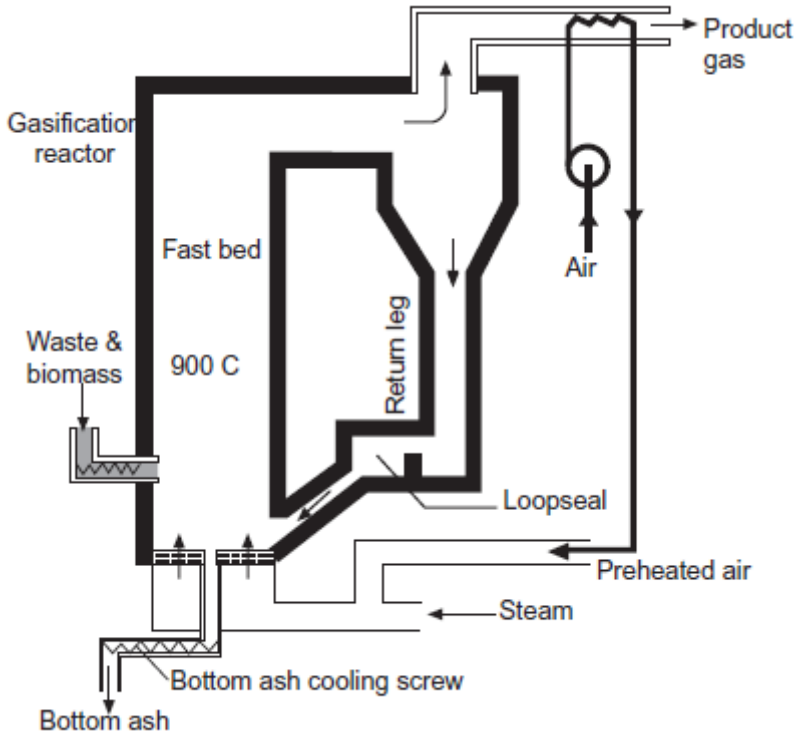


Figure 1.14 Circulating fluidized bed gasifier [49]

In a CFB gasifier, the solids are dispersed throughout the tall riser, enabling an extended residence time for both the gas and the fine particles. The fluidization velocity in a CFB is considerably higher (ranging from 3.5 to 5.5 m/s) compared to that in a bubbling bed (which typically ranges from 0.5 to 1.0 m/s). Additionally, there is significant migration of solids out of the CFB riser, which are then captured and continuously returned to the base of the riser for recirculation.

### *1.7.3 Entrained-flow gasifiers*

The entrained-flow gasifier stands as the most successful and widely adopted type for large-scale gasification of coal, petroleum coke, and refinery residues. This gasifier type is particularly well-suited for most coal types, excluding low-rank coal such as lignite and biomass due to their high moisture content. Additionally, high-ash coal is less desirable because the efficiency of cold-gas diminishes as the ash content increases. For coal fed as slurry, the economic limit for ash content is around 20%, while for dry feed, it's about 40%.

However, the suitability of entrained-flow gasification for biomass raises questions for several reasons. The short residence time (only a few seconds) in entrained-flow reactors necessitates finely ground fuel, which poses challenges, especially when dealing with fibrous biomass [50].

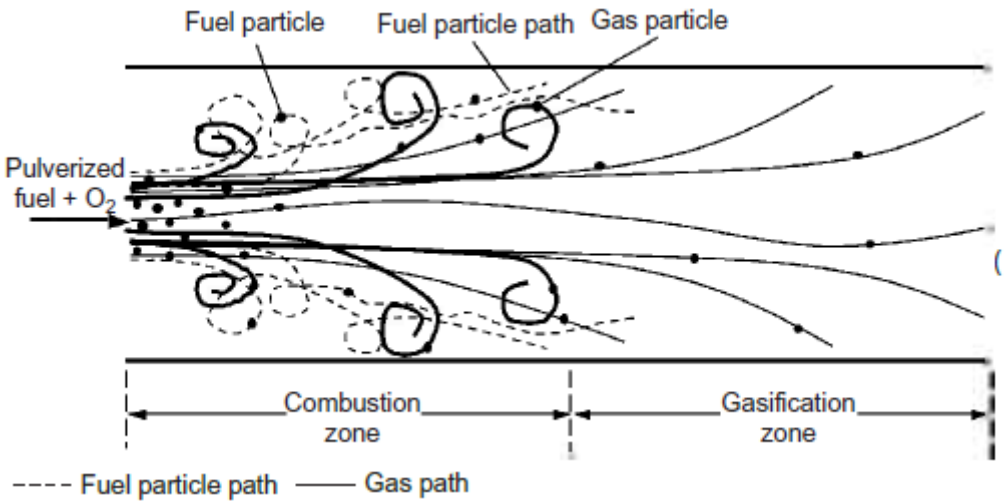


Figure 1.15 Simplified schematic of gas solid flow in an entrained-flow [7]

In an entrained-flow gasifier, a simplified sketch illustrates its working principle. A high-velocity jet forms a recirculation zone near the entry point. Fine fuel particles are rapidly heated by radiative heat from the hot walls of the reactor chamber and from the hot gases downstream, initiating combustion in excess oxygen. The majority of the fuel is consumed near the entrance zone through devolatilization, where temperatures may soar as high as 2500 °C.

## 1.8 Application of gasification for methanol production

Interest in biomass as a chemical feedstock is on the rise due to its renewable nature and carbon-neutral characteristics. There's a noticeable shift towards the production of "green chemicals" and "green fuels," which are derived from carbon-neutral biomass sources.

With the advancement of the chemical industry and the implementation of new environmental regulations, the utilization of charcoal for the purification of industrial wastes has significantly increased. Gasification and pyrolysis stand out as effective and robust methods for converting biomass (or other fuels) into energy, chemicals, and transportation fuels. Additionally, carbonization and torrefaction play crucial roles in converting biomass into effective adsorbents and reducing agents. These processes contribute to the sustainable utilization of biomass resources and align with efforts to mitigate environmental impact.

Methanol ($CH_3OH$) serves as a significant raw material for manufacturing transportation fuels and various chemicals. The conversion of methanol into gasoline constitutes a well-established industrial process. Methanol production involves synthesizing syngas, a mixture of carbon monoxide (CO) and hydrogen ($H_2$), typically in the presence of catalysts (refer to Figure 1.17) (Higman & van der Burgt, 2008a):

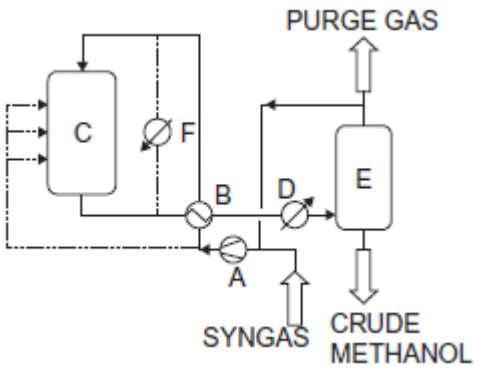


Figure 1.16 Methanol production [51].

$$CO + 2H_2 \overset{Catalyst}{\longleftrightarrow} CH_3OH \qquad -91\ KJ/mol \qquad (1.23)$$

Methanol synthesis is an exothermic reaction influenced by both temperature and pressure. The equilibrium concentration of methanol in this reaction increases with pressure within the range of 50 to 300 atmospheres but decreases with temperature within the range of 240 to 400 degrees Celsius. Without a suitable catalyst, the actual yield of methanol is very low. Therefore, catalysts based on zinc (Zn), copper (Cu), aluminum (Al), and chromium (Cr) are commonly employed.

Syngas, which serves as the feedstock for methanol production, can be generated from biomass through either thermal or hydrothermal gasification. However, one of the most commonly utilized commercial methods involves using natural gas (CH4) as the feedstock. This process employs steam reforming of methane, as illustrated in the equation below:

$$CH_4 + H_2O \rightarrow CO + 3H_2 \qquad + 206\ KJ/mol \qquad (1.24)$$

We observe here that for every mole of carbon monoxide (CO) produced, three moles of hydrogen ($H_2$) are generated. However, in the methanol synthesis reaction (Equation (1.26)), only two moles of hydrogen are required for every mole of carbon monoxide. Consequently, there is an excess of one hydrogen molecule for each mole of methanol produced. In this scenario, if carbon dioxide ($CO_2$) is available, it can be utilized in the following reaction to generate an additional methanol molecule, utilizing the surplus hydrogen[52]:

$$CO_2 + 3H_2 \overset{Catalyst}{\longleftrightarrow} CH_3OH + H_2O \qquad \text{- 50KJ/mol} \qquad (1.25)$$

Methanol synthesis can occur under both high pressure (above 30 MPa, at temperatures between 300°C to 400°C) and low pressure (between 5 to 10 MPa, at temperatures from 220°C to 350°C) conditions.

In the high-pressure process, syngas is initially compressed. The pressurized syngas is then introduced into either a fixed- or fluidized-bed reactor for synthesis in the presence of a catalyst at pressures ranging from 300 to 350 atmospheres and temperatures from 300 to 400 °C. A fluidized bed offers continuous catalyst regeneration and efficient heat removal. The catalyst typically used is an oxide of zinc (Zn) and chromium (Cr). The resulting product is subsequently cooled to condense the methanol. Due to low conversion rates, the unconverted syngas is recycled back into the reactor for further conversion. Currently, the most commonly used catalyst consists of a mixture of copper, zinc oxide, and alumina [47].

The low-pressure process resembles the high-pressure one but operates at lower pressures and temperatures. In one variant, a fixed bed containing a Cu/Zn/Al catalyst is employed at pressures of 5 to 10 MPa and temperatures of 220°C to 290°C.

Another option, liquid-phase synthesis, is still under development but shows promise for achieving significantly higher conversion rates (over 90%) compared to around 20% for the high-pressure process. In this approach, syngas is mixed with recycled gas and introduced into a slurry of catalysts in a suitable solvent. The compressed syngas mixture is then heated to the

desired reactor inlet temperature, typically around 220 to 230 degrees Celsius. In a cold-quench operation, only a portion of the feed gas is preheated, while the remainder is used to cool the product gas between individual catalyst layers [53].

## 1.9 Conclusion

This chapter has outlined the critical role of biomass as a renewable energy resource and its immense potential in fostering sustainable energy solutions. Biomass, derived from organic materials such as agricultural residues, forestry waste, and other biodegradable materials, represents a versatile feedstock for energy production. Its vast availability and renewability make it an attractive alternative to fossil fuels, particularly in the context of global efforts to combat climate change and reduce carbon emissions. The discussion of biomass and its products highlighted its diverse forms, including solid, liquid, and gaseous derivatives, each with unique applications in energy and industrial sectors.

Understanding the properties of biomass is essential for optimizing its utilization in energy systems. Variability in composition, moisture content, and calorific value significantly influences the choice of conversion technology and its efficiency. These intrinsic characteristics necessitate tailored approaches to biomass processing, ensuring that its energy potential is fully harnessed while minimizing waste and emissions. This variability also underscores the importance of pre-treatment and conditioning processes, which enhance biomass suitability for specific conversion methods.

The motivation for biomass conversion technologies lies in addressing the growing demand for cleaner and more sustainable energy solutions. Biomass offers the dual advantage of energy generation and carbon sequestration, positioning it as a critical component of the circular economy. Technologies such as combustion, pyrolysis, and gasification enable the transformation of biomass into energy carriers like heat, electricity, bio-oil, and syngas. Among these, gasification stands out due to its high efficiency and adaptability.

The detailed exploration of gasification processes in reactors illustrated its versatility in handling different feedstocks and producing valuable syngas. This syngas, a mixture of carbon monoxide, hydrogen, and other gases, serves as a precursor for various industrial applications, including chemical synthesis and power generation. Gasification reactors, such as fixed-bed, fluidized-bed, and entrained-flow systems, each have unique designs that cater to specific operational requirements. These reactors not only enhance conversion efficiency but also allow for better control of product quality.

One of the most significant applications of gasification is in methanol production, a process that demonstrates the industrial relevance of biomass-based energy systems. Methanol, a key chemical in the production of plastics, resins, and fuels, can be synthesized from syngas derived from biomass. This pathway offers a sustainable and low-carbon alternative to conventional methanol production, which typically relies on natural gas or coal. By integrating biomass into methanol synthesis, industries can reduce their carbon footprint and contribute to global sustainability goals.

The commercial attraction of biomass gasification lies in its ability to provide economically competitive and environmentally friendly solutions. With growing regulatory pressures and societal demand for greener energy systems, the adoption of biomass gasification technologies is becoming increasingly feasible. Investments in research, development, and scaling of these technologies are creating opportunities for industries to capitalize on biomass as a sustainable energy source. Additionally, the potential for integrating gasification with carbon capture and utilization (CCU) technologies further enhances its viability as a cornerstone of the renewable energy landscape.

In summary, this chapter has provided a comprehensive understanding of biomass, its properties, conversion technologies, and the specific significance of gasification. By exploring its application in methanol production and emphasizing its commercial relevance, we have established a solid foundation for the subsequent chapters. The focus will now shift to the ambitious Reffect Africa Project, a groundbreaking initiative aimed at leveraging biomass resources to promote sustainable energy solutions across the African continent. Additionally, we will describe our active participation in this large-scale project, detailing our contributions, objectives, and role in addressing the complex challenges it aims to solve.

# Chapter 2 Reffect Africa project

## 2.1 Introduction

The number of people without electricity in Africa is projected to rise in 2020, reversing a six-year trend of improvement. Significant progress had been made, with the population lacking electricity dropping from nearly 860 million in 2018 to 770 million in 2019—a notable achievement in recent years. However, the Covid-19 pandemic has stalled these advancements [54].

Reliable electricity is a cornerstone of any modern economy, particularly in the era of digital transformation. For African countries aiming to drive economic growth and transformation, ensuring dependable electricity supply must be a top priority. Yet, access to electricity alone is insufficient; many households and businesses face daily power outages. Even when electricity is available, frequent brownouts hinder its effective use, limiting its impact on end users.

In order to tackle this, the present proposal REFFECT AFRICA will demonstrate innovative, reliable and adapted sustainable energy solutions based on the valorisation of biomass wastes from agriculture and the food industry through biomass gasification.

The REFFECT AFRICA initiative aims to adapt and optimize biomass gasification technologies to process a diverse range of biomass wastes prevalent across different regions. These include olive mill residues, almond hulls and husks, millet, rice, sorghum, peanut waste, sugarcane bagasse, and more. The project will establish three full-scale demonstrators in Morocco, Ghana, and South Africa to address the energy needs of both urban and rural communities, considering varying socio-economic conditions.

Comprehensive Life Cycle Analyses (LCAs) will be conducted for each supply chain, evaluating the climate adaptation and mitigation potential of the technology against alternative solutions within African social, economic, and environmental contexts. REFFECT AFRICA aims to advance renewable energy development by offering tailored solutions for both on-grid and off-grid communities, integrating renewable energy generation, transmission, and storage systems into existing energy infrastructures.

To strengthen the water-energy-food nexus, the project will produce biochar from the gasification process, enhancing its properties to create a high-quality fertilizer for local farmers. Demonstrators will also incorporate water testing laboratories to provide essential services for assessing drinking and irrigation water quality, often unavailable in the targeted locations.

The socio-economic objectives include job creation and capacity building across Africa, with training programs for plant operators, biomass suppliers, and related stakeholders. This approach aims to foster improved public health, economic growth, and employment opportunities. Electrification, coupled with job creation, is key to enabling income-generating activities. Without it, a significant portion of the population cannot afford meaningful electricity use. By aligning electrification efforts with job creation, REFFECT AFRICA seeks to attract investments and enhance the financial sustainability of the energy sector.

The primary goal of REFFECT AFRICA is to develop, validate, and demonstrate an effective biomass valorisation technology for generating energy and biochar in three targeted African regions:

- A rural off-grid application in Ghana (in the Sawla-Tuna-Kalba District Assembly, at a school compound, which includes a small medical clinic).
- An on-grid application at a food industry in Morocco (at the premises of the olive oil mill Dar Azzaytoune in in Douar El Hachia).
- An urban application at Clairewood Bulk Market, a large-supply market connected on-grid in the eThekwini Municipality, which belongs to the city of Durban (**South Africa)**.

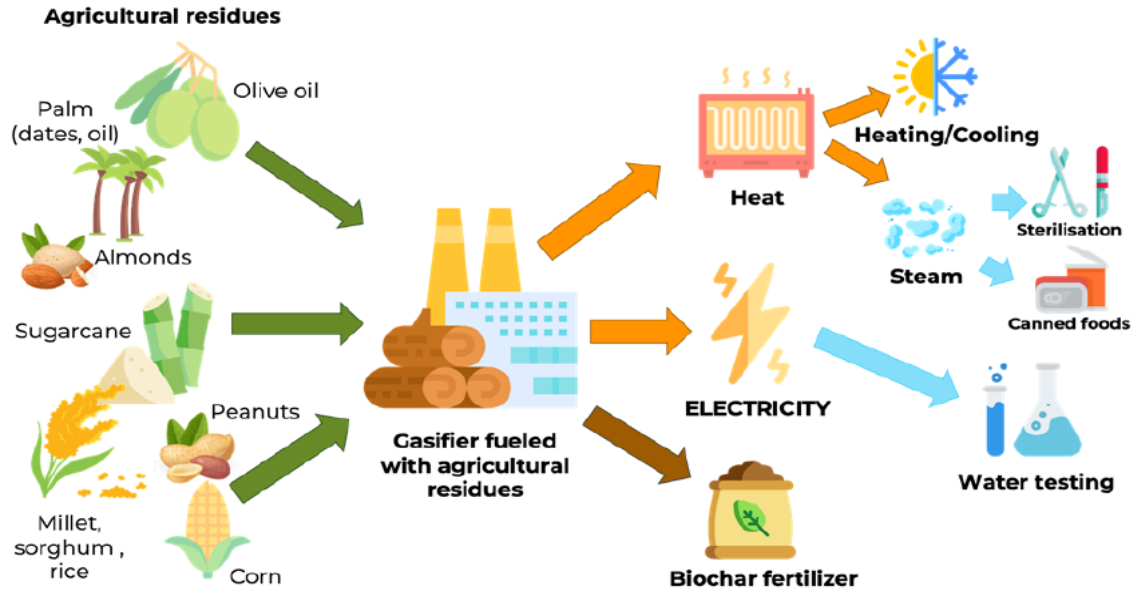


Figure 2.1 The Reffect Africa waste valorisation concept

## 2.2 Objectives

### *2.2.1 Performance objectives :*

- To develop a technology concept for in situ treatment and energetic reuse of the most important agri-food value chains: olive oil and sugarcane industries, as well as other crops such as rice, dates, almonds, corn, sorghum, millet, cassava, peanuts, etc.
- To cover the energy consumption of the three real scenarios by valorising local agri-food residues: 50% of the electricity and 80% of the heat demanded by the olive oil mill, 100% of the electricity supply in Ghana (a school and a small medical clinic) and 20% of the electrical and thermal energy demanded by the market in South Africa.
- To make the African agri-food sector self-sufficient in terms of energy supply and independent from energy price fluctuations.
- To generate new jobs, income streams and business models for the residents of these areas.

### *2.2.2 Scientific objectives*

- To update the state-of-the-art of the four most representative agri-food chains of Africa focusing on the current waste valorisation techniques and their suitability for the crops addressed.
- To identify and carry out the experimental validation of the valorisation technology in 3 real scenarios located in Africa. Assessment of the outcomes: bioenergy, biofertilizer, biochar and water treatment/production.
- To build and start operation of three water testing labs, in order to increase health and living standards in the demonstration sites.
- To establish three Living Labs in the demonstrators to allow further research and the improvement of the technologies addressed.
- To ensure the supply of biomass to the plants creating an Online Supply and Demand Marketplace.

### *2.2.3 Environmental objectives*

- To enable the broad implementation of renewable energies in Africa by using waste-to-energy approaches.
- To perform a Life Cycle Assessment (LCA) and Life Cycle Costing (LCC) analysis “from cradle-to gate” evaluating the improvements proposed: environmental and economic.

### *2.2.4 Socio-economic objectives*

- Socio- To increase access to electricity of the populations addressed.
- To reduce the energy bills (electricity and heat).
- To increase the competitiveness of the African agri-food sector and to create new jobs in the installation and operation of the REFFECT AFRICA gasification systems.
- To identify technical, vocational and educational needs of the workforce in the 11 African countries included in the consortium and to train and transfer the outcomes to local stakeholders (the unemployed, especially youth, food industry sectors, academia, policymakers, public administrations and governments and funding institutions.
- To create a new income stream for farmers as biomass suppliers to the gasifiers via the Online Supply and Demand Marketplace taking advantage of the Digital Era.
- To provide training and capacity building on new skills especially to the young and unemployed.

## 2.3 Concept

The demonstration plants developed under REFFECT AFRICA will supply electricity and heat tailored to the diverse technical and socio-economic needs of rural and urban areas in three African countries. Additionally, each plant will offer secondary services customized to the specific requirements of the locations, including biochar-based fertilizers (enhanced through methods like co-composting), heating and cooling solutions, and a water testing facility.

This comprehensive approach aims to deliver a 360º service to the host communities by providing affordable electricity generated from locally available biomass waste, enhancing soil fertility and agricultural productivity through closed nutrient loops, and improving health

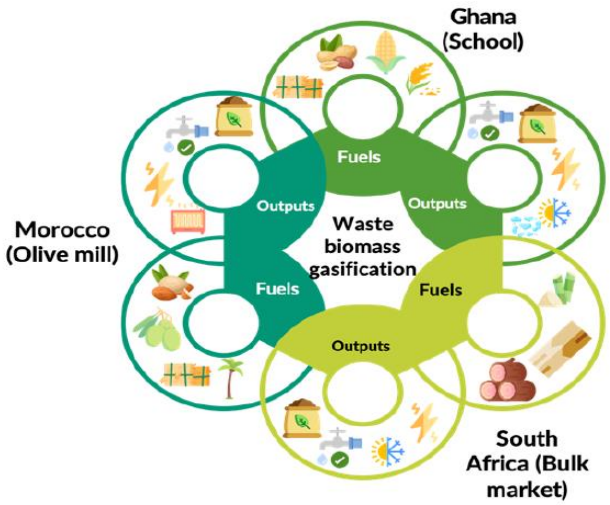


Figure 2.2 Summary of the three demonstrators, their feedstocks, and outputs

outcomes by ensuring access to safe drinking water and services such as sterilization of medical equipment.

Moreover, REFFECT AFRICA is committed to fostering job creation and skills development, equipping individuals with new competencies to build a skilled and highly employable workforce, thereby maximizing the initiative's long-term impact on community well-being and economic growth.

## 2.4 Methodology

REFFECT AFRICA is centered on the on-site and real-time demonstration of an innovative system for enhancing the gasification of agricultural and agri-food sector wastes. The project employs a multi-faceted approach to ensure success across various domains. Technically, it focuses on gasifying diverse agricultural wastes while delivering secondary benefits to the host communities, such as heating or cooling solutions, biochar production, steam for sterilization or food processing, and water and pathogen analysis. These efforts aim to close the energy-food-water cycle comprehensively.

In addition to the technical advancements, REFFECT AFRICA leverages digital tools to optimize operational and economic outcomes for plant operators and entrepreneurs. The initiative also seeks to influence policymakers to accelerate Africa’s transition to renewable energy and to train and empower a new generation of stakeholders, raising awareness about the potential of sustainable energy solutions.

Three demonstration plants will be constructed, with the locations already determined, and landowners and end-users directly engaged as key stakeholders. Each plant will address specific needs across different countries and sectors. The demonstrator coordinates are as follows: Morocco (32º11'36.4"N, -7º45'01.7"W) which has been transferred to Zouyout Essaouira Cooperative, and has been inaugurated on December 2024. Ghana (9º17'55.0"N, 2º25'45.0"W), and South Africa (29º54'50.41"S, 30º59'36.33"W). This collaborative approach ensures that local communities are actively involved in and benefit from the project's success.

In Morocco, the demonstration plant was inaugurated in December 2024 at the Zouyout Essaouira Cooperative, an olive mill located in Essaouira. The plant is designed to valorize olive mill residues, including husks, pits, dates, and pruning materials. It will generate 50% of the cooperative's electricity needs and 80% of its heat requirements. Additionally, the plant incorporates a distillation system to treat olive mill wastewater, providing access to clean water.

In Sawla, Ghana, the demonstration plant will be established at a school that offers professional training programs for boys and girls, focusing on coding and IT skills. The plant will utilize residues from local subsistence crops such as cassava, peanuts, millet, sorghum, and maize as feedstocks. The electricity generated will meet the entire demand of the school while also supporting nearby agricultural activities. This includes powering farm machinery such as water pumps for irrigation, cooling systems for fruits and vegetables, and crop-drying processes. The plant will be constructed on land owned by the Sawla District Assembly, with its location already identified.

In Durban, South Africa, the demonstrator will be installed at the Clairwood Bulk Market, a key supply hub for supermarkets, restaurants, and local farmers. This location offers ample space for building the valorisation plant and co-composting biochar produced through the gasification process. Farmers who supply the market will benefit directly, as the biochar can be sold to them as-is or co-composted with vegetable residues to create a high-quality biofertilizer. The plant will feature a trigeneration setup, providing electricity, heat, and cooling to the market, enhancing its operational efficiency. The site is located on land owned by the project partner, Ethekwini Municipality (ETHEK).

To achieve these outcomes, the project will begin with an initial research phase to assess the specific technological requirements of each demonstration site. This includes optimizing supply chains, selecting the most suitable plant configurations for each location, and implementing necessary transformations to ensure strong commercial performance. Based on these assessments, the three demonstration plants will be designed and constructed.

REFFECT AFRICA includes an extended demonstration phase, involving 5,000 hours of operation for each plant, during which the systems will be optimized to achieve their maximum output. Throughout this phase, the project will engage key stakeholders, including industry representatives, policymakers, farmers, and agricultural associations, to promote awareness of the centres' benefits and highlight the business opportunities they offer in rural areas. These engagements will also emphasize the advantages of adopting circular economy principles. The project aims to attract over 300 participants to its various demonstration events.

Replicability is a core objective for the consortium. To ensure the broader application of its findings, the results from the research and demonstration phases will undergo comprehensive environmental, economic, and social evaluations through Life Cycle Assessments (LCAs). These results will inform the development of methodologies for replicating REFFECT

AFRICA plants in other regions. By creating tailored business models, the project will demonstrate opportunities for both rural and urban settings, empowering entrepreneurs with actionable insights to establish their own ventures.

Additionally, the consortium plans to establish the three demonstration sites as living labs, fostering innovation through open exploration, experimentation, and evaluation. These living labs will serve as collaborative platforms where users and producers can co-create advancements. Remote access to these facilities will further enable researchers worldwide to contribute to and advance the development of gasification technologies and waste valorisation processes.

## 2.5 Ambition

Around 600 million people across the continent lack access to electricity, while approximately 730 million rely on traditional biomass combustion systems for energy. Figure 2.3 illustrates the disparities in electricity access: about 50% of West Africans, 75% of East Africans, and the majority of Southern Africans are without electricity, although in South Africa, only 15% lack access. In contrast, North Africa consumes, on average, eight times more electricity per capita compared to the rest of the continent, excluding South Africa

Currently, Africa's energy needs are met through a combination of biomass and fossil fuels. Biomass constitutes nearly half of the continent's total primary energy supply. Fossil fuels also play a significant role, with coal and natural gas each accounting for around 14% and oil contributing 22%. Regarding electricity generation, fossil fuels dominate the energy mix, comprising approximately 30% coal, 40% natural gas, and 10% oil [55]

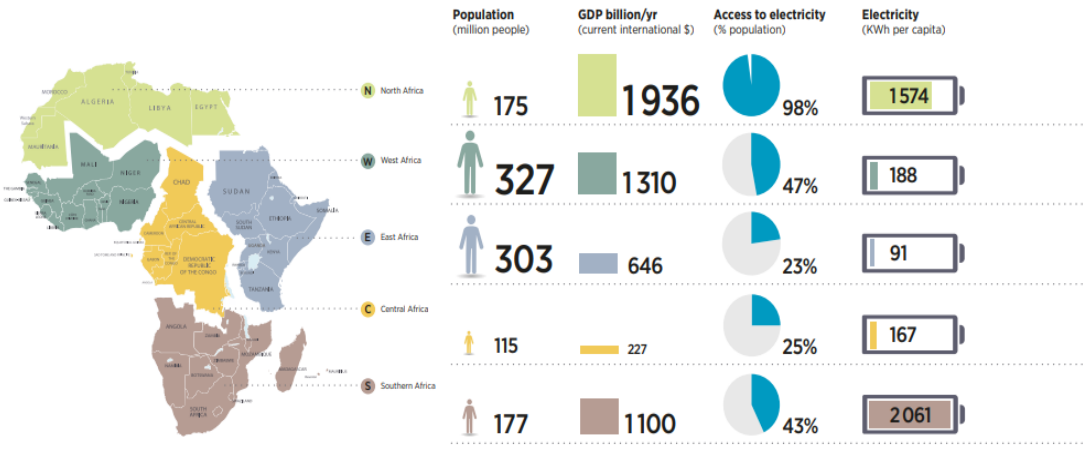


Figure 2.3 Africa's energy landscape [55]

In this context, new initiatives and projects proposing technologically robust and economically viable solutions, particularly those centered on renewable energy sources for on-grid and off-grid applications, are essential for Africa's sustainable development. Biomass gasification, especially when applied to agri-food wastes, stands out as one of the most promising methods for waste-to-energy conversion. It offers a viable alternative to fossil fuels, particularly for distributed power generation and off-grid applications[47]. Furthermore, the process yields biochar as a solid byproduct, which has significant potential as a soil amendment and fertilizer.

Gasification is a thermochemical process that converts biomass into gaseous fuels with a usable heating value via partial high-temperature oxidation. Depending on the oxidation agent used (air, oxygen, or steam), the resulting producer gas (or syngas) has various applications. Air gasification, in particular, is well-suited for power generation and can be employed in combined heat and power (CHP) systems, allowing simultaneous heat and electricity production[56]. However, systems combining gasification with boilers and steam turbines often face challenges such as high capital costs and low net electrical efficiency (10–20%), making them less attractive for small-scale applications.

Internal combustion engines and gas turbines, in contrast, offer better efficiency at small scales. These systems, however, require ultra-clean gas to prevent damage to filters and fuel injectors. Over the last decade, downdraft gasifiers have gained traction for producing green energy, particularly in remote areas where extending the electrical grid is cost-prohibitive. In these contexts, decentralized biomass CHP systems using local biomass sources can provide efficient and sustainable power solutions.

Although biomass gasification's energy efficiency (75–85%) is slightly lower than that of biomass combustion boilers (>90%), it produces fewer CO2 emissions, NOx, and particulates due to its lower reaction temperatures (<1000°C) and higher carbon conversion efficiency. Several studies illustrate the potential of biomass gasification in Africa:

Ben Hassen Trabelsi et al. [57]demonstrated that gasification of Tunisian solar-dried sewage sludge produced a high-calorific syngas, with values of 8.02 MJ/kg. Allesina et al. [58] investigated biomass gasification using cotton residues in Mozambique. A 20 kW plant achieved a net electrical efficiency of 14% and a specific consumption of 1.16 kg/kWh. Abd El-Sattar et al. [59] simulated a CHP plant in Egypt using corn stover, highlighting its potential as a local biomass resource.

Ozonoh et al. [60] conducted a techno-economic analysis of a 5 MW co-gasification power plant in South Africa, identifying coal and pine sawdust blends as the most efficient feedstock. Arranz-Piera et al. [61] provided technical and financial insights into decentralized electrification in Ghana using agricultural waste gasification.

European projects, such as RESOLIVE and OLIVEN, have demonstrated the techno-economic feasibility of downdraft gasifiers for the agri-food industry, particularly in olive oil production. However, these studies have yet to integrate a comprehensive approach combining electricity, heat, and biochar production with Life Cycle Assessment (LCA) and Life Cycle Costing (LCC). This gap underscores the need for further research and implementation of such integrated systems, particularly in regions like Africa, where renewable energy solutions are critical for sustainable development.

REFFECT AFRICA approaches the implementation of renewable energies with the potential of becoming a whole new line of services and businesses in Africa. The approach chosen will allow biomass wastes to become products, used as feedstocks of the gasifiers. The most representative biomass wastes from agrifood value chains (olive oil, dates, sugarcane, rice, almond, etc.) will be the fuel of the gasification plant. The biomass gasifier (composed of a downdraft reactor, gas cleaning and cooling system and an internal combustion engine) generates three products: electricity, heat (in the way of cooling water and exhaust gases from the engine) and biochar (around 20% of the biomass input by weight). Depending on the final application and local necessities (energy, water and/or bio-fertilizer), the demonstrator will produce the following products:

- Biochar (used directly on the soils) and/or bio-fertilizer (i.e.: through co-composting with manure from local suppliers).
- Electricity for on-grid (distributed generation) or off-grid applications. 1st and 3rd demos are on-grid applications in an operative olive oil mill (Morocco) and an urban bulk food market in South Africa; and an off-grid application in a school (2nd demo in Ghana).
- Heating: in the way of steam (sterilization, vegetable processing, cooling), hot water for cogeneration or distilled water. Here, the heat recovery unit (HRU) will be assessed and optimized.

Other by-products and business models approach proposed in REFFECT AFRICA are the following:

- Water testing.
- Biomass supply (waste biomass from the farmer's own land).
- Biomass logistics (collecting biomass from several producers and delivering it to the plant).

The common denominator in the cases chosen by the project is the need for a solution for the wastes, long studied and desired, but the lacking in funds to cover the investment, lack of technical support to adapt any system to specific circumstances or training to operate the machines after their installation have made it impossible to achieve success. REFFECT AFRICA will tackle all these obstacles and ensure success, and the creation of a new economic sector around the valorisation of agricultural waste.

## 2.6 Conclusion

Chapter 2 provided an in-depth overview of the Reffect Africa project, a transformative initiative dedicated to addressing Africa's pressing energy, environmental, and socio-economic challenges through innovative biomass utilization, the project gather more than 10 African countries such as Egypt, Tunisia, Morocco and Algeria in addition to Spain the unique country representing the EU. The objectives of the Reffect Africa project focus on transforming Africa's agri-food sector through sustainable energy solutions. It aims to valorize agricultural residues to meet energy demands, foster self-sufficiency, and create jobs. Scientifically, the project seeks to validate waste valorization technologies, establish labs, and develop a biomass supply marketplace. Environmentally, it promotes renewable energy adoption via waste-to-energy methods with life cycle assessments. Socio-economically, it enhances energy access, reduces costs, and provides training, empowering communities, particularly youth and farmers. These goals integrate technological innovation with socio-environmental impact to drive Africa's renewable energy transition.

The concept of the project involves developing demonstration plants in three African countries to provide electricity, heat, and secondary services like biochar-based fertilizers, water testing, and sterilization. The initiative enhances energy access, agricultural productivity, health, and job creation, while fostering skills development for sustainable, long-term community well-being.

Reffect Africa's methodology centers on the real-time demonstration of an innovative system for enhancing agricultural waste gasification. It employs a multi-disciplinary approach, focusing on the integration of heating, cooling, biochar production, and water treatment to close

the energy-food-water cycle. The project leverages digital tools to optimize outcomes and advocates for policy changes to accelerate Africa's renewable energy transition. Three demonstration plants in Morocco, Ghana, and South Africa will cater to local needs, involving stakeholders directly. The project's success will be evaluated through comprehensive Life Cycle Assessments, promoting replicability and sustainable entrepreneurship in rural and urban settings. Based on the scientific objectives of the project, the next chapter will focus on the modelling of biomass gasification and methanol synthesis, highlighting key methodologies and recent advancements in these areas.

# Chapter 3 Literature review

## 3.1 Gasification models

The efficient conversion of the chemical energy of biomass or other solid fuels into the desired gas relies heavily on the appropriate configuration, sizing, and selection of gasifier operating conditions. In industrial settings, determining the optimal operating conditions often involves trials conducted on the unit itself or experiments conducted on pilot plants. Although costly, experiments can provide more dependable design data compared to what can be obtained through modelling or simulation. However, there is a significant drawback associated with experimental data. If any of the variables of the original process change, the optimal operating condition determined from specific experimental conditions may no longer be valid. Additionally, an optimum parameter identified through experimentation may be specific to the size of the gasifier used; meaning, the optimal operating condition for one gasifier size may not necessarily be applicable to another size. Hence, making the right decision between experimentation and modelling is crucial for ensuring a reliable design.

### *3.1.1 Simulation versus experiment*

Simulation, or mathematical modelling, of a gasifier may not offer pinpoint accuracy in predicting its performance, but it can certainly provide qualitative insights into the impact of design, operating conditions, or feedstock parameters. By employing simulation, designers or plant engineers can effectively optimize plant operation or design using available experimental data from pilot plants or the current facility [62].

Moreover, simulation can pinpoint operational limits and identify potentially hazardous or undesirable operating zones, if any exist. Modern gasifiers often operate under high temperature and pressure conditions, exposing them to extreme environments. Attempting to push operations to even more extreme conditions to enhance gasifier performance can pose risks, particularly if undertaken without prior understanding of how the gasifier might respond at such conditions. In such cases, modelling offers a comparatively less expensive means of evaluating potential benefits and associated risks.

### *3.1.2 Gasifier simulation models*

Gasifier simulation models can be categorized into several groups, including:

- Thermodynamic equilibrium.
- Kinetic.

- Computational fluid dynamics (CFD).
- Artificial neural network (ANN) models.

The thermodynamic equilibrium model predicts the maximum achievable yield of a desired product from a reacting system. In essence, if the reactants are allowed to react for an infinite time, they will reach equilibrium yield. This model provides the yield and composition of the product under these conditions, focusing solely on the reaction without considering the gasifier's geometry. However, in practical applications, reactants have only a finite time to react in the gasifier. Therefore, while the equilibrium model offers an ideal yield, practical applications require the use of kinetic models to predict product formation within a specified reaction time. Kinetic models track the progression of reactions within the reactor, providing product compositions at various positions along the gasifier. These models consider both the reactor's geometry and its hydrodynamics [62].

CFD models, specifically Eulerian-type models, solve a set of simultaneous equations governing the conservation of mass, momentum, energy, and species within discrete regions of the gasifier. Consequently, they offer insights into temperature distribution, concentration, and other parameters within the reactor. When the reactor's hydrodynamics are well understood, CFD models provide highly accurate predictions of temperature and gas yield throughout the reactor.

Neural network analysis represents a relatively new simulation tool for modeling gasifiers. It operates in a manner akin to an experienced operator who draws upon years of expertise to forecast how a gasifier will perform under specific conditions. This approach necessitates minimal prior knowledge about the process; instead, the neural network autonomously learns from sample experimental data [63].

### *3.1.3 Thermodynamic equilibrium models*

Thermodynamic equilibrium calculations are not contingent upon gasifier design, making them convenient for studying the impact of fuel and process parameters. While chemical or thermodynamic equilibrium may not be fully attained within the gasifier, this model offers the designer a reasonably accurate prediction of the maximum achievable yield of the desired product. Nevertheless, it lacks the capability to forecast the influence of hydrodynamic or geometric parameters, such as fluidizing velocity, or design variables like gasifier height.

Chemical equilibrium is determined by either of the following [50]:

- Equilibrium constant (stoichiometric model)
- Minimization of the Gibbs free energy (non-stoichiometric model)

Before 1958, all equilibrium computations relied on the equilibrium constant formulation of the governing equations [64]. However, in later years, the computation of equilibrium compositions by minimizing Gibbs free energy became an accepted alternative.

The thermodynamic model of a gasification system requires the following inputs:

1. The elemental composition and immediate analysis of the biomass, along with the standard heats of formation of fuels and their higher and lower heating values.
2. The standard enthalpies and entropies, as well as the temperature dependence, of all species of substances involved in the various phenomena constituting gasification.

To achieve this, the following equations need to be developed [50]:

a. The elemental balance of the relevant species (C, H, O, N, S), considering the mass conservation of ashes. Ash is treated as a single substance, and its elemental composition is not taken into account.
b. The energy balance by applying the first principle of thermodynamics to the various processes, which considers the enthalpies of formation of products and reactants, along with the addition or removal of sensible and latent heats in the different processes.
c. The definition of equilibrium conditions, either in the form of equilibrium constants of constituent reactions, or as Gibbs functions of constituent fluxes to be minimized for the process to achieve equilibrium.

By solving the system of equations obtained, the model will be able to predict the composition of the syngas, its calorific value, and the oxidant/fuel ratio. Parametric analysis will enable the study of the influence of operating parameters such as pressure, gasification temperature, and fuel characteristics on the composition of the produced gas. After defining the optimal operating conditions, various efficiencies are calculated.

This section presents a simplified approach to equilibrium modelling of a gasifier based on the following overall gasification reactions:

$$C + CO_2 \rightarrow 2CO \quad 3.1)$$

$$C+H_2O \rightarrow CO+H_2 \quad 3.2)$$

$$C+2H_2 \rightarrow CH_4 \quad 3.3)$$

$$CO+H_2O \rightarrow CO_2+H_2 \quad 3.4)$$

From a thermodynamic standpoint, the equilibrium state represents the maximum conversion attainable for a given reaction condition. In this context, the reaction is regarded as zero-dimensional, implying no changes over time. Equilibrium modelling proves particularly effective at higher temperatures (above 1500 K), where it can reveal valuable trends in variations of operating parameters [65]. For equilibrium modelling, one may employ stoichiometric or nonstoichiometric methods [47].

### *3.1.3.a Stoichiometric equilibrium models*

In the stoichiometric process, the model integrates the chemical reactions and species involved. Typically, it begins by selecting all species containing dominant elements like C, H, and O. If other elements contribute minimally to the product gas, they are often disregarded.

For instance, consider the gasification of 1 mole of biomass in the presence of d moles of steam and e moles of air. The reaction of biomass with air (3.76 moles of nitrogen, 1 mole of oxygen) and steam can be represented as follows [66]:

$$CH_aO_bN_c + dH_2O + e(O_2 + 3.76N_2) \rightarrow n_1C + n_2H_2 + n_3CO + n_4H_2O + n_5CO_2 + n_6CH_4 + n_7N_2 \quad (3.5)$$

In this representation, $n1,\ldots,n7$ represent stoichiometric coefficients. Here, $CH_aO_bN_c$ denotes the chemical representation of the biomass, where $a$, $b$, and $c$ are the mole ratios (H/C, O/C, and N/C) determined from the ultimate analysis of the biomass. With $dd$ and $ee$ as input parameters, the total number of unknowns is seven.

An atomic balance of carbon, hydrogen, oxygen, and nitrogen yields:

$$C: \quad n_1 + n_3 + n_5 + n_6 = 1 \quad 3.6)$$

H: $2\,n_2 + 2\,n_4 + 4n_6 + a + 2d$ 3.7)

O: $n_3 + n_4 + 2\,n_5 = b + d + 2e$ 3.8)

N: $n_7 = c + 7.52e$ 3.9)

During the gasification process, reactions R1, R2, R3, and R7 (as listed in Table 1.7) occur. The water-gas shift reaction, R7, can be viewed as a consequence of subtracting the steam gasification and Boudouard reactions. Therefore, we focus solely on the equilibrium of reactions R1, R2, and R3. The equilibrium constants for these reactions, denoted by $R_1$, $R_2$, and $R_3$, respectively, are determined for a gasifier pressure, $P$ [29]:

$$K_{e_1} = \frac{y_{CO}^2 P}{y_{CO_2}} \quad R1 \qquad (3.10)$$

$$K_{e_2} = \frac{y_{CO}^1\, y_{H_2} P}{y_{H_2O}} \quad R2 \qquad (3.11)$$

$$K_{e_3} = \frac{y_{CH_4}}{y_{H_2}^2 P} \quad R3 \qquad (3.12)$$

where $y_i$ is the mole fraction for species i of CO, $H_2$, $H_2O$, and $CO_2$. The two sets of equations (stoichiometric and equilibrium) may be solved simultaneously to find the coefficients, (n1,…, n7), and hence the product gas composition in an equilibrium state.

Therefore, by solving seven equations (Eqs. 3.6) to ( 3.12)), we can determine the values of seven unknowns ($n_1$,…,$n_7$) which provide both the yield and the product of gasification for a given air/steam-to-biomass ratio. This approach relies on the simplified reaction path and the chemical formula of the biomass.

### *3.1.3.b Nonstoichiometric equilibrium models*

In nonstoichiometric modelling, there's no requirement for knowledge about a specific reaction mechanism to solve the problem. In a reacting system, a stable equilibrium state is achieved when the Gibbs free energy of the system is minimized. Therefore, this method revolves around minimizing the total Gibbs free energy. The only input required is the elemental composition of the feed, which is discerned from its ultimate analysis. This method is especially well-suited for fuels such as biomass, where the exact chemical formula may not be explicitly known [67].

The Gibbs free energy, $G_{total}$ for the gasification product comprising N species ($i = 1, \dots, N$) is given by:

$$G_{total} = \sum_{i=1}^{N} n_i \Delta G_{f,i}^{0} + \sum_{i=1}^{N} n_i RT ln\left(\frac{n_i}{\sum n_i}\right) \quad (3.13)$$

where $\Delta G_{f,i}^{0}$ is the Gibbs free energy of formation of species i at standard pressure of 1 bar.

Equation 3.13 is to be solved for unknown values of $n_i$ to minimize $G_{total}$, bearing in mind that it is subject to the overall mass balance of individual elements. For example, irrespective of the reaction path, type, or chemical formula of the fuel, the amount of carbon determined by ultimate analysis must be equal to the sum total of all carbon in the gas mixture produced. Thus, for each jth element we can write [29]:

$$\sum_{i=1}^{N} a_{i,j} n_i = A_j \quad (3.14)$$

Where $a_{i,j}$ is the number of atoms of the $j$th element in the $i$th species, and $A_j$ is the total number of atoms of element $j$ entering the reactor. The value of $n_i$ should be determined such that the total Gibbs free energy ($G_{total}$) is minimized. To solve these equations, we can employ the Lagrange multiplier method L.

$$L = G_{total} - \sum_{j=1}^{K} \lambda_j \left( \sum_{i=1}^{N} a_{ij} n_i - A_j \right) \quad kJ/mol \quad (3.15)$$

where $\lambda_{\varphi}$ is the Lagrangian multiplier for the $j$th element. To find the extreme point, we divide Eq. ( 3.15) by RT and take the derivative:

$$\left(\frac{\partial L}{\partial n_i}\right) = 0 \quad (3.16)$$

Substituting the value of Gtotal from Eq. (3.13) in Eq. (3.15), and then taking its partial derivative, the final equation is of the form given by:

$$\left(\frac{\partial L}{\partial n_i}\right) = \frac{\Delta G_{f,i}^0}{RT} + \sum_{i=1}^{N} ln\left(\frac{n_i}{n_{total}}\right) + \frac{1}{RT}\sum_{j=1}^{K} \lambda_j \left(\sum_{i=1}^{N} a_{ij} n_i\right) = 0 \qquad (3.17)$$

### *3.1.4 Kinetic models*

Gas composition measurements from gasifiers often deviate significantly from those predicted by equilibrium models [68–70]. This discrepancy highlights the limitations of equilibrium models and emphasizes the necessity of kinetic models to accurately simulate gasifier behaviour.

A kinetic model provides insight into the gas yield and product composition achieved by a gasifier after a finite time (or within a finite volume in a flowing medium). As such, it incorporates parameters such as reaction rate, particle residence time, and reactor hydrodynamics. Given a specific operating condition and gasifier configuration, the kinetic model can predict the profiles of gas composition and temperature within the gasifier, as well as the overall gasifier performance.

The model integrates the gasifier reactor's hydrodynamics with the kinetics of gasification reactions occurring inside it. At low reaction temperatures, the reaction rate is sluggish, necessitating a lengthy residence time for complete conversion. Therefore, kinetic modeling is particularly suitable and accurate at relatively low operating temperatures (below 800°C) ([65]). Conversely, at higher temperatures where reaction rates are faster, the equilibrium model may be more applicable.

To account for the finite time available for reactions, a kinetic model is necessary. This model considers the progression of a reaction as it occurs within the reactor, taking into account the geometry and fluid flow, and thus the residence time. The approach outlined in this section involves modelling each phase that comprises the gasification process, namely drying, pyrolysis, combustion, and reduction.

#### *3.1.4.a Drying*

In this zone, the water contained in the biomass particle diffuses outward due to the moisture concentration gradient, transitioning from its equilibrium moisture content to the ambient temperature around the particle. Thus, the drying process is determined by heat and mass transfer within the biomass bed and the particles.

It is often estimated that thermal diffusivity is much faster than mass transfer. Consequently, the assumption that the particle is in thermal equilibrium with its environment is valid. In this case, it is considered that mass transfer determines the drying rate. This process starts at a temperature of 95°C and stops at 200°C [71].

The rate at which the drying reaction occurs is determined by the following equation:

$$r_d = K_d C_{h_2O,l} \quad (3.18)$$

$$K_d = A_d e^{\frac{-E_d}{RT_d}} \quad (3.19)$$

Where $A_d$ is a preexponential constant, R is the universal gas constant, and E is the activation energy for the reaction.

The constants used in this model are presented in the following table.

***3.1.4.b Pyrolysis***

Pyrolysis occurs through the successive decomposition of the main constituents (hemicellulose, lignin, cellulose) at different temperature levels. The breakdown of bonds and the rearrangement process of the polymers that make up the biomass lead to a very large number of products, which are grouped into three classes:

- Charcoal: Solid residues composed mainly of carbon.
- Condensables (tars, pyroligneous juice): These are volatiles at the pyrolysis temperature but condense at ambient temperature.
- Non-condensables: These are permanent gases with low molecular weight (CO, $H_2$, $CH_4$, $CO_2$, etc.).

A multitude of models have been developed to better represent the often complex mechanisms of pyrolysis based on different approaches. The simplest approach is to consider this phenomenon as a single reaction that transforms the solid into char. This approach does not concern itself with the composition of the produced gas and tars, but only allows for knowing the mass evolution of the solid[72]. The mechanism is then modelled with a single equation:

If the mechanism involves degradation, the following equation is used:

$$\frac{dt}{dm_{wood}} = -K \cdot m_{wood} \quad (3.20)$$

If the mechanism involves devolatilization, the following equation is used:

$$\frac{d(m_{bois} - m_{char})}{dt} = -K(m_{bois} - m_{char}) \quad (3.21)$$

The second approach is to estimate the pyrolysis products through primary and secondary reactions that divide the products into gas, char, and tars. These are more elaborate models and are simple to use. This approach is by far the most used, and several models arise from this approach [72]:

The Broido-Shafizadeh model:

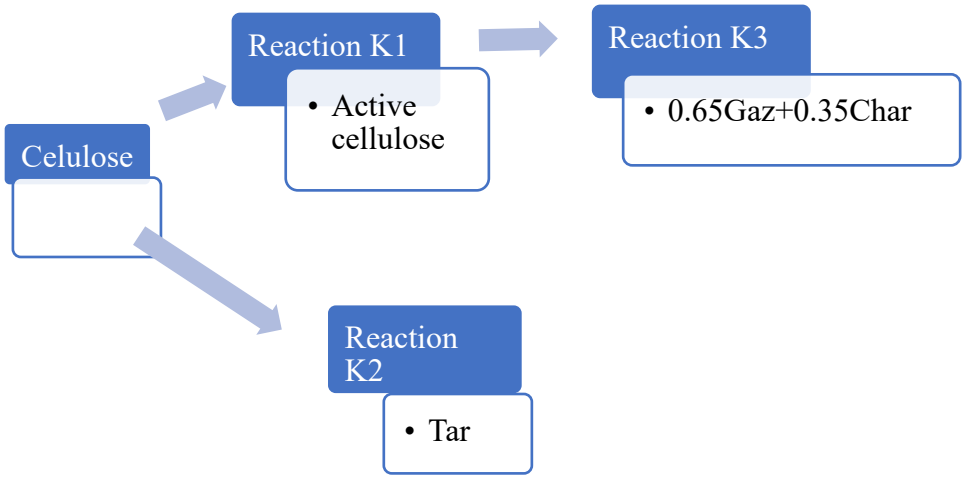


Figure 3.1 Broido-ShafizadehCelulose model[73]

The values 0.65 and 0.35 represent the mass stoichiometric coefficients of the products resulting from the pyrolysis of cellulose. The first step begins at 200°C and leads to the formation of active anhydrous cellulose through reaction K1.

At 280°C, the cellulose that has not been converted into active anhydrous cellulose undergoes depolymerization, leading to the formation of tars via reaction K2.

Finally, the active cellulose formed undergoes pyrolysis, producing a fraction of light gases and char through the exothermic reaction K3.

### *3.1.4.c Oxidation*

During the oxidation phase, the combustion of some pyrolysis products provides the heat required for the drying, pyrolysis, and gasification phases. The air-to-fuel ratio is sub-stoichiometric. The reactions occurring in this zone and their respective reaction rates are listed

in Tables 3.1 [74,75]. The pyrolysis products are oxidized in an order determined by the reaction rates:

- Complete oxidation of hydrogen (R1): Occurs first.
- Oxidation of CO (R2): Takes place immediately after hydrogen oxidation.
- Methane oxidation (R3): If oxygen remains after the previous reactions, methane is oxidized.
- Oxidation of charcoal and tars (R4, R5): If additional oxygen is available, charcoal and tars are oxidized.

The oxidation reaction rate can be described by the Arrhenius equation:

$$r_o = Ae^{\left(\frac{-E_a}{RT}\right)}.[Reactant1]^n[Reactant]^m \quad (3.22)$$

Where:

- $r_o$ is the rate of oxidation (mol/s),
- A is the pre-exponential factor (reaction rate constant at standard conditions, typically related to the frequency of collisions between reactants),
- $E_a$ is the activation energy (kJ/mol),
- R is the universal gas constant (8.314 J/mol·K),
- T is the temperature (K),
- n and m are reaction orders.

Table 3.1 Reactions Occurring During the Oxidation Phase [74,75].

| R | Reaction | Reaction rate ($mole\ m^3\ s^{-1}$) |
|---|---|---|
| **1** | $H_2+0.5O_2 \leftrightarrow H_2O$ | $r_{H_2} = A_{H_2}e^{\left(\frac{-E_{H_2}}{RT}\right)}.[H_2][O_2]^{0.5}$ |
| **2** | $CO+0.5O_2 \leftrightarrow CO_2$ | $r_{CO} = A_{CO}e^{\left(\frac{-E_{CO}}{RT}\right)}.[CO][O_2]^{0.5}$ |
| **3** | $CH_4+1.5O_2 \leftrightarrow CO+2H_2O$ | $r_{CH_4} = A_{CH_4}e^{\left(\frac{-E_{CH_4}}{RT}\right)}.[CH_4][O_2]^{1.5}$ |
| **4** | $C+0.5O_2 \leftrightarrow CO$ | $r_{CO} = A_Ce^{\left(\frac{-E_C}{RT}\right)}.[C][O_2]^{0.5}$ |

### *3.1.4.d Reduction*

The gasification process itself begins during this phase, where the char formed during pyrolysis is converted into synthesis gas under the action of an oxidizing agent. Ideally, the volatiles released during pyrolysis are transformed into carbon dioxide and water vapor. Giltrap et al.

[76] modelled the reduction zone based on the reaction kinetics values observed during this phase, as reported by Wang and Kinoshita [77]. The reactions included in this model are presented in the following table:

Table 3.2 Reaction Rate during the Gasification sub-process

| R | Reaction | Reaction rate ($mole\ m^3\ s^{-1}$) |
|---|---|---|
| **1** | $C + CO_2 \rightarrow 2CO$ | $r_1 = A_1 e^{\left(\frac{-E_1}{RT}\right)} \left(y_{CO_2} - \frac{y_{CO}^2}{K_1}\right)$ |
| **2** | $C + H_2O \leftrightarrow CO + H_2$ | $r_2 = A_2 e^{\left(\frac{-E_2}{RT}\right)} \left(y_{H_2O} - \frac{y_{CO}\, y_{H_2}}{K_2}\right)$ |
| **3** | $C + 2H_2 \leftrightarrow CH_4$ | $r_3 = A_3 e^{\left(\frac{-E_3}{RT}\right)} \left(y_{H_2}^2 - \frac{y_{CH_4}}{K_3}\right)$ |
| **4** | $CH_4 + H_2O \leftrightarrow CO + 3H_2$ | $r_4 = A_4 e^{\left(\frac{-E_4}{RT}\right)} \left(y_{Ch_4} y_{H_2O} - \frac{y_{CO}\, y_{H_2}^3}{K_3}\right)$ |

### *3.1.5 Computational fluid dynamics (CFD)*

CFD can play a significant role in modelling a fluidized-bed gasifier. A CFD-based code solves the equations for mass, momentum, species, and energy conservation over a defined region or domain. These equations are formulated for an element, considering the fluxes of the mentioned quantities entering and exiting the element, with appropriate boundary conditions. A CFD code for gasification typically incorporates various sub-models that represent processes such as the vaporization of a biomass particle, its pyrolysis (devolatilization), secondary reactions during pyrolysis, and char oxidation [78,79]. More advanced features, such as a subroutine for fuel fragmentation during gasification and combustion, have also been developed [80]. These subroutines can be integrated with transport phenomena, particularly in the case of a fluidized-bed gasifier.

For laminar flow situations, the hydrodynamic or transport phenomenon is fully described by the Navier-Stokes equations. However, in turbulent flow scenarios, finding a solution becomes more complex. A complete time-dependent solution to the instantaneous Navier-Stokes equations exceeds current computational capabilities [81], making it necessary to apply turbulence models. The Reynolds-averaged Navier-Stokes equations are often used in The Navier-Stokes equations, along with turbulence models like the k-ε model or large eddy simulation filters, are commonly used to account for turbulence in fluid flow. In the case of fluidized beds, flow is typically modelled using the Eulerian-Lagrange approach, where the

discrete phase applies to the particle flow and the continuous phase to the gas. Overmann et al. [82] utilized both Euler-Euler and Euler-Lagrange models to simulate wood gasification in a bubbling fluidized bed, with preliminary results showing that both models provided similar agreement with experimental data. If the flow is sufficiently dilute, particle-particle interactions and the particle volume in the gas phase are often neglected.

Another CFD approach is the two-fluid model. Discretization methods such as finite difference, finite element, and finite volume are used in this model. Commercial software like ANSYS, ASPEN, Fluent, Phoenics, and CFD2000 are available for solving these models [83]. A review and comparison of these software tools can be found in Xia and Sun and Norton et al. [84,85]

Recent advancements in the numerical solution and modelling of complex gas-solid interactions have made CFD a more powerful tool for simulating real-life processes. If these models are successful, they could serve as an essential tool for the optimization and even design of thermochemical reactors such as gasifiers [81]. CFD models are particularly effective in simulating entrained-flow gasifiers, where the gas-solid flows are simpler than in fluidized beds and the solid concentration is low. Several researchers have developed models that incorporate sophisticated reaction kinetics and complex particle-particle interactions. However, most of these models rely on submodels, fitting parameters, or major assumptions in areas where precise data is unavailable. These "weak links" can make the final results sensitive to the accuracy of the assumptions or parameters used. When the final results are known, they can be used to back-calculate the values of unknown parameters or to refine the underlying assumptions.

Thus, while a CFD model can predict the behaviour of a gasifier across a broader range of parameters using data from one scenario, the prediction may not be accurate if applied to a different gasifier with significantly different input parameters.

### *3.1.6 Neural network models*

An alternative to the detailed modelling of complex processes, particularly those that are not well understood, is the use of Artificial Neural Networks (ANNs). ANNs simulate the functioning of the human brain and replicate certain human-like problem-solving abilities [86]. While they do not provide analytical solutions, they are capable of delivering numerical results. This approach has been successfully applied to predict gas yield and composition from the gasification of materials such as bagasse, cotton stems, pine sawdust, and poplar in fluidized beds [87] as well as Municipal Solid Waste (MSW) in fluidized bed systems [88]

ANN models are well-suited to address complex gasification challenges, utilizing a high-speed architecture that includes three hidden neuron layers [89]: an input layer for receiving data, a processing layer, and an output layer for delivering results. Figure 3.2 illustrates the arrangement of neuron layers and their interconnections. Kalogirou [89] proposed an empirical formula to determine the optimal number of hidden neurons:

$$Number\ of\ hiden\ neurons = \frac{1}{2}(inputs + outputs) + \sqrt{Number\ of\ training\ patterns} \quad (3.23)$$

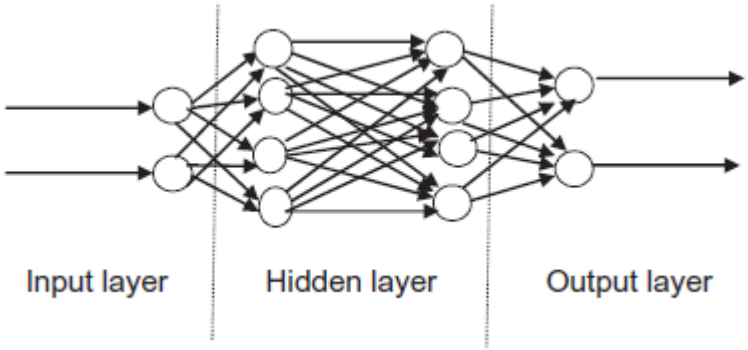


Figure 3.2 Schematic diagram of a multilayer feedforward neural network [89].

The input layer operates with two key components: inputs and weights. Weights facilitate the transfer of data between layers. Initially, the nodes process the input data, perform a summation, and pass the result through an activation function. The output of this process, referred to as the node's "activation value," is then multiplied by its corresponding weight and sent to the subsequent node in the network.

Training modifies the connection weights in some orderly fashion using learning methods [90]. It begins with a set of data (with inputs and outputs targeted); the weights are adjusted until the difference between the neural network output and the corresponding target is minimum [89]. When the training process satisfies the required tolerance,

the network holds the weights constant and uses the network to make output predictions. After training, the weights contain meaningful information.

A back-propagation algorithm is used to train the network. Multilayer feed-forward neural networks are used to approximate the function.

Puig-Arnavat et al. [91] investigated the application of artificial neural networks (ANNs) to model the biomass gasification process in fluidized bed reactors. Two ANN architectures are presented: one for circulating fluidized bed (CFB) gasifiers and another for bubbling fluidized bed (BFB) gasifiers. These models predict the producer gas composition (CO, CO2, H2, CH4) and gas yield using published experimental data to train the ANNs.

A neural network may return poor results for data that differ from the original data it was trained with. This happens sometimes when limited data are available to calibrate and evaluate the constants of the model ([92]). After structuring the neural network, information starts to flow from the input layer to the output layer according to the concepts described here.

## 3.2 State of the art gasification

### *3.2.1 Gasification modelling*

Despite its simple design and construction, the gasification process is highly complex from a modelling perspective due to the interaction of various phenomena, particularly during the oxidation and reduction phases. Extensive research conducted on different modelling approaches over the past decades highlights the importance of understanding the fundamental mechanisms of gasification.

Several thermodynamic models predicting the behaviour of the gasification process have been reported in the literature.

Zainal et al. [93] proposed a model combining chemical and thermodynamic equilibria for biomass gasification in a co-current gasifier. In this model, all reactions are assumed to be at equilibrium, the products from pyrolysis are completely oxidized before reaching the reduction zone, and all charcoal is converted into syngas. This model predicts the syngas composition and its calorific value using wood as the biomass feedstock. However, the chemical formula for wood in this model includes only carbon, hydrogen, and oxygen (C, H, O).

Melgar et al. [94] adopted a similar approach, developing a model based on Gibbs free energy minimization. The difference lies in the inclusion of nitrogen ($N_2$) and sulfur (S) in the biomass chemical formula, modifying the global gasification equation to include $SO_2$ and unconverted oxygen ($O_2$) in the product gases. Their parametric study showed that the gasification yield reaches its maximum (80%) when the air-to-fuel ratio is within the range [2.5–5], and the biomass moisture content is below 25%.

Sharma [95] developed a more detailed equilibrium model also based on Gibbs free energy minimization. This model accounts for unconverted charcoal in the reduction zone, heat losses through the reactor walls, and bed thermal conductivity. Using pine bark as the biomass feedstock, the results indicated that optimal conversion occurs within a moisture content range of [10–20%], an equivalence ratio (ER) between [0.3–0.45], and a gasification temperature exceeding 1200 K. The results from Sharma's model were validated with experimental data from [96].

Prins et al. [97] conducted a comparative study on air and steam gasification using a stoichiometric model, calculating energy and exergy efficiencies based on the type of oxidizing agent. The results indicated that steam gasification has a higher efficiency compared to air gasification, with efficiencies of 87.6% and 80.5%, respectively. Additionally, steam gasification produces a gas rich in methane and carbon dioxide, while hydrogen, carbon monoxide, and steam dominate the syngas composition during air gasification.

Altafini et al. [65] developed a thermodynamic model to simulate the gasification of Elliott pine waste. A parametric study analyzed the influence of moisture on syngas composition and calorific value, with the model's performance validated using previously obtained experimental data. To better represent gasifier operation, the authors created more complex models using the Cycle-Tempo software, which employs a Gibbs free energy minimization approach. The study found this method to be valid for gasification temperatures above 1200K.

Fortunato et al. [98] built upon Altafini's model by simulating each gasification phase pyrolysis, combustion, and reduction—separately using Cycle-Tempo. Modifications included bypassing some methane produced during pyrolysis into the oxidation zone and preheating oxidation air before entering the gasifier. The model introduced an empirical relationship between the equivalence ratio (ER) and biomass parameters, such as ash content, particle size, and moisture, extending its applicability to diverse biomass types.

Thermodynamic models, while relatively simple and effective for assessing the influence of biomass and operating parameters, cannot capture the intrinsic behaviour of gasifiers, necessitating the use of kinetic models [99].

Giltrap et al. [76] developed a kinetic model focusing on the reduction zone. It predicts gas composition and temperature while assuming all pyrolysis products are cracked in the combustion zone. The model uses reaction rates provided by [77] and incorporates the Char Reactivity Factor (CRF) to represent the reactivity of different char types. Applying mass and

energy balances to the reduction zone resulted in seven first-order differential equations. Additionally, empirical equations estimate velocity and pressure throughout the bed. While the model provides reasonable predictions, it overestimates methane ($CH_4$) composition. Giltrap suggested refining initial conditions and varying CRF along the bed for improved accuracy.

Patra & Sheth [99] extended Giltrap's model by varying the CRF linearly (1 to 10,000) and exponentially along the reduction zone. Exponential variation yielded better predictions for gas temperature and composition, aligning with experimental results from Jayah et al. [96].

Dejtrakulwong et al. [100] reported kinetic modelling of all four phases in a co-current gasifier, modelling each zone separately. They observed that increasing fuel moisture extended drying and pyrolysis zones while reducing the critical reduction zone length from 0.53 m to 0.25 m.

Salem et al. [75] adopted a similar approach, predicting temperature and pressure distributions, zone heights, and the composition of gases and ash. Their model introduced an optimized reduction zone length to ensure complete char consumption from the pyrolysis zone. Results indicated that biomass with less than 10% moisture and an equivalence ratio of 0.3–0.35 produced higher syngas output with low tar content. Remarkably, olive wood with 10% moisture yielded a syngas with a calorific value of 6.4 MJ/Nm³.

Awais et al. [101] conducted an experimental study evaluating the performance of a filtration and cleaning system for syngas derived from the gasification of wood chips and corn cobs. The system, comprising four integrated filters within a co-current gasifier, demonstrated significant tar reduction. Specifically, the tar content in syngas from wood chips was reduced from 6600 mg/Nm³ to 112 mg/Nm³, while for corn cobs, it decreased from 7500 mg/Nm³ to 220 mg/Nm³. In a subsequent study, Awais et al. [101] investigated a co-current gasifier fueled by sugarcane bagasse and coconut shells at varying moisture levels. The results showed that 1 kg of sugarcane bagasse produced 3.1 Nm³ of syngas, whereas the same amount of coconut shells yielded 2.97 Nm³. Moreover, increasing the equivalence ratio (ER) from 0.17 to 0.22 led to a rise in CO and $H_2$ concentrations from 14% to 17.9% and 7.5% to 9.6%, respectively. This increase in ER also enhanced the lower heating value (LHV) of the syngas from 4.4 MJ/Nm³ to 5.4 MJ/Nm³.

### *3.2.2 Gasification of date palm waste*

Sait et al. [102] executed the kinetics of DPW for combustion and pyrolysis process using a thermogravimetric analyser to define the physical properties of the process The results revealed that the date palm seed and leaf possess high calorific values and volatile content compared to

the leaf stem. The kinetic analysis emphasizes the potential of these biomass materials as promising sources of energy, chemicals, and bio-char.

Bensidhom et al. [103] experienced different date palm waste from Tunisia, namely Date Palm Rachis (DPR), Date Palm Leaflets (DPL), Empty Fruit Bunches (EFB), and Date Palm Glaich (DPG), was performed in a fixed-bed reactor from room temperature to 500 °C, with a heating rate of 15 °C/min and a condensation temperature of −5 °C, to produce bio-oil, biochar, and syngas using a fixed bed reactor The highest biochar yield (36.66 wt%) was obtained from DPL, while the lowest (31.66 wt%) was derived from DPG. The syngas production varied between 39.10 wt% for DPR and 46.31 wt% for DPL.

Pyrolysis process of date palm waste has been attracting the lion's share so far, date palm gasification process is getting more interest in the recent years. Bassyouni et al. [104] developed an Aspen Hysys model simulation for steam gasification of DPW to predict the optimal operating condition, A set of six reactor models was employed to simulate the various reaction zones of a downdraft gasifier in accordance with its hydrodynamic behaviour. Biomass decomposition in the pyrolysis zone was modelled using a conversion reactor, while the combustion of char and volatiles in the combustion zone was represented by equilibrium and Gibbs reactor models, respectively. The gasification zone was modelled using both Gibbs and equilibrium reactors. Simulation results were validated against experimental data obtained from a parametric variability study conducted on a laboratory-scale gasifier. The simulations indicated that the proportion of synthesis gas increased with temperature, as evidenced by the variations in concentration, molar fraction, and partial pressure. In contrast, CO2 and CH4 concentrations in the product gases decreased with increasing temperature. At 800 °C, the exit gas achieved a stable molar composition of $H_2$ (56.27%), CO (21.71%), $CO_2$ (18.24%), and $CH_4$ (3.78%). Moreover, an increase in the steam-to-biomass ratio resulted in higher levels of $CO_2$ and $H_2$, with a concomitant decrease in CO, driven by the shift reaction. Steam induction was found to increase methane content, thereby enhancing the heating value of the product gas.

After, AlNouss et al. [105] developed an air-steam gasification of date pits based on a thermos-equilibrium method on Aspen plus, the syngas composition varied from 40.40% $H_2$ and 20.20% CO.

Sulaiman et al. [106] investigated the impact of particle size and temperature on gas composition, for an air gasification of date palm on a downdraft gasifier. The findings indicated that temperature plays a crucial role in determining gas composition, with notable impacts on

the concentrations of $H_2$ and CO. Elevated temperatures led to higher levels of $H_2$ and CO in the product gas. Moreover, a more desirable gas composition, in terms of $H_2$, CO, $CH_4$, and $CO_2$ contents, was observed when larger particle sizes were used, as compared to smaller particles.

Kabli et al. [107], studied the hydrogen enrichment from Saudi Arabian date palm waste air gasification. A simulation model based on an equilibrium process was developed using Aspen Plus and validated against experiments. The impact of temperature, particle size, and air flowrate were analysed on gasification performance, The results demonstrated that $H_2$ concentration was enhanced with increasing temperature and particle size, ranging from 12.12 to 26 vol.% and 26.02 to 26.89 vol.%, respectively. This increase in $H_2$ concentration was attributed to the activation of endothermic and methane-reforming reactions, with $CH_4$ concentration decreasing to 12.6 vol.% as the temperature rose. The higher heating value of syngas, carbon conversion efficiency, and cold gas efficiency all exhibited an upward trend with elevated temperature and air flowrate.

Martis et al. [108] simulated biochemical and thermochemical routes for date palm waste conversion via Aspen plus, leading to 56kg of hydrogen via gasification and 233kg of ethanol via fermentation. The gas composition and yield of syngas created are influenced by gasifying agent and temperature [109]. The temperature has a significant part in the gasification process. It affects water gas shift, methane reforming, and Boudouard reactions, which influence the gas composition [110].

The gasification medium influences the gas products and yield. Steam could be a reasonable choice for hydrogen enrichment since it boosts the water shift reaction [14].

### *3.2.3 Gasification of date palm for methanol production*

Moreover, methanol is a stable liquid produced based on syngas with important energy density, for this it is considered as a valuable sustainable alternative to fuel. Methanol is widely used in engines, chemicals industry due to several advantages, among which, the higher boiling points, and lower production cost [111]. 90% of methanol are produced from natural gas so far [112].

Giuliano et al. [113] in their study evaluate methanol production from digestate-derived syngas through air gasification and carbon capture. Results show a significant CO2 savings of 71 ktCO2eq/year, making waste-based methanol a promising sustainable option.

Another study employs Aspen Plus software to simulate methanol synthesis using H2-rich biomass-derived syngas from interconnected fluidized beds. It investigates the impact of operating parameters, including gasification temperature, pressure, steam/biomass ratio (S/B), and catalyst choice. The results indicate that using CaCO3 catalysis, a gasification temperature of approximately 750°C, ambient pressure, and an S/B ratio of 0.4-0.5 are optimal conditions, yielding a maximum of 12.19 mol/(kg biomass) of methanol [114]

## 3.3 Conclusion:

This chapter provides a comprehensive review of gasification models and their application in understanding and optimizing the conversion of biomass into syngas. Several key points emerge from the analysis:

- Comparison of Simulation and Experimentation: While experiments provide reliable data for gasifier design, they are often costly and limited in scalability. Simulation models offer a cost-effective alternative, delivering qualitative and predictive insights into gasifier performance.
- Model Categories: Gasifier models are categorized into thermodynamic equilibrium, kinetic, computational fluid dynamics (CFD), and artificial neural networks (ANNs). Each has distinct strengths, from predicting maximum yields to detailed hydrodynamic behaviours.
- Thermodynamic Models: These models, including stoichiometric and nonstoichiometric approaches, offer valuable predictions of gas compositions and efficiencies, but they lack the capacity to capture dynamic and geometric influences.
- Kinetic Models: Essential for low-temperature operations, these models account for reaction rates and residence times, providing detailed insights into phase-specific phenomena such as drying, pyrolysis, combustion, and reduction.
- Among these, the future holds significant promise for ANN models, largely due to the vast amounts of data now available from experimental studies, industrial operations, and advanced simulations. The increasing availability of big data allows ANNs to train on diverse datasets, improving their accuracy, adaptability, and ability to capture nonlinear relationships in complex systems.
- State-of-the-Art Advancements: Contemporary research highlights the critical role of modeling in addressing challenges such as temperature, particle size, and gasifying agents, particularly for novel biomass like date palm waste. Applications range from optimizing syngas composition to producing methanol as a sustainable fuel.

This bibliographic review underscores the pivotal role of gasification modelling in advancing renewable energy technologies. By bridging experimental limitations and offering predictive capabilities, these models enhance our understanding of biomass conversion processes, enabling more efficient and sustainable designs. Furthermore, the exploration of date palm waste as a biomass feedstock demonstrates the potential for region-specific solutions to global energy challenges, contributing to a circular economy and reducing dependence on fossil fuels.

However, a notable gap in the literature is the limited exploration of methanol synthesis from date palm waste gasification. While methanol is a valuable sustainable fuel, studies specific to this biomass feedstock remain scarce. Addressing this gap through targeted research could unlock significant opportunities for renewable fuel production and support the transition to a more sustainable energy future.

# Chapter 4 Materials and methods

## 4.1 Introduction

The previous chapters have highlighted the abundance and significant potential of Algerian date palm waste as a renewable biomass resource. Despite its vast availability, there remains a notable gap in research and development focusing on the gasification of this biomass and its subsequent utilization for methanol synthesis, particularly in Algeria. Addressing this gap is crucial for leveraging date palm waste as a sustainable energy source and exploring its role in producing valuable chemicals like methanol.

This chapter aims to bridge this gap by presenting a detailed discussion of the materials and methods employed in this study. It begins by quantifying the biomass potential of Algerian date palm waste, establishing a foundation for its feasibility as a feedstock. Following this, the characterization of the biomass is discussed to provide insight into its chemical and physical properties, which play a pivotal role in determining its gasification behaviour.

Additionally, this chapter introduces the Aspen Plus® model developed to simulate the gasification process and methanol synthesis. The model is designed specifically for date palm waste, incorporating essential assumptions and parameters to ensure accurate and realistic predictions.

## 4.2 The Algerian biomass potential

This work forms part of the Reffect Africa initiative, which aims to explore sustainable energy solutions through the utilization of biomass resources across the continent. Within this framework, one of the primary objectives is to identify and characterize the most significant biomass resources available in Algeria.

The first step in this approach involves collecting comprehensive data on the various types of biomasses in the region, focusing on their availability, distribution, and potential for energy production.

The current biomass potential in Algeria is estimated at approximately 37 Mtoe (million tons of oil equivalent)[38]. However, the recoverable potential is significantly lower, at around 3.7 Mtoe, indicating that only 10% of the total potential is utilized. This low recovery rate highlights the substantial waste of resources, with nearly 5 million tons of urban and agricultural waste remaining unrecycled. This untapped biomass represents an additional energy resource of approximately 1.33 Mtoe per year, underscoring the need for improved waste management

systems and biomass recovery strategies to enhance the utilization of this renewable resource for energy generation and other value-added applications [115].

This study aims to identify and quantify the potential of organic waste by conducting an analysis within the agricultural sector.

The agricultural potential of biomass can be calculated by categorizing the waste into three main types based on their origin and characteristics.

### *4.2.1 Waste from primary processing of the harvest*

This includes residues generated during the processing of crops, such as:

- Husks, shells, and stalks from cereals (e.g., wheat, rice, maize).
- Seed coats and other by-products from oilseed crops like sunflower or sesame.

### *4.2.2 Waste left in the fields during harvest*

Residues that remain on the field after harvesting, often serving as natural ground cover or organic material, include:

- Straw from cereals.
- Leaves, stems, and other plant matter not collected during harvesting.

### *4.2.3 Waste remaining in the ground*

These are the parts of the plant left in the soil after the crop has been harvested, such as:

- Roots and underground biomass (e.g., tubers, root stumps).

### *4.2.4 Olive trees*

The olive sector in Algeria has experienced remarkable growth over the years, demonstrating its increasing importance within the country's agricultural landscape. By 2016, olive groves covered a total area of 471,657 hectares. This expansion underscores the significance of olive cultivation as a priority in Algeria's agricultural development. The total number of olive trees saw a significant rise, increasing by 10% in just one year to nearly 6.2 million trees. Between 2015 and 2016, 2,439,033 olive trees entered production, bringing the total number of trees in the country to approximately 35 million, up from 32 million in 2015. Certain regions have been particularly instrumental in this growth. The wilayas of Béjaia, Skikda, Saida, Djelfa, and Chlef accounted for 64% of the national increase in olive trees planted, reflecting their critical role in driving the sector forward. Over the longer term, the evolution of olive tree cultivation in Algeria has shown consistent growth. Between 2000 and 2020, there was a steady increase in both the number of trees and the area dedicated to olive groves, driven by rising domestic and global demand, figure 4.1 illustrates the evolution of olive trees in Algeria from 2000 to 2020. [115].

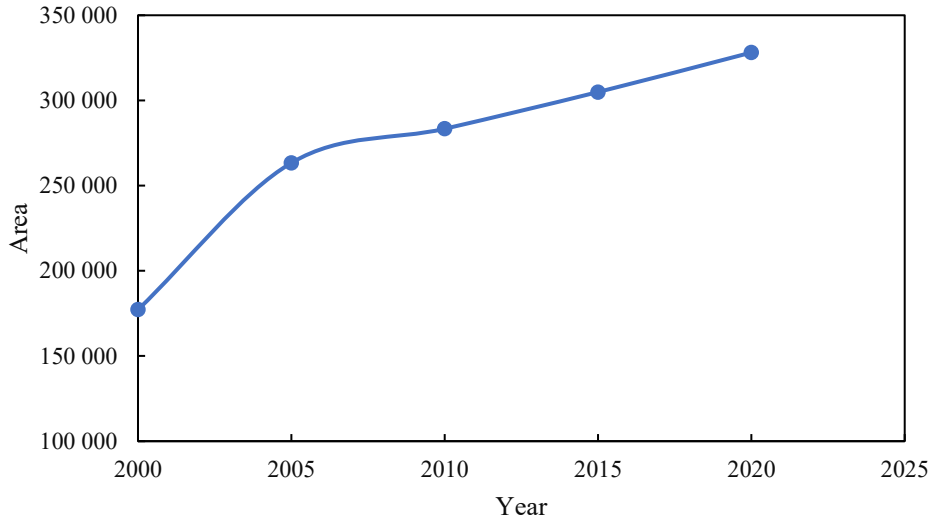


Figure 4.1 Evolution of the area of olive trees (2000-2020)[115]

This expansion not only highlights Algeria's potential in olive oil production but also presents opportunities for biomass valorisation. By-products such as olive pits, husks, and wastewater could be leveraged for renewable energy generation and biochar production, contributing to a sustainable and circular economy.

### *4.2.5 Wheat*

In the 2023/24 season, Algeria's wheat cultivation area is estimated at just over 2 million hectares, with the majority of production concentrated in the coastal Mediterranean zones and the high plateaus. Currently, less than 10% of the country's wheat production originates from the southern regions. However, cereal production in Algeria's desert biome is steadily increasing, aligning with the government's objective to cultivate one million hectares of cereals in the south by 2030. If realized, this would represent about one-third of Algeria's total cereal-planted area.

To achieve this target, the government has implemented various measures to attract investors to develop agriculture in the Sahara. As a result, significant foreign investments have been established, particularly in cereal production. According to Algeria's official outlet APS [116], as of June 23, 2024, cultivated crop areas in the south have reached 500,000 hectares, of which 153,000 hectares are attributed to foreign investments. However, specific data on the wheat-planted area within this figure has not been disclosed.

For the 2024/25 marketing year, Algeria's wheat production is forecast at 3 million metric tons (MT), while barley production is estimated at 1.2 million MT. In southern Algeria's hot and dry regions, the harvest period typically runs from late April to early May. This year's harvest in the south is reportedly favourable, with irrigated areas achieving higher yields, ranging from 45 to 80 quintals per hectare (equivalent to 4.5-8 MT/ha), surpassing the yields of northern regions.

The southern provinces are expected to contribute approximately 222,000 MT of grain to Algeria's total production, accounting for about 7% of the national output. Key contributions include more than 85,000 MT from El Menea, 37,000 MT from El-Oued, and over 100,000 MT from Adrar in the southwest. This reflects the growing importance of southern Algeria in the country's agricultural strategy and its potential to significantly boost cereal production in the coming years [117].

### *4.2.6 Date palm*

During the 1980s, new agricultural zones were developed in the Sahara, particularly in regions such as Adrar, El Oued, Biskra, Ouargla, and Ghardaïa. This period also saw the establishment of an electric power network and the mobilization of new water resources, which facilitated

agricultural expansion. In these areas, the number of date palms grew from 8 million in 1990 to 9 million, primarily through the creation of large date palm plantations in Biskra, El Oued, El Guerrara, El Meniaa, Adrar, and In Salah.

Since 2000, Algerian date palm groves have experienced substantial growth. By 2002, the number of date palms reached 13.5 million, occupying 120,830 hectares. Today, the country boasts 18 million date palms spread across 169,380 hectares[118]. As a result, there is a substantial quantity of biomass waste material produced, such as leaflets, bunches petioles, among others, which amounts to approximately 40 kg per date palm tree[119]. These date palm plantations are predominantly located in the oasis regions south of the Saharan Atlas Mountains. Geographically, their cultivation stretches from the Moroccan border in the west to the Tunisian-Libyan border in the east. From north to south, the date palm groves extend from the southern foothills of the Saharan Atlas Mountains at Reggane in the west, Tamanrasset in the center, and Djanet in the east.

In Algeria, the cultivation of date palms is distributed across several key regions, each characterized by unique geographical and agricultural conditions:

- In the Atlas Mountains foothills: The Ksour Ouled Naïl, Zibans, and Aures regions form an oasis chain that marks the transition to the Sahara.
- In the east: The Zibans (Biskra), Oued Ghir, Oued Souf (El Oued), and the Ouargla basin are prominent areas known for their cultivation of the Deglet Noor variety, which holds high commercial value.
- In the west: Regions like Saoura (Beni Abbes), Touat (Adrar), Gourara (Timimoun), and Tidikelt (Reggane) have palm groves with cultivars of relatively lower commercial quality. However, this area is significant for hosting the Taqerbucht cultivar, the only known variety resistant to the Bayoud disease.

- At the center: Areas such as El Golea, M'zab (Ghardaïa), and Laghouat also feature extensive date palm cultivation.

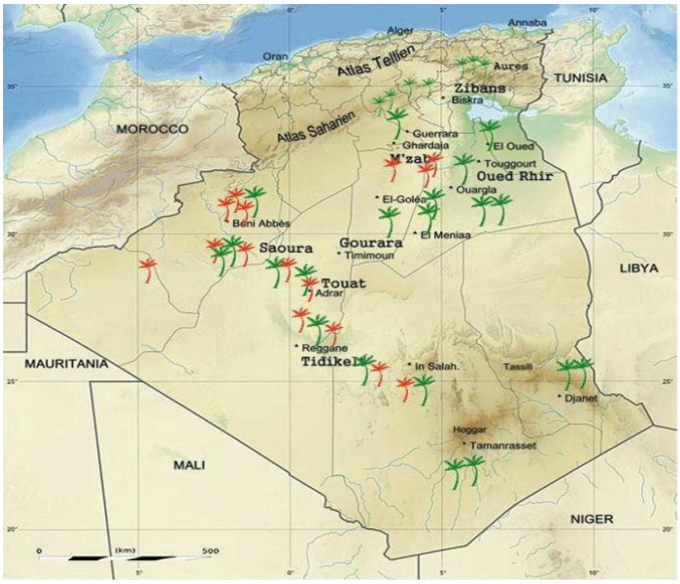


Figure 4.2 Map of Algeria indicating the different areas with date palms[120]

## 4.3 Characterization of biomass

The used methods for biomass characterization are mostly adapted from those used for coal characterization. Proximate and ultimate analyses are determined experimentally to represent the quality of the biomass. Proximate analysis gives the volatile matter, moisture, fixed carbon and ash composition. Ultimate analysis gives results that are more comprehensive on the elemental composition of the fuel (i.e. C, H, N, and O). These analyses are critical for evaluating the biomass's energy potential.

In addition to these analyses, we calculate the **lower heating value (LHV)** and **higher heating value (HHV)** to quantify the energy content of the biomass and other characteristics. This data is essential for assessing the feasibility of using these resources in various bioenergy applications.

### *4.3.1 Ultimate analysis*

#### *4.3.1.a Simple preparation for Date Palm Waste (DPW)*

The raw date palm waste (DPW), including fronds, leaves, and trunks, was collected from the region of Biskra. The samples were air-dried to reduce moisture content to below 10% and subsequently ground to a particle size of ≤1 mm using a mechanical grinder, as specified *in ISO*

*14780:2017*. The prepared samples were stored in airtight containers to prevent moisture uptake and contamination before analysis.

#### *4.3.1.b Analytical method*

The total carbon (C), hydrogen (H), and nitrogen (N) content of the date palm waste were determined in accordance with NF EN ISO 16948:2015, which prescribes instrumental methods for solid biofuels. The analysis was performed using an elemental analyser (CHNOS analyser, EA3100series), which utilizes a combustion method followed by gas chromatography to quantify the elemental concentrations.

- Weighing and Loading: Approximately 0.1–0.2 g of each prepared DPW sample was weighed using an analytical balance with an accuracy of ±0.1 mg. The sample was placed in a tin capsule for precise combustion.
- Combustion: The samples were combusted in the analyser at a temperature of approximately 900–1000°C in an oxygen-rich atmosphere.
- Detection: The evolved gases were carried through a thermal conductivity detector (TCD) or a mass spectrometer for quantification. Calibration of the equipment was performed prior to analysis using certified reference materials such as acetanilide or similar

### *4.3.2 Proximate analysis*

The proximate analysis of DPW was conducted to determine its moisture content, volatile matter, ash content, and fixed carbon, in accordance with ISO standards for solid biofuels:

#### *4.3.2.a Moisture content (CM)*

Moisture content was determined following ISO 18134-1:2015. Approximately 1 g of the prepared sample was weighed and dried in an oven at 105 ± 2°C for 24 hours. After cooling in a desiccator, the weight loss was calculated to determine the moisture content:

$$Moisture\ content\ (\%) = \frac{Initial\ weight - Dry\ weightal\ weight}{Initial\ weight} \times 100 \qquad (4.1)$$

#### *4.3.2.b Volatile matter (VM)*

The volatile matter was analysed according to ISO 18123:2015. 1 g of the sample was heated in a muffle furnace at 900 ± 10°C for 7 minutes in a lidded crucible to prevent air ingress. The weight loss, excluding moisture, was recorded as the volatile matter.

#### *4.3.2.c Ash content*

The ash content was determined following ISO 18122:2015. Approximately 1 g of the sample was combusted in a muffle furnace at 550 ± 10°C for 4 hours until a constant weight was achieved. The residue was weighed to calculate the ash content :

$$Ash\ content\ (\%) = \frac{Weight\ of\ residue}{Initial\ weight} \times 100 \qquad (4.2)$$

#### *4.3.2.d Fixed carbon*

Fixed carbon content was calculated by difference, as follows:

$$\text{Fixed carbon}\ (\%) = 100 - (\text{MC} + \text{VM} + \text{Ash content}) \qquad (4.3)$$

Each analysis was performed in triplicate to ensure reproducibility and reliability. Calibration of the furnace and weighing equipment was performed prior to analysis.

### *4.3.3 High heating value (HHV)*

The Higher Heating Value (HHV) and Lower Heating Value (LHV) of DPW were determined following ISO 18125:2017 for solid biofuels. The HHV was measured using a bomb calorimeter ([insert model and manufacturer]). 1 g of the ground sample was placed in the bomb calorimeter, and the combustion was carried out in an oxygen atmosphere under controlled conditions:

- **Combustion:** The sample was ignited, and the heat released was measured as the temperature rise in the surrounding water bath.
- **Calculation:** The HHV (expressed in MJ/kg) was calculated using the following formula:

$$HHV = \frac{\Delta T \times W}{m} \qquad (4.4)$$

where $\Delta T$ is the temperature rise (°C), W is the calorimeter's water equivalent (kJ/°C), and mmm is the mass of the sample (kg).

### *4.3.4 Low heating value (LHV)*

The LHV was calculated from the HHV by accounting for the latent heat of water vapor formed during combustion. The formula used was:

$$\mathrm{LHV} = \mathrm{HHV} - (2.447 \cdot \mathrm{H} \cdot 8.94) \qquad (4.5)$$

where HHH is the hydrogen content of the sample (measured using elemental analysis, NF EN ISO 16948:2015), and 2.447 is the energy required to vaporize 1 g of water (MJ/kg).

the table below summarize the characterization of the most important biomass.

Table 4.1 the characterization of the 3 most important biomass in Algeria

| Proximate analysis (wt. %) | Olive oil | | | Date palm | | | | | Wheat Waste | |
|---|---|---|---|---|---|---|---|---|---|---|
| | **Olive pomace (3-phase)**[121] | **Olive tree pruning**[121] | **Olive leaves and twigs** [121] | **Petioles** [74,75] | **Rachis** [121] | **Brunch**[38] | **Fibrilium** [74,75] | **Palm** [74,75] | **Wheat Straw** [122] | **Wheat Husk** |
| **Moisture content (as received)** | 15 (ELIAS & Boumeddane, 2021) | 20 | 5 | 7.3 | 4.4 | 4.8 | 5.7 | 3.9 | 9.67 | 5.98 |
| **Ash content (dry basis)** | 5 | 8,6 | 4.41 | 6.4 | 3.2 | 5.2 | 5.7 | 5..2 | 12.59 | 12.11 |
| **Volatile matter (dry basis)** | 77.38 | 71,41 | 74.73 | 74 | 86 | 79 | 78 | 68 | 71.74 | 69.19 |
| **Fixed carbon (dry basis)** | 17.6 | 19,88 | 16.31 | 28.05 (Bousdira, et al., 2018) | 23.3 (Bousdira, et al., 2018) | 25.3 (Bousdira, et al., 2018) | 18 (Bousdira, et al., 2018) | 18.1 (Bousdira, et al., 2018) | 9.67 | 12.72 |
| **C** | 51.31 | 45,08 | 47.1 | 45.04 | 43.6 | 46.06 | 45.39 | 41.09 | 43.5 | 41.47 |
| **H** | 6.38 | 5,89 | 6.18 | 5.56 | 6.4 | 5.59 | 5.62 | 5.47 | 5.93 | 5.83 |
| **N** | 1.82 | 0,52 | 0.55 | 0.38 | - | 5.77 | 0.49 | 0.76 | 3.43 | 2.55 |
| **S** | 0.16 | 0.09 | 0.1 | 0.15 | - | 0 | 0.07 | 0.22 | 0.00 | 0.10 |
| **O (by difference)** | 44.35 | 39.7 | 41.66 | 38.31 | 40.3 | 42.68 | 39.35 | 34.49 | 34.35 | 37.97 |
| **LHV (MJ/kg)** | 16.836 | 17.2 | 16.73 | - | - | - | - | 16.85 | 14.77 | 18.18 |

| | | | | | | | | | | |
|---|---|---|---|---|---|---|---|---|---|---|
| **HHV (MJ/kg)** | 14.48 | 16.41 | 17.74 | 18.3 | 17.5 | 18.6 | 18.6 | 18 | 18.91 | 19.55 |
| **Ash melting point (°C)** | - | - | - | - | - | - | - | - | 850-900 | - |
| **Bulk density (kg/$m^3$)** | 700 | 272-374.9 ( Francisco , et al., 2020) | 108 | 160 | 635 | 555 | 209 | - | 160.75 | 750 |
| **Particle size distribution (mm)** | 1-3mm 10%<br>3-5 mm 60%<br>5-8 mm 30 % | >100 mm | 30-50mm 10<br>50-70mm 70%<br>>70mm 20%( | 0.4-100 ( Almi, Benchabane, Lake, & Kriker, 2015) | 0.60-0.75 ( Almi, Benchabane, Lake, & Kriker, 2015) | 0.3-05 ( Almi, Benchabane, Lake, & Kriker, 2015) | 0.5-08 ( Almi, Benchabane, Lake, & Kriker, 2015) | 3.22–14.89 mm (0.79%) [123] | 0.5mm± 0.2mm for a large variety of straw wheat (6.64%) | 50-100 µm<br>100-200 µm<br>200-300 µm<br>300-400 µm<br>400-650 µm<br>>650 µm |

## 4.4 Date palm sample

The biomass selected is a date palm waste (DPW) sample from the region of Biskra (Algeria). The Table 4.2 illustrates the ultimate and proximate analysis of the date palm sample. The proximate and ultimate analysis were done according to the standards UNE 15104:2011 , UNE–EN ISO18123, UNE 32-004-84 and UNE 32-002-95 at the Research Centre Scientific And Technical In Analyses Physical (CRAPC) in Algeria [124,125].

Table 4.2 Ultimate and proximate analysis for date palm waste

| **Ultimate analysis (wt.%)*** | | | | | **Proximate analysis (wt.%)*As-received** | | | |
|---|---|---|---|---|---|---|---|---|
| C | H | N | S | O*diff | Ash | VM | FC*diff | Moisture |
| 44.27 | 5.59 | 0.38 | 0.07 | 49.69 | 5.2 | 79 | 11 | 4.8 |

O*diff: % of oxygen calculated from difference of C,H, N and S; VM*: Volatile matter. FC*diff The fixed carbon content is calculated by subtracting the sum of moisture content volatile matter and Ash from 100%.

## 4.5 Aspen Plus modelling

Aspen Plus software permits the combination of different processes, such as biomass drying, syngas cleaning, combustion systems and chemicals production. Therefore, Aspen Plus simulator is considered as an advantageous tool to design new processes and develop present ones with a reliable prediction [126].

Figure 4.3 shows the Aspen Plus flowsheet for the methanol production from date palm waste. The steps involved in the methanol synthesis from DPW are: gasification process, gas treatment and methanol synthesis. In order to simplify the explanation of the simulation, the three primary units will be explained sequentially. Firstly, the feedstock is gasified using steam as gasifying medium. The product gas is then fed to the gas treatment unit in which the gas is to be cleaned from impurities such as ash. Finally, the cleaned syngas is fed to the methanol synthesis unit to produce methanol. The units and their functions are tabulated in Table 4.3.

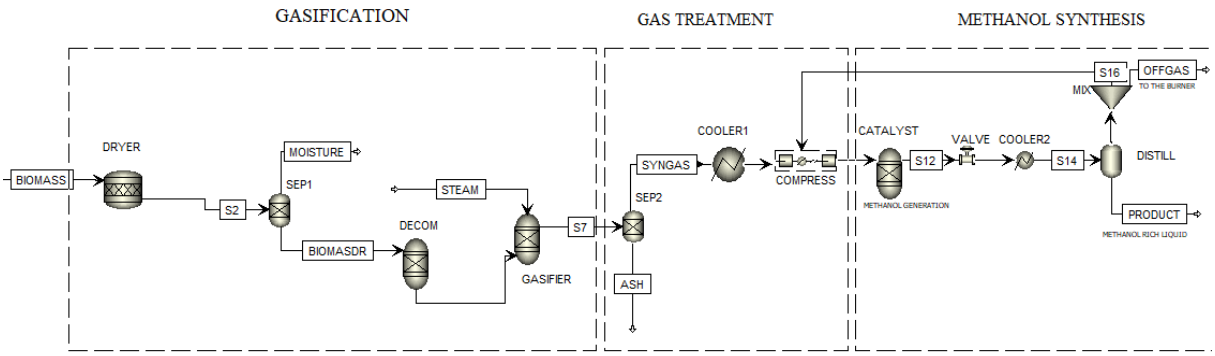


Figure 4.3 AspenPlus flowsheet process

Table 4.3 The Aspen Plus blocks and their corresponding descriptions.

| Name | Type | Temperature (°C) | Pressure (Bar) | Description |
|---|---|---|---|---|
| Dryer | RSTOIC | 100 | 1 | Model the drying mechanism for the purpose of extracting moisture content from the initial raw material. |
| Sep1 | Sep | 100 | 1 | Separate moisture and feedstock |
| Boiler | HEATER | 100 | 1 | The heater simulates the heat exchangers, enabling the recovery of the heat losses for heating the water to a temperature of 100°C. |
| Decom | RYIELD | 800 | 1 | This scientific process involves transforming non-conventional raw materials into conventional elements, as determined by analysing their elemental composition. |
| Gasifier | RGIBBS | 800 | 1 | The process of gasification reaction is simulated using a reactor that utilizes Gibbs free energy. |
| Sep2 | SEP | 800 | 1 | Separate ash from syngas |
| Cooler1 | HEATER | 120 | 1 | Lower the temperature of syngas. |

| | | | | |
|---|---|---|---|---|
| compress | COMPRESSOR | 200 | 50 | Increase the pressure of syngas by subjecting it to compression. |
| Catalyst | RSTOIC | 220 | 50 | A reactor designed specifically for the purpose of synthesizing methanol. |
| Valve | VALVE | 213 | 10 | Use to decrease the pressure of the methanol produced |
| Cooler2 | HEATER | 60 | 1 | Lower the temperature of produced methanol temperature |
| Distill | FLASH2 | 60 | 1 | Separate the gas, water and the methanol |
| MIX | MIX FSplit | 60 | 1 | Separate the portions of gas |

### *4.5.1 Component*

A fundamental prerequisite for reliable process simulation in Aspen Plus is the accurate definition and classification of all components involved in the system. In this study, a mixture of conventional and nonconventional components was defined to represent the various materials and chemical species present throughout the biomass gasification and methanol synthesis processes. The complete list of components is provided in Table 4.4.

Table 4.4 The list of components

| **Component ID** | **Type** | **Component name** | **Formula** |
|---|---|---|---|
| Biomass (DPW) | Nonconventional | - | - |
| Ash | Nonconventional | - | - |
| C | Solid | CARBON | C |
| CO | Conventional | CARBON MONOXIDE | CO |

| | | | |
|---|---|---|---|
| $CO_2$ | Conventional | CARBON DIOXIDE | $CO_2$ |
| $CH_4$ | Conventional | METHANE | $CH_4$ |
| $CH_3OH$ | Conventional | METHANOL | $CH_3OH$ |
| $H_2$ | Conventional | HYDROGEN | $H_2$ |
| $H_2O$ | Conventional | WATER | $H_2O$ |
| $O_2$ | Conventional | OXYGEN | $O_2$ |
| $N_2$ | Conventional | NITROGEN | $N_2$ |
| $H_2S$ | Conventional | HYDROGEN SULFIDIC | $H_2S$ |
| $SO_2$ | Conventional | SULFUR-DIOXIDE | $SO_2$ |
| HCL | Conventional | HYDROGEN-CHLORIDE | HCL |

Conventional components—including hydrogen ($H_2$), carbon monoxide (CO), carbon dioxide ($CO_2$), methane ($CH_4$), water ($H_2O$), nitrogen ($N_2$), hydrogen sulfidic ($H_2S$), and methanol ($CH_3OH$)—were selected from Aspen Plus' built-in component database. These compounds have well-defined molecular structures and associated thermodynamic and transport property data, enabling the software to calculate a wide range of properties such as enthalpy, entropy, density, heat capacity, and fugacity using the selected thermodynamic model (PR-BM in this case).

In contrast, the biomass (DPW) feedstock and ash were modelled as nonconventional components due to the absence of well-defined molecular formulas. These materials are typically complex, heterogeneous mixtures of lignocellulosic biomass and inorganic residues, for which traditional molecular-based property estimation is not feasible. As such, they were defined using proximate and ultimate analysis data, which characterize biomass in terms of elemental composition (C, H, O, N, S, ash content) and physical behaviour (moisture content, volatile matter, fixed carbon, etc.).

Aspen Plus accommodates such nonconventional solids by treating them using specialized property estimation models originally developed for coal-derived materials, which share similar combustion and gasification behaviour with biomass. These models were employed to calculate only the properties that are meaningful for nonconventional solids—primarily enthalpy and density. The HCOALGEN model was used for estimating enthalpy, based on the correlations

derived from heat-of-combustion measurements of solid fuels, while the DCOALIGT model was used to estimate the solid-phase density.

Although originally tailored for coal, these models have been widely validated and adapted for lignocellulosic biomass simulation in thermochemical applications. Their use ensures thermodynamic consistency during process simulation, particularly in energy balance calculations and in the RYIELD block, where the biomass is decomposed into its elemental constituents before entering the equilibrium gasifier

### *4.5.2 Gasification process*

In this simulation via Aspen Plus, the biomass and ash were defined as a non-conventional (NC) component, a Peng-Robinson equation of state with Boston-Mathias alpha function (PR-BM) was selected to estimate the physical properties of the conventional components such as $H_2$, CO, $CO_2$, $CH_4$, $H_2O$, $N_2$, H2S, and $CH_3OH$.

This method is suitable for gasification systems that operate at elevated temperatures (700–1000 °C) and moderate to high pressures (1–50 bar), particularly in systems involving polar and non-ideal gases such as H2, CO, CO2, CH4, and methanol [127].

The original Peng-Robinson EOS is a cubic equation of state suitable for non-polar and mildly polar substances at high pressures and moderate to high temperatures. It is commonly used in simulations involving hydrocarbon systems and syngas production.

The equation is expressed as :

$$P = \frac{RT}{V-b} - \frac{a}{V^2+2Vb-b^2} \tag{4.6}$$

Where:

- P: Pressure (Pa)
- T: Temperature (T)
- V: Molar volume $(m^3/mol)$
- R: Gas constant (J/(mol.k)

- a, b: Substance-specific parameters that account for intermolecular attractions and molecular volume (Pa. $(m^3/mol)^2$) and $(m^3/mol)$ respectively.

This equation provides reasonable accuracy for gasification-related components like CO, CO2, CH4, and H2 under elevated temperatures.

The PR-BM method enhances the original PR-EOS by incorporating an improved temperature dependency for the alpha function, making it more reliable for polar compounds and associating species like methanol and water. The modified attraction term becomes temperature-dependent:

$$a(T) = a \times \alpha(T) \tag{4.7}$$

When Peng-Robinson with the Boston-Mathias alpha function (PR-BM) is selected as the global thermodynamic method in Aspen Plus, the software utilizes this equation of state as the central framework to compute all thermophysical and phase equilibrium properties for conventional components.

Aspen Plus retrieves the component-specific critical properties: critical temperature ($T_c$), critical pressure ($P_c$), and the acentric factor (ω). These are used to calculate the attraction parameter a(T) and the co-volume parameter b of the Peng-Robinson equation. The temperature dependence of a(T) is refined through the Boston-Mathias alpha function, which improves the accuracy of the model for polar and associating compounds. The PR-BM took place in the RGibbs reactor and it it calculates phase equilibria and chemical equilibrium based on minimization of Gibbs free energy.

The choice of PR-BM in our study is due to the gasification and methanol synthesis processes which involve polar and non-ideal gases such as water vapor, methanol, hydrogen, and carbon monoxide. The PR-BM method was therefore chosen due to its:

- Proven accuracy in modelling non-ideal, associating components.
- Compatibility with high-temperature, moderate-to-high pressure systems.
- Standard use in biomass gasification and syngas-to-methanol simulations in literature.

To further understand the assumptions, the Aspen Plus simulation employed a simplified gasification equilibrium model, which was subsequently verified through successful validation

against experimental data. This equilibrium-centric approach specifically accounts for equilibrium products, encompassing methane, hydrogen, carbon monoxide, carbon dioxide, water, and compounds containing sulfur and nitrogen that emerge within the reactor. Notably, it omits the consideration of higher molecular weight hydrocarbons, such as tars and oils, which typically result from the intrusion of pyrolysis byproducts, as they are less likely to form under equilibrium conditions and are consequently excluded from the simulation. This equilibrium state offers a conducive environment for conducting a comprehensive optimisation study, with a primary focus on critical process parameters including gasification temperature, steam-to-biomass ratio, and the nature of the gasifying medium. It thereby simplifies the analysis by disregarding the intricacies associated with gasifier hydrodynamics and reaction kinetics [128].

The foremost assumptions considered in this unit of the process are:

1. The process is developed at steady state condition.
2. Isothermal conditions with no pressure change inside the gasifier.
3. Char is considered 100% carbon.
4. Tar is not considered in the system.
5. All gases are assumed to be ideal.
6. No unconverted carbon is present in the product.
7. All reactions have reached thermodynamic equilibrium based on Gibbs' free energy minimization.

The gasification process unit is composed of three principal blocks. Drying (DRYER), decomposition (DECOM) and gasification (GASIFIER). We first introduce the biomass by specifying its ULTANAL and PROXANAL analysis to the RSTOIC reactor (DRYER) where the moisture is evaporated at 1 atm and 100°C, to be extracted by the separator (SEP1). Next, the BIOMASDR that has been dried is subjected to decomposition in the RYIELD reactor (DECOM) at a temperature of 800°C and 1 atm pressure. This process utilises the calculator block specified in Table 4.5 to determine the elemental composition (C, H, O, N, S) based on the mass composition provided by the proximate and ultimate analysis shown in Table 4.2. After that, the decomposed biomass and steam at 100°C that has been produced by the Boiler, are fed into the RGIBBS Reactor (GASIFER) where the gasification process took place to estimate syngas composition by minimizing Gibbs-free energy at 1atm and different temperature ranges.

Table 4.5 The calculator block utilised to convert non-conventional to conventional components

| |
|---|
| Water=PROXANAL (1) |
| H2O=WATER/100 (2) |
| Ash=UTM1/100*((100-WATER)/100) (3) |
| Carbon=UTM2/100*((100-WATER)/100) (4) |
| H2=UTM3/100*((100 WATER)/100) (5) |
| Nitrogen=UTM4/100*((100-WATER)/100) (6) |
| O2=UTM5/100*((100-WATER)/100) (7) |
| Sulfur=UTM6/100*((100-WATER)/100) (8) |

The gasification reactions involved in this process are as below:

| | | | |
|---|---|---|---|
| Water Gas: | $C + H_2O \leftrightarrow CO + H_2$ | $\Delta H = 131 Kj/mol$ | (4.6) |
| Water gas shift: | $CO + H_2O \leftrightarrow CO_2 + H_2$ | $\Delta H = -41 Kj/mol$ | (4.7) |
| Steam reforming: | $CH_4 + H_2O \leftrightarrow CO + 3H_2$ | $\Delta H = 206\ Kj/mol$ | 4.8) |
| Boudouard: | $C + CO_2 \leftrightarrow 2CO$ | $\Delta H = 172\ kJ/mol$ | 4.9) |

### *4.5.3 Gas cleaning process*

The objective of this stage was to purify the gas exiting the gasification process, with the goal of obtaining a high-grade syngas suitable for methanol synthesis.

In the gasification process, the gas produced from the reaction between the feedstock and steam is typically contaminated with impurities such as ash, which can have a negative impact on downstream processes, The syngas utilised for methanol production must meet a specific criterion [129,130], the ratio of $H_2$ to CO ranging from 2.4 to 2.5.

$$\frac{H_2}{CO} = 2.4 - 2.5 \qquad (4.10)$$

Therefore, it is necessary to remove these impurities before further processing. This is achieved by introducing the gas stream (S7), as shown in Figure 4.4, into a separator reactor (Sep2), where the ash is separated from the gas phase.

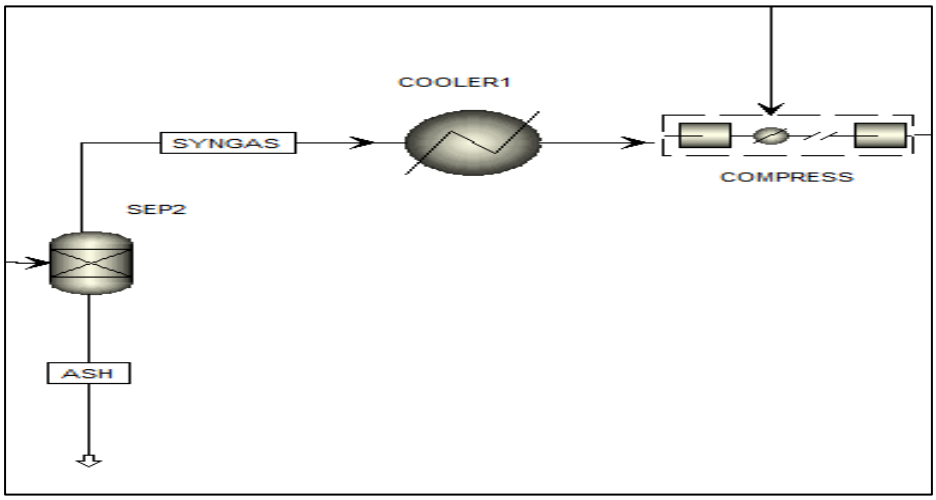


Figure 4.4 Gas treatment

Once the syngas is cleaned from impurities such as ash, it is necessary to reduce its temperature to meet the compression requirements of downstream processes. To achieve this, the cleaned syngas is introduced to an exchanger (COOLER1), where it is cooled down to 120 °C. The cooled syngas is then fed to a compressor (COMPRESS), where the pressure is increased to 50 atm, while the temperature is raised to 200°C. This is required to meet the standard operating conditions for methanol production [130].

By compressing the syngas, its energy content is increased, allowing it to be more efficiently utilised in downstream processes. Additionally, the increased pressure of the syngas facilitates its transport and storage, while the higher temperature helps to avoid the formation of condensation and corrosion in the downstream equipment. Overall, this process configuration allows for the production of high-quality syngas that is well-suited for further conversion into valuable chemicals such as methanol.

### *4.5.4 Methanol synthesis*

After the cleaned syngas has been compressed, as shown in Figure 4.5 and mentioned in Appendix A, it is introduced into a reactor where the methanol production takes place in the presence of a Zn and Cu oxide catalyst. Different temperature ranges and pressures will be tested to identify the appropriate operating condition for methanol production. This type of catalyst is chosen due to its commercial availability, as described in reference [129]. The reactions involved during the methanol synthesis are as follow:

$$CO + 2H_2 \overset{Catalyst}{\longleftrightarrow} CH_3OH \qquad \text{-91 KJ/mol} \qquad (4.11)$$

$$CO_2 + 3H_2 \overset{Catalyst}{\longleftrightarrow} CH_3OH + H_2O \qquad \text{-50KJ/mol} \qquad (4.12)$$

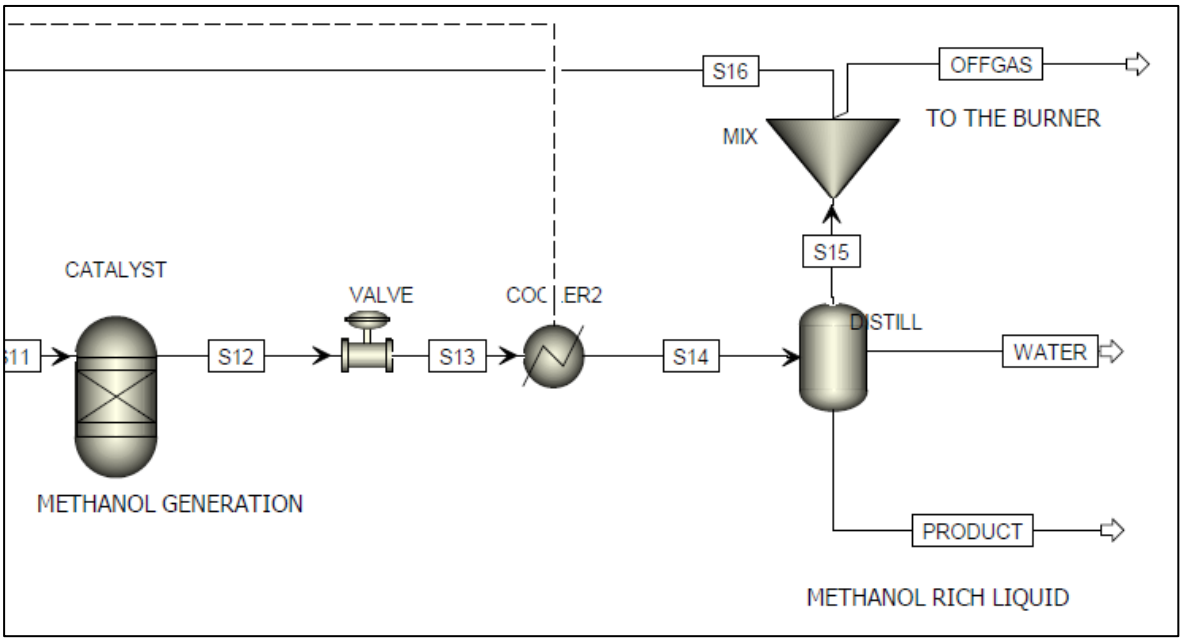


Figure 4.5 Methanol synthesis using Aspen plus

The product stream from the methanol reactor is expanded through a valve (VALVE) and then cooled using a heat exchanger (COOLER2), reducing its pressure to 1 bar and temperature to 60°C and, which are appropriate conditions for methanol condensation [52]. Next, the stream is introduced to a separator (Flash2), where the pure methanol is extracted, leaving behind the unreacted syngas. Afterward, 20% of the syngas undergoes recycling through stream (S16) and enters the compressor (COMPRESS) where its pressure and temperature rise. This leads to an elevated rate of methanol production, while the remaining 80% is utilised to fuel burners for other purposes, which will be further investigated in future research.

## 4.6 Conclusion

The chapter was divided into four key sections. The first section identified olive, wheat, and date palm wastes as the three most important biomass resources in Algeria in alignment with the tasks outlined in the REFFECT AFRICA project.

The second section detailed the physicochemical characteristics of these biomass types, including proximate and ultimate analyses, heating values, and elemental compositions.

The third section delved deeper into date palm waste, specifically focusing on its abundance in the Biskra region. Date palm residues were identified as a particularly promising feedstock due to their high availability and favourable composition for gasification processes.

The final section explored the Aspen Plus modelling of steam gasification using date palm waste from Biskra. The model simulated the gasification process, optimizing key parameters such as temperature, steam-to-biomass ratio, and gasifier design. The syngas produced was then used as a feedstock for methanol synthesis, showcasing a complete biomass-to-methanol pathway.

# Chapter 5 Results and discussion

## 5.1 Introduction

This chapter is dedicated to presenting and discussing the results of the study in detail. It starts with a sensitivity analysis aimed at evaluating the influence of key parameters on gas production. Specifically, the effects of temperature and the steam-to-biomass ratio are analysed to understand their roles in optimizing the process and enhancing gas yields. These parameters are critical for identifying operational conditions that maximize efficiency and performance in biomass conversion processes.

Following the sensitivity analysis, the chapter delves into the methanol synthesis process, presenting the results obtained under various operating conditions. This section focuses on the relationship between the synthesis process and the intermediate outputs from the gasification stage, emphasizing how the process parameters influence the final yield and quality of methanol.

To ensure the reliability and accuracy of the proposed model, a validation step is included. The results are compared with data available in the literature, highlighting the model's capacity to predict trends and outputs effectively.

The chapter concludes with an analysis of optimal process improvements based on the results obtained. The focus is on proposing actionable recommendations to enhance the overall process efficiency, reduce energy consumption, and improve the sustainability of the system.

## 5.2 Sensitive analysis

### *5.2.1 Impact of temperature on gas production*

Temperature is one of the most influential variables governing the gasification process, as it directly affects the equilibrium position of the principal chemical reactions occurring in the reactor. In this study, three gasification temperatures—800°C, 900°C, and 1000°C—were simulated using Aspen Plus to evaluate their effect on the composition of the resulting syngas, with particular emphasis on hydrogen, carbon monoxide, carbon dioxide, and methane.

The simulation results (Figures 5.1–5.4) indicate that as the temperature increases, the molar fraction of carbon monoxide (CO) rises significantly, while the concentrations of carbon dioxide ($CO_2$) and methane ($CH_4$) decrease. Interestingly, the concentration of hydrogen ($H_2$) remains relatively stable over the temperature range considered.

This behaviour is consistent with the thermodynamic nature of the key gasification reactions. The Boudouard reaction ($C + CO_2 \rightleftharpoons 2CO$), the steam reforming of methane ($CH_4 + H_2O \rightleftharpoons CO + 3H_2$), and the water-gas reaction ($C + H_2O \rightleftharpoons CO + H_2$) are all strongly endothermic. According to Le Chatelier's principle, an increase in temperature shifts the equilibrium of these reactions toward the product side, thereby enhancing CO and $H_2$ production. Consequently, the decline in $CH_4$ and $CO_2$ concentrations with rising temperature reflects their conversion into more thermodynamically favoured products under high-temperature conditions.

On the other hand, the water-gas shift reaction ($CO + H_2O \rightleftharpoons CO_2 + H_2$) is exothermic and thus thermodynamically favoured at lower temperatures. At elevated temperatures, the equilibrium shifts backward, reducing $CO_2$ and $H_2$ formation in favour of CO and $H_2O$. This explains the reduction in $CO_2$ and the apparent plateau in $H_2$ concentration, despite the concurrent promotion of other hydrogen-producing reactions. The nearly constant hydrogen output is the result of a dynamic balance between competing $H_2$-generating and $H_2$-consuming reactions at high temperatures. These observations are consistent with previous studies [131,132].

Moreover, Figure 5.5 illustrates the variation in the $H_2$/CO molar ratio as a function of temperature. The data show a declining trend in this ratio as temperature increases. This is attributed to the disproportionately higher increase in CO production relative to $H_2$, especially due to the prominence of the Boudouard reaction at elevated temperatures. Although steam reforming and water-gas reactions contribute to $H_2$ formation, the suppression of the water-gas shift reaction and enhancement of CO-forming reactions reduce the relative hydrogen yield.

In summary, the temperature sensitivity analysis reveals that higher gasification temperatures enhance the yield of CO while reducing the presence of $CO_2$ and $CH_4$. Hydrogen remains relatively stable due to counteracting thermodynamic effects. These findings underscore the importance of carefully selecting operating temperatures based on the desired syngas composition and the target $H_2$/CO ratio, particularly in downstream applications such as methanol synthesis, where stoichiometric balance is critical.

### *5.2.2 Impact of steam to biomass (S/B) mass flowrate ratio*

In thermochemical biomass conversion, particularly steam gasification, the steam-to-biomass mass flowrate ratio (S/B) is a fundamental operational parameter that significantly influences the equilibrium composition of the produced syngas. In this study, the effect of varying the S/B ratio between 0.5 and 1.0 was evaluated at three different gasification temperatures: 800 °C,

900 °C, and 1000 °C. The resulting changes in the molar fractions of major gas species—$H_2$, CO, $CO_2$, and $CH_4$—were simulated using Aspen Plus and are presented in Figures 5.5.

The results reveal that increasing the S/B ratio led to a progressive increase in the concentrations of hydrogen ($H_2$) and carbon dioxide ($CO_2$), accompanied by a decrease in carbon monoxide (CO) and methane ($CH_4$). These trends are thermodynamically consistent with the stoichiometry and equilibrium shifts of several key gas-phase reactions involved in steam gasification.

The increase in $H_2$ yield with rising S/B is primarily due to the enhancement of the following endothermic reactions:

Steam reforming of methane:

$$CH_4 + H_2O \rightleftharpoons CO + 3H_2 \qquad \Delta H = +206 \text{ kJ/mol}$$

Water-gas reaction:

$$C + H_2O \rightleftharpoons CO + H_2 \qquad \Delta H = +131 \text{ kJ/mol}$$

Water-gas shift reaction:

$$CO + H_2O \rightleftharpoons CO_2 + H_2 \qquad \Delta H = -41 \text{ kJ/mo}$$

At higher steam concentrations, the water-gas shift reaction becomes increasingly dominant, converting more CO into $CO_2$ and $H_2$. This explains both the decline in CO concentration and the simultaneous rise in $H_2$ and $CO_2$ concentrations with increasing S/B ratio. This reaction is also exothermic, and although thermodynamically more favourable at lower temperatures, it is kinetically promoted by the higher partial pressure of steam, which drives the equilibrium toward the products even at elevated temperatures.

In parallel, the reduction in $CH_4$ content can be attributed to its participation in steam reforming reactions, particularly under conditions of excess steam. The availability of more steam molecules promotes the cracking of methane into CO and $H_2$, further contributing to the increase in hydrogen concentration. However, the extent of $CH_4$ reforming tends to reach a limit, and in some temperature ranges (notably at 1000 °C), $CH_4$ levels become nearly constant, indicating that methane is largely depleted or reforming reaches equilibrium saturation.

Furthermore, these reactions occur within the RGIBBS reactor in Aspen Plus, which assumes that all equilibrium reactions reach their thermodynamically favoured compositions based on Gibbs free energy minimization. The presence of additional steam shifts the chemical equilibrium in favour of reactions that consume steam (i.e., reforming and shift reactions), thus modifying the syngas composition predictably.

The effect of the S/B ratio on the $H_2$/CO molar ratio is especially relevant for downstream synthesis applications. As shown in Figure 5.5, increasing the steam input leads to a notable rise in the $H_2$/CO ratio. This is primarily a result of enhanced $H_2$ formation and the simultaneous suppression of CO via the water-gas shift reaction. From a process integration perspective, this ratio is a critical control parameter in determining the suitability of the syngas for methanol synthesis or Fischer–Tropsch synthesis, which both require specific stoichiometric $H_2$/CO ratios [129].

For instance, methanol synthesis conventionally requires an $H_2$/CO ratio of approximately 2.4. Based on the simulation results, this ratio can be achieved at an S/B mass flowrate ratio of 0.9 and a gasification temperature of 800 °C, under equilibrium conditions. Hence, selecting an appropriate S/B ratio is not only vital for maximizing hydrogen production but also for tailoring syngas composition to meet the specific requirements of downstream catalytic processes.

In conclusion, increasing the S/B ratio promotes reactions that enhance $H_2$ and $CO_2$ formation at the expense of CO and $CH_4$. These trends align with equilibrium thermodynamics and reflect the role of steam as both a reactant and a shift-inducing agent. The findings reinforce the importance of S/B optimization in designing gasification systems intended for synthesis gas production with specific compositional targets.

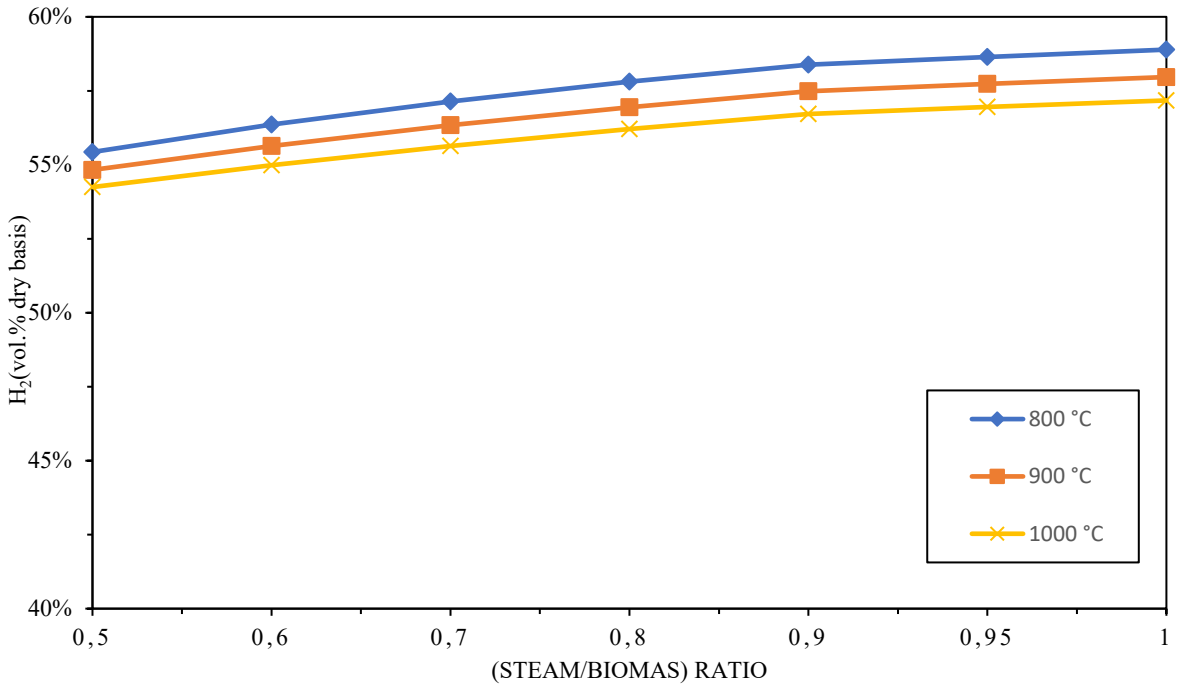


Figure 5.1: Influence of the S/B ratio on the syngas composition H2 at the three investigated gasification temperatures.

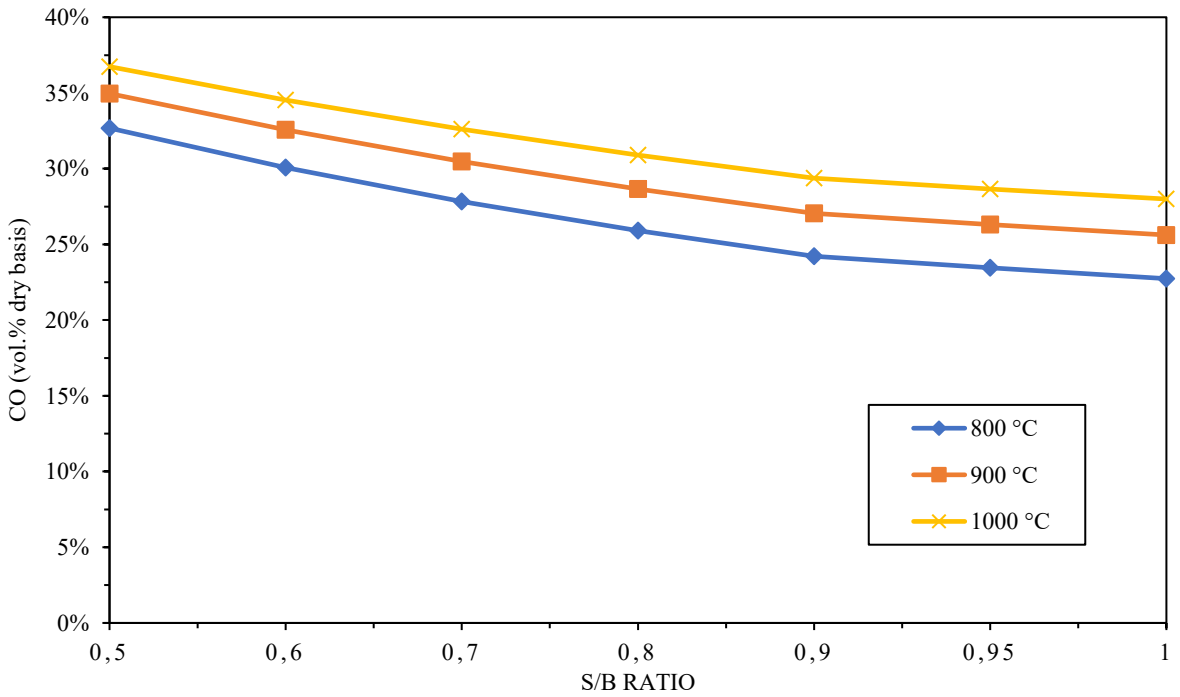


Figure 5.2 : Influence of the S/B ratio on the syngas composition; CO; at the three investigated gasification temperatures

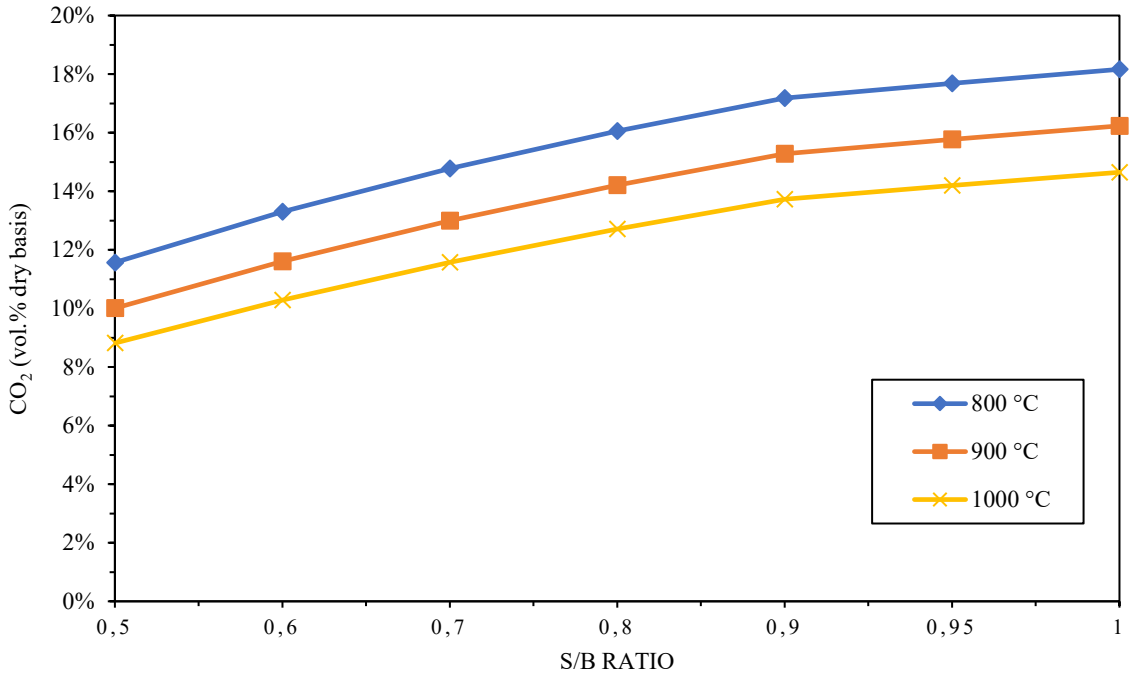


Figure 5.3: Influence of the S/B ratio on the syngas composition; CO2; at the three investigated gasification temperatures

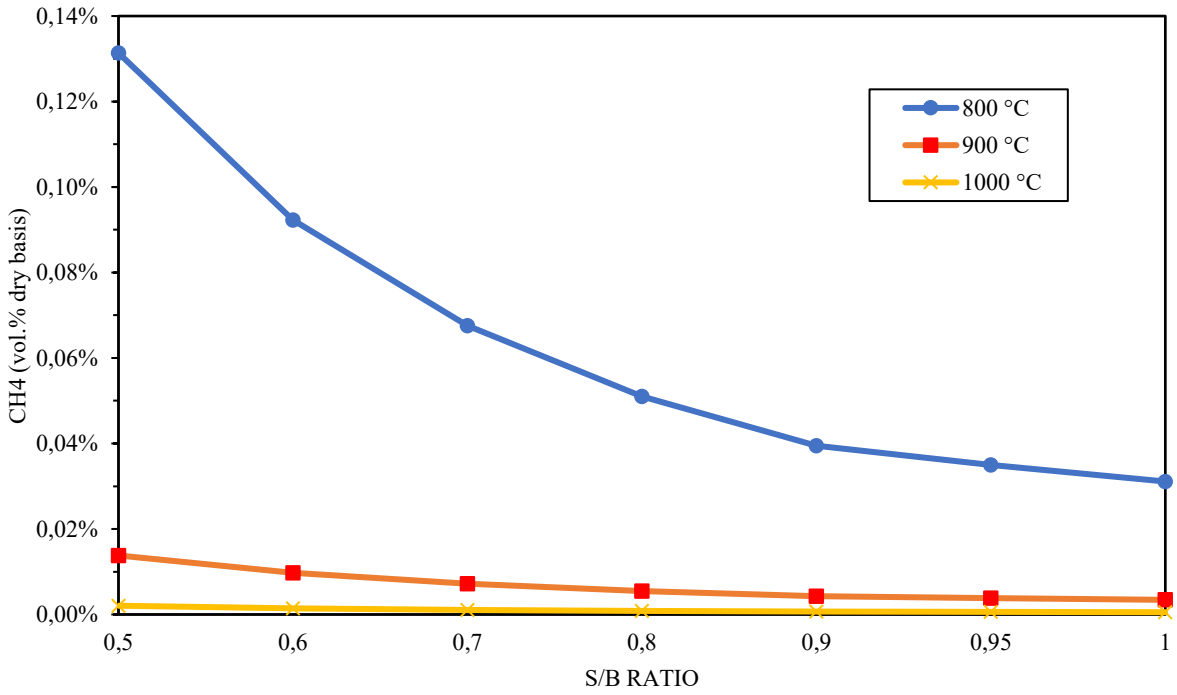


Figure 5.4: Influence of the S/B ratio on the syngas composition; CH4; at the three investigated gasification temperatures

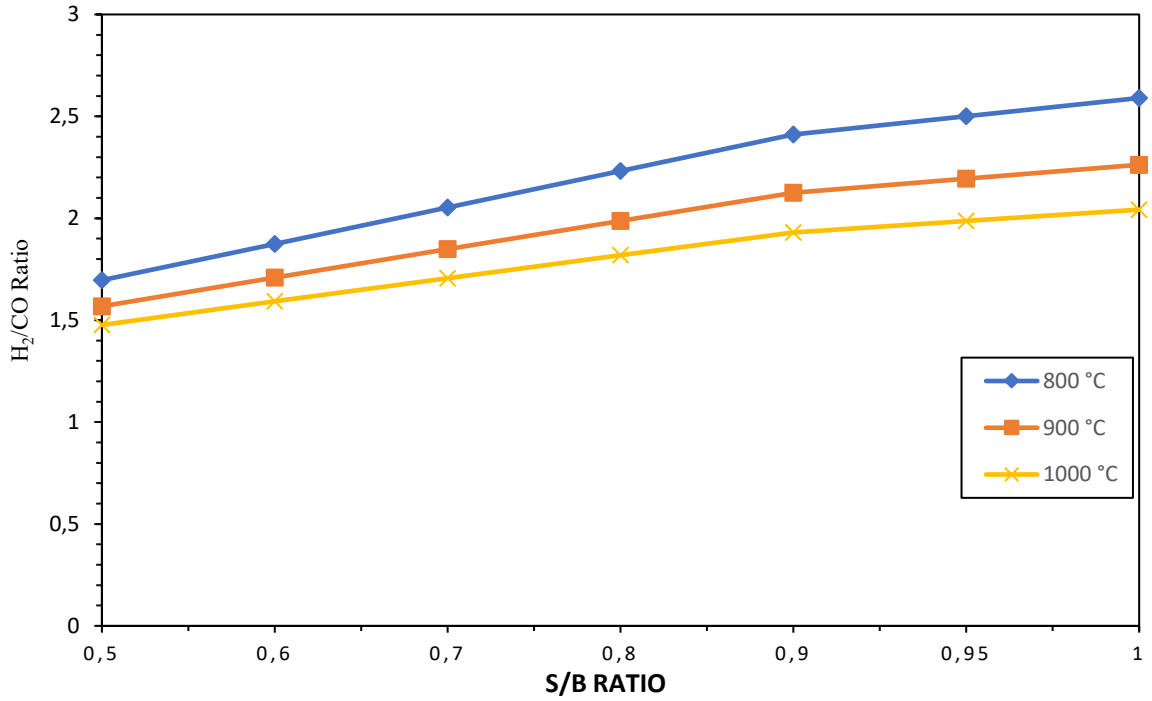


Figure 5.5: Impact of steam to biomass ratio on the H2/CO ratio

## 5.3 Methanol synthesis

To The synthesis of methanol from syngas (a mixture primarily composed of CO, $CO_2$, and $H_2$) is a catalytic process highly sensitive to thermodynamic and kinetic parameters, particularly temperature and pressure. In this section, the effects of these two parameters on methanol yield were investigated through simulation using Aspen Plus, with a focus on identifying optimal operating conditions that balance production efficiency and process feasibility.

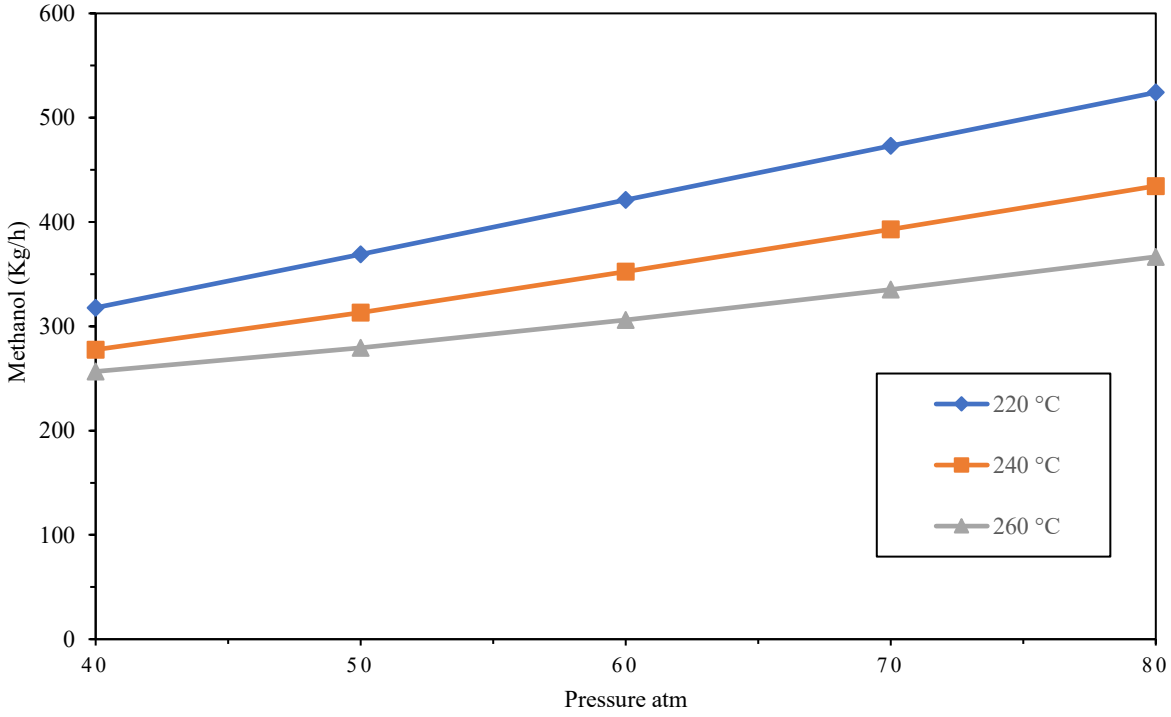


Figure 5.6 Impact of temperature and pressure on methanol production capacity

Based on a review of industrial practices and literature reports [130,133], the typical operational window for methanol synthesis lies within a temperature range of 220–280 °C and a pressure range of 50–100 bar. These conditions represent a compromise between kinetic activity and thermodynamic favourability, given the complex nature of the reactions involved.

Methanol is synthesized via two principal reversible reactions:

Hydrogenation of carbon monoxide:

$$CO + 2H_2 \rightleftharpoons CH_3OH \qquad \Delta H = -91 \text{ kJ/mol}$$

Hydrogenation of carbon dioxide:

$$CO_2 + 3H_2 \rightleftharpoons CH_3OH + H_2O \qquad \Delta H = -50 \text{ kJ/mol}$$

Both reactions are exothermic and accompanied by a reduction in the total number of moles of gas. From a thermodynamic standpoint, this implies that low temperatures and high pressures favor the forward reactions, as predicted by Le Chatelier's principle. Increasing pressure drives the equilibrium toward methanol formation due to the reduction in gas-phase volume, while decreasing temperature enhances the extent of conversion by shifting the equilibrium in favor of exothermic product formation.

However, practical considerations impose constraints on the extent to which these variables can be manipulated. High temperatures, although beneficial for accelerating reaction rates, can lead to catalyst degradation through sintering, fusing, and loss of active surface area. On the other hand, very low temperatures reduce the kinetic rate of methanol formation, requiring larger reactor volumes or longer residence times to achieve sufficient conversion. Similarly, while increasing pressure improves yield, it also imposes mechanical and economic limitations, including higher equipment costs, increased compressor energy demand, and safety considerations.

To assess these effects, a parametric simulation study was conducted using the RSTOIC reactor block in Aspen Plus, covering a range of pressures (30, 50, and 70 bar) and temperatures (220, 250, and 280 °C). The resulting methanol production capacities are illustrated in Figure 5.6.

The simulation results confirm that methanol yield increases with pressure and decreases with temperature, in line with the exothermic, volume-reducing nature of the reactions. Among the pressure levels studied, 50 bar was selected as the operating point, representing a trade-off between maximizing conversion and avoiding the operational complexities and cost escalations associated with pressures above 70 bar.

At this selected pressure, varying the temperature demonstrated the typical inverse relationship between temperature and methanol production: lower temperatures enhanced yield due to favorable equilibrium positioning, but excessively low values were avoided to maintain acceptable reaction kinetics.

In conclusion, the study underscores the delicate balance between thermodynamic optimization and practical operation in methanol synthesis. The use of moderate temperatures (220–250 °C) and elevated pressures (~50 bar) provides a viable path for maximizing methanol output from syngas derived from date palm waste gasification, while maintaining catalyst integrity and system efficiency. These findings align with industrial practice and support the feasibility of integrating biomass-derived syngas into methanol production systems.

## 5.4 Statistical analysis and comparison with literature

Although date palm waste is an important waste material, it has not been extensively investigated for its potential for syngas production through gasification, and there has not been reporting on methanol synthesis using the produced syngas. Previous in the literature have mostly been simulation-based, and in this section, we compare some of these reported studies to our current research. Inayat et al.[134] studied the configuration of a kinetic-based model using MATLAB for the steam gasification of date seeds and reported a 64 vol% $H_2$ production and a lower CO production of 19 vol%. We have also employed an additional experimental study of Bassyouni et al. [104] for comparative validation of our simulation. In this comparison, we maintained consistent operating conditions, utilising date palm waste as the feedstock, while keeping the temperature at 800 °C and ranging the steam-to-biomass ratio from 0.5 to 1.

Figures 5.7 to 5.10 depict the results of our comprehensive comparison between simulation and experimental data. Our simulation outcomes closely parallel the results reported in the referenced experimental study. Specifically, at S/B ratio of 1, our findings indicate a syngas composition of 58.88 mol% H2, 22.27 mol% CO, 18.16 mol% CO2, and 0.3 mol% CH4. This stands in contrast to the experimental results of 56.27 mol% H2, 21.71 mol% CO, 14 mol% CO2, and 3 mol% CH4. The primary distinctions arise from employing an equilibrium model in the simulation we proposed, as opposed to the experimental data that considered reaction kinetics, resulting in more rigorous outcomes. The errors observed were merely 5% for H2 and 3% for CO, both falling within acceptable margins. Consequently, the simulation can be deemed valid for replicating a gasification process. [17].

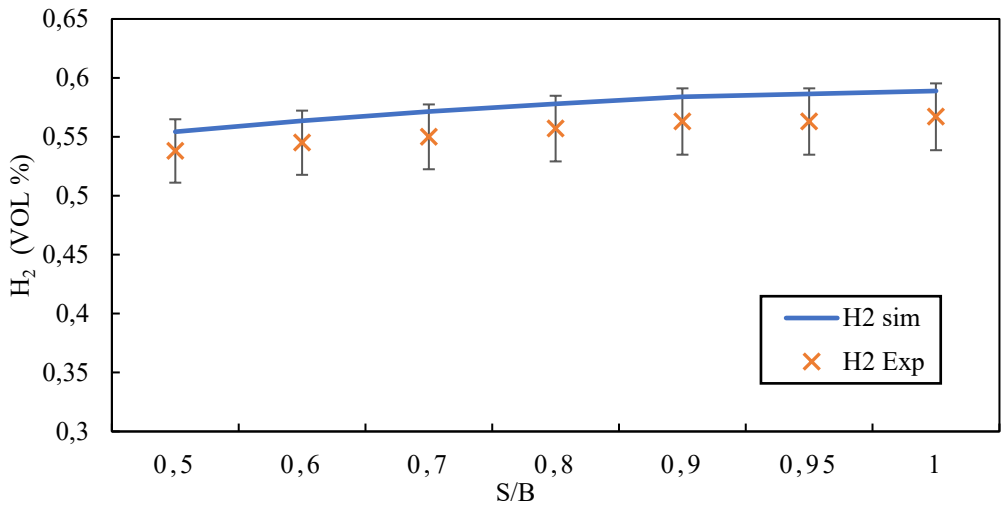


Figure 5.7 Hydrogen comparison between simulation values and experimental values

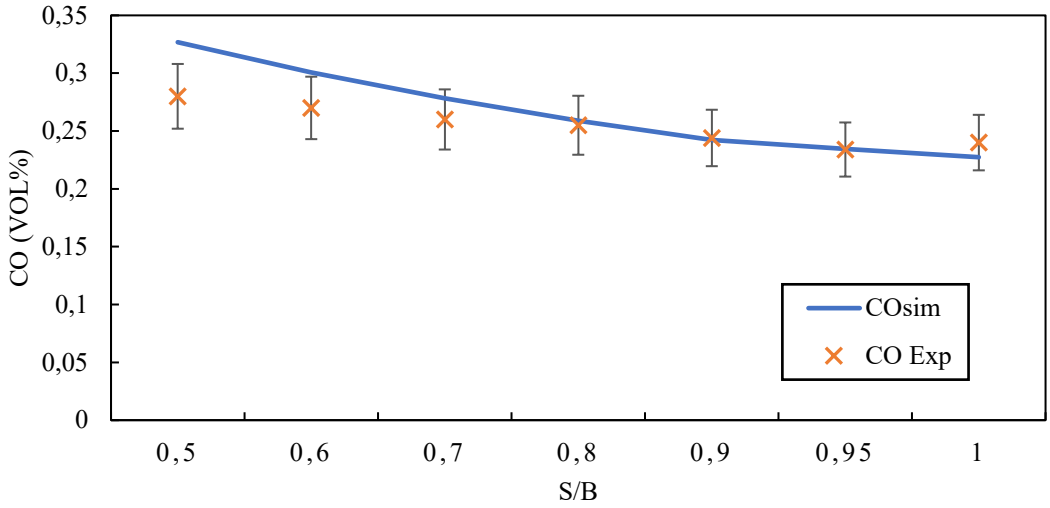


Figure 5.8: Carbon-monoxide comparison between simulation values and experimental values

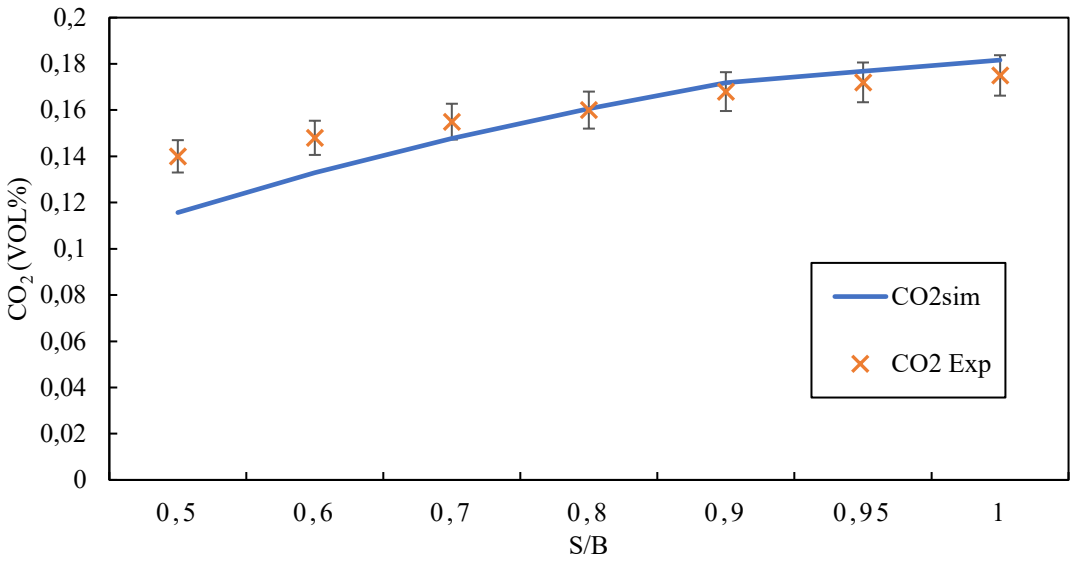


Figure 5.9 Carbon-dioxide comparison between simulation values and experimental values

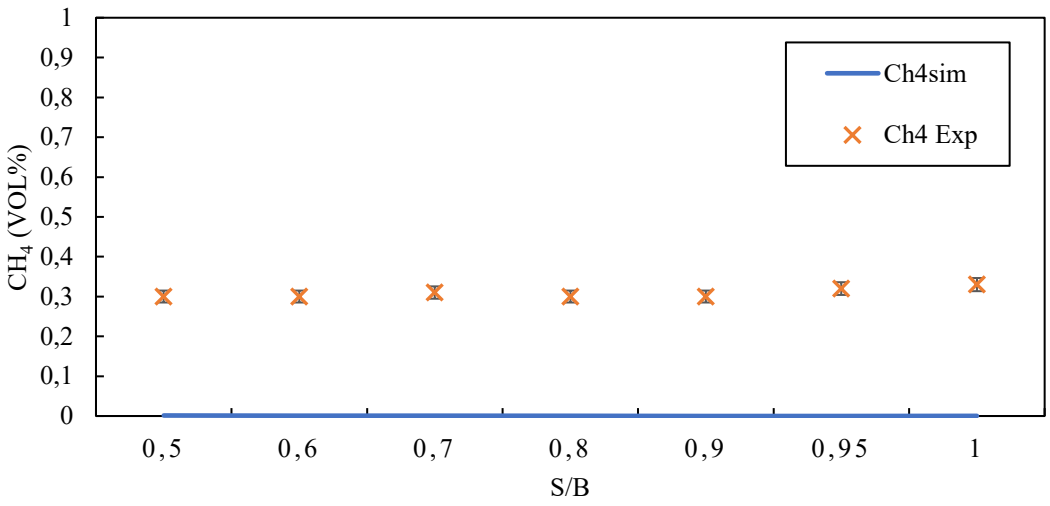


Figure 5.10 Methane comparison between simulation values and experimental values

Another study used Aspen Plus to configure a model that included other biomass, and when 99% of the feed was date pits, the syngas composition was reported as 45.25 vol% $H_2$, 22.67 vol% CO, 19.72 vol% $CO_2$, and 12.25 vol% $CH_4$ [105]. Babiker et al. [135] investigation of date palm seed steam gasification through both experimental and simulation methods produced a syngas with 35 vol% $H_2$, 29 vol% CO, 21 vol% $CO_2$, and 15 vol% $CH_4$. Finally, in the reference [132]a steam gasification of date palm is studied through an Aspen Plus process modelling with $H_2$ 37.88 vol%, CO 14.24 vol%, $CO_2$ 11.29 vol% and $CH_4$ 0.001 vol% at S/B ratio of 1 and 850 °C. Our current study achieved satisfactory composition of syngas, as compared to previous studies, with further details provided in Table 5.1.

Regarding the production of methanol from waste materials, there has been no documentation of studies investigating the utilisation of date palm waste for methanol synthesis. To address this gap in the literature, we conducted a comparative analysis of methanol production using pine biomass, this comparison is particularly relevant as both feedstocks exhibit similar ultimate and proximate analysis characteristics. Specifically, [129]. Puig-Gamero et al investigated the methanol synthesis from syngas produced through the steam gasification of pine biomass, utilising Aspen Plus simulation software. The study achieved a methanol production rate of 32kg/h for 100kg/h of pine biomass, operating at 220°C and 55atm.

for the waste stream of the methanol synthesis [136]. In our present study, we obtained satisfactory methanol production capacity in comparison to previous research, with more detailed information provided in Table 5.1.

Table 5.1 Comparison of syngas composition and methanol production with previous studies.

| Reference | Process parameters | Approach | Gas composition |
|---|---|---|---|
| **Present model** | • Feed: Date palm waste.<br>• T=800 °C.<br>• S/B= 1.<br>• T=220 °C.<br>• P= 50 Bar. | Aspen plus equilibrium modelling | $H_2$ 58.88 mol%, CO 22.27 mol%, $CO_2$ 18.16 mol%, $CH_4$ 0.3 mol% (DRY basis).<br>CH3OH = 368.92 Kg/h |
| **Bassyouni et al.** [104] | • Feed: date palm waste<br>• T = 800 °C<br>• S/B= 1 | Experimental Aspen HYSYS | $H_2$ 56.27 mol%, CO 21.71 mol%, $CO_2$ 14 mol%, $CH_4$ 3 mol% (DRY basis) |
| **Inayat et al.** [134] | • Feed: date seed<br>• T = 850 ◦C<br>• S/B= 1<br>• | Kinetic modelling Simulation | $H_2$ 64 vol%, CO 19 vol%, $CO_2$ 14 %, $CH_4$ 3 vol% |
| **AlNouss et al.** [105] | • Feed: date pits<br>• T = 850 ◦C<br>• S/B =1 | Aspen Plus equilibrium modelling | $H_2$ 45.25 vol%, CO 22.67 vol%, $CO_2$ 19.72 vol%, $CH_4$ 12.25 vol (dry basis) |
| **Babiker et al.** [135] | • Feed: Date palm seed<br>• T = 800°C<br>• S/B = 1 | Simulation and experimental | $H_2$ 35 vol%, CO 29 vol%, $CO_2$ 21 vol%, $CH_4$ 15 vol% |
| **Ali et al.** [132] | • Feed: Date palm<br>• T=850°C<br>• S/B= 1 | Aspen Plus, equilibrium modelling | $H_2$ 37.88 vol%, CO 14.24 vol%, $CO_2$ 11.29 vol%, $CH_4$ 0.001 vol% |

| | | | |
|---|---|---|---|
| **Puig-Gamero et al.** [129] | • Feed: pine biomass<br>• T= 220 °C<br>• P= 55 atm | Simulation and experimental Sociometric reactor & equilibrium reactor | $H_2$ 45–55vol%, CO 21–25vol%, $CO_2$ 18–22vol%, $CH_4$ 2–4 vol% (Dry Basis)<br>$CH_3OH$= 320kg/h |

## 5.5 Optimal process improvement

Following the successful calibration and validation of the methanol synthesis model, an optimization step was implemented to improve the overall efficiency and yield of the process. This improvement centred on the recovery and partial recycling of unreacted syngas from the product stream using a flash separation unit (SEP3), strategically integrated downstream of the methanol reactor.

In the baseline process configuration, the output from the methanol synthesis reactor contains a mixture of methanol, water, and unreacted syngas (primarily $H_2$, CO, and minor amounts of $CO_2$ and $CH_4$). To enhance methanol recovery while minimizing raw material losses, a flash unit was introduced to separate volatile, non-condensable gases from the condensed liquid product. The unreacted gas stream (stream 15) was extracted from the top outlet of the flash separator, while the condensed methanol-rich phase exited from the bottom.

To optimize conversion efficiency and reduce waste, 20% of the unreacted gas stream was recycled back to the methanol synthesis reactor. This recycled gas, compressed to reactor inlet pressure using a dedicated compressor unit, supplements the fresh syngas feed. The remaining 80% of the unreacted stream is directed to an energy recovery system, such as a combined heat and power (CHP) unit, which is the subject of a future energy integration study to be presented in a forthcoming publication.

The impact of recycling on methanol production capacity was significant. As illustrated in Figure 5.11, the introduction of the gas recycle loop increased the methanol production rate from 368.92 kg/h to 419.00 kg/h, corresponding to an absolute gain of 50.08 kg/h. This enhancement is attributed to the reintroduction of unconverted reactants—principally $H_2$ and CO, which are essential for methanol formation via the reversible exothermic reactions:

$$CO + 2H_2 \rightleftharpoons CH_3OH \qquad \Delta H = -91 \text{ kJ/mol}$$

$$CO_2 + 3H_2 \rightleftharpoons CH_3OH + H_2O \qquad \Delta H = -50 \text{ kJ/mol}$$

By enriching the feed with these key reactants, the reactor operates with a higher reactant-to-product conversion potential, effectively increasing the space-time yield without requiring additional fresh syngas input. Moreover, the partial recycling reduces the overall molar flow of inert species and low-value byproducts, improving the selectivity toward methanol.

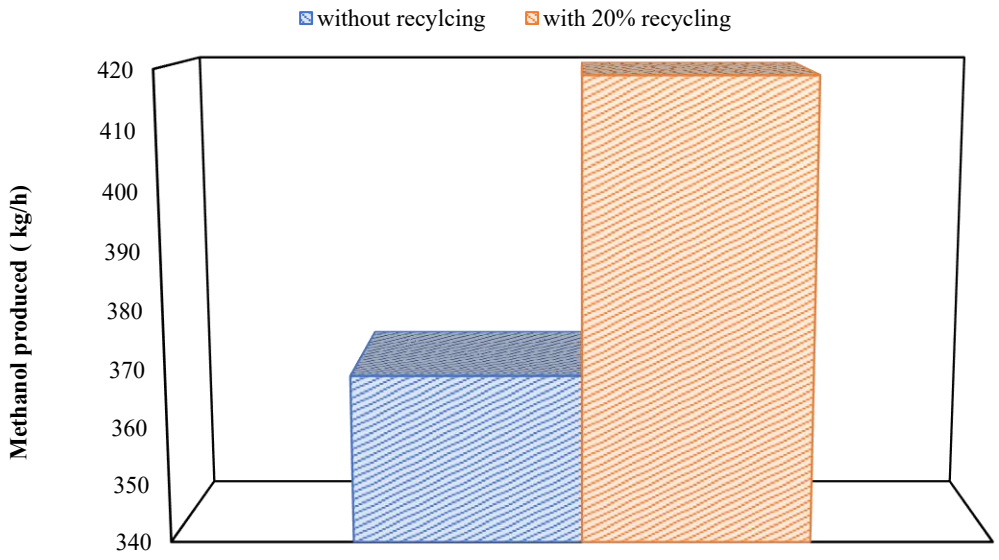


Figure 5.11 Comparison between methanol production (kg/h) with recycling 20% of unreacted syngas and without recycle.

From a thermodynamic standpoint, the recycling strategy also mitigates some of the equilibrium limitations inherent in the synthesis reactions. By continuously removing products (via condensation in the flash separator) and replenishing reactants (via recycling), the chemical equilibrium is favourably shifted toward methanol formation, in accordance with Le Chatelier's principle.

In summary, the integration of a flash separation unit combined with partial syngas recycling constitutes a cost-effective and energy-conscious process intensification strategy. It not only improves methanol yield but also enhances the overall resource utilization efficiency of the system. This approach is widely adopted in industrial-scale methanol plants and demonstrates the potential scalability of the proposed biomass-to-methanol process when optimized through smart recirculation and energy recovery techniques.

## 5.6 Conclusion

This chapter presented a comprehensive analysis of the steam gasification of date palm waste using Aspen Plus, highlighting the impact of key parameters on gas production and its downstream applications. Sensitivity analysis was conducted to evaluate the influence of gasification temperature and the steam-to-biomass (S/B) mass flow rate ratio, followed by methanol synthesis simulations, statistical validation, and process optimization.

The results underscored the pivotal role of gasification temperature in determining syngas composition. Higher temperatures (800°C–1000°C) favoured the production of CO while maintaining a nearly constant concentration of $H_2$. This behaviour was attributed to the dominance of endothermic reactions, including the Boudouard and water-gas reactions, over exothermic processes like the water-gas shift reaction. Conversely, increasing the S/B mass flow rate ratio enhanced hydrogen production by promoting steam reforming reactions, but with diminishing returns at higher ratios due to saturation effects.

Methanol synthesis from syngas was also examined, with results demonstrating that the $H_2$/CO molar ratio significantly impacts methanol yield. The gasification conditions yielding the optimal syngas composition for methanol production were identified, providing a pathway for integrated process development.

Statistical validation of the proposed model showed good agreement with experimental data and literature, affirming its reliability in simulating steam gasification processes. Comparative analysis revealed that the model accurately captured the complex dynamics of temperature and S/B ratio effects, further supporting its robustness.

Finally, optimal process conditions were proposed to improve the efficiency of syngas production and downstream methanol synthesis. These improvements pave the way for enhanced utilization of date palm waste as a sustainable biomass feedstock, contributing to renewable energy solutions and waste valorisation.

In conclusion, this chapter highlights the importance of multi-parameter optimization in biomass gasification processes. By integrating thermodynamic principles, sensitivity analysis, and statistical validation, this work provides a strong foundation for advancing sustainable energy technologies. The insights gained will guide future research in process enhancement and the development of efficient biomass-to-energy systems.

# Chapter 6 General conclusion

The research presented in this thesis investigates the potential of biomass gasification as a sustainable pathway for energy production, focusing on the valorisation of Algerian date palm estimated at approximately 2000 ton per day, present a remarkable opportunity for biomass energy valorisation. Through comprehensive bibliographic analysis, detailed modelling, and experimental validation, the work contributes to advancing knowledge on the thermodynamic, kinetic, and operational aspects of steam gasification processes. The findings are particularly relevant within the framework of the Reffect Africa project, which seeks to leverage agricultural waste for energy independence and environmental sustainability in African countries.

Biomass gasification holds significant promise as a technology for converting organic waste into high-value energy products, including syngas and methanol. This thesis underscores the relevance of gasification in addressing regional energy needs while aligning with global sustainability goals. Olive, Wheat and Date palm waste revealed to be the 3 most important solid agri-food in Algeria. Date palm waste a readily available but underutilized agricultural byproduct, was identified as an ideal candidate for this study due to its abundance and potential for energy recovery. By focusing on this feedstock, the research highlights opportunities for waste valorisation and renewable energy generation tailored to local contexts.

The study employed Aspen Plus modelling to simulate the steam gasification of date palm waste and systematically analysed the effects of key process parameters. Sensitivity analyses revealed that gasification temperature plays a pivotal role in determining syngas composition. Increasing the temperature from 800°C to 1000°C was shown to favour the production of carbon monoxide (CO) while maintaining a relatively constant hydrogen ($H_2$) concentration. This trend was attributed to the thermodynamic dominance of endothermic reactions, such as the Boudouard and water-gas reactions, at higher temperatures. Conversely, the steam-to-biomass (S/B) mass flow ratio significantly influenced hydrogen production, with higher ratios promoting steam reforming but exhibiting diminishing returns beyond certain levels due to reaction saturation.

Further, the integration of syngas with methanol synthesis was explored, demonstrating the critical influence of the $H_2$/CO molar ratio on methanol yield. Optimal gasification conditions were identified to maximize syngas quality for methanol production, enhancing the economic and practical viability of the overall process. Statistical analysis and validation against

experimental data and literature confirmed the robustness of the proposed model, highlighting its capability to accurately predict the complex dynamics of biomass gasification.

The findings of this thesis have several implications. First, they demonstrate the feasibility of utilizing date palm waste as a sustainable biomass feedstock, contributing to waste management and energy production in regions where such resources are abundant. Second, they provide actionable insights into the optimization of gasification processes to tailor syngas composition for specific applications. Third, they pave the way for integrating gasification with value-added chemical production, such as methanol synthesis, thereby enhancing the overall efficiency and sustainability of the biomass-to-energy chain.

Despite these achievements, the research also identifies areas for future investigation. Feedstock variability remains an important challenge, as the composition and properties of biomass can significantly influence gasification performance. Additionally, the potential for catalytic enhancement of reaction kinetics and syngas quality merits further exploration. Moreover, comprehensive techno-economic and life cycle analyses are needed to assess the scalability and environmental impact of the proposed processes. Finally, integrating biomass gasification with other renewable energy technologies, such as solar or wind power, offers exciting opportunities for decentralized and hybrid energy systems.

In conclusion, this thesis demonstrates that biomass gasification is a transformative technology with the potential to address pressing energy and environmental challenges. By leveraging locally available resources, such as date palm waste, the research contributes to the development of innovative, sustainable energy solutions that align with regional needs and global sustainability goals. The methodologies and findings presented herein provide a foundation for further research and technological development, fostering progress toward a low-carbon, energy-resilient future.

While the findings of this thesis contribute significantly to advancing biomass gasification research, several opportunities for further exploration remain, particularly in the realm of techno-economic studies. These analyses are essential for evaluating the feasibility and scalability of the proposed processes in real-world applications, especially in contexts such as Algeria, where the economic landscape is influenced by the availability and low cost of natural gas.

## 6.1 Techno-economic analysis of gas production

In Algeria, natural gas is not only abundant but also subsidized, resulting in a very low market price. This presents a dual challenge and opportunity for biomass-based syngas production. A detailed techno-economic study is needed to assess whether biomass gasification can compete economically with natural gas for energy production or industrial applications. Such an analysis would need to account for:

- Feedstock Costs: Estimating the cost of collecting, transporting, and processing date palm waste.
- Operational Costs: Evaluating the energy input and maintenance costs associated with steam gasification.
- Environmental Benefits: Quantifying the potential carbon credits or other incentives that could offset production costs.
- Market Applications: Identifying niche markets or applications where biomass-based syngas could provide added value, such as in regions lacking natural gas infrastructure or for renewable energy certification.

The economic competitiveness of biomass gasification in Algeria will depend on these factors, as well as potential government policies supporting renewable energy and waste valorisation. Insights from such studies could guide investment decisions and policy recommendations to promote biomass gasification technologies in the country.

## 6.2 Techno-economic analysis of methanol synthesis

Methanol synthesis presents another critical avenue for techno-economic evaluation. Algeria, with its extensive natural gas reserves, already produces methanol using conventional steam reforming of natural gas. Introducing biomass-based syngas as an alternative feedstock raises questions about cost competitiveness, scalability, and environmental impact. A comparative techno-economic analysis is necessary to address the following:

- Cost of syngas production: assessing the cost of producing syngas from biomass versus natural gas.
- Process efficiency: comparing the efficiency and yield of methanol production from biomass-derived syngas with that from natural gas.
- Market dynamics: evaluating how fluctuations in natural gas prices and global methanol demand might affect the economic viability of biomass-based methanol synthesis.

- Environmental impact: considering the carbon footprint and lifecycle emissions of each process to highlight the sustainability benefits of biomass-derived methanol.

Such studies are crucial for determining whether biomass gasification can complement or compete with natural gas-based methanol production. They can also help identify hybrid approaches, where biomass and natural gas are co-fed into methanol synthesis processes to optimize costs and sustainability.

These techno-economic analyses will be instrumental in bridging the gap between laboratory-scale findings and industrial-scale implementation. By addressing cost and market dynamics, this research could lay the groundwork for integrating biomass gasification technologies into Algeria's energy and chemical industries. Moreover, these studies would provide valuable insights into the role of renewable energy technologies in a region heavily reliant on fossil fuels, fostering a transition to more sustainable and diversified energy systems.

# References


[1] Remigijus L, Kent N, Alejandra L. Global bioenergy statistics report 10th Edition. Stockholm: 2023.

[2] Loppinet-Serani A, Aymonier C, Cansell F. Current and foreseeable applications of supercritical water for energy and the environment. ChemSusChem 2008;1:486–503. https://doi.org/10.1002/CSSC.200700167.

[3] Nicolas S. Clarifications on definition of biomass and consideration of changes In carbon pools due to a cdm project activity. Bonn: 2005.

[4] Hodge B. K. Alternative Energy Systems and Applications-Wiley-(2017) 2017:460.

[5] International Organization for Standardization. ISO 17225-1:2021 – Solid biofuels – Fuel specifications and classes – Part 1: General requirements. Geneva: 2021.

[6] CEN – European Committee for Standardization. EN 15234-1:2011 – Solid biofuels – Fuel quality assurance – Part 1: General requirements. Brussels: 2011.

[7] Basu P, Kaushal P. Introduction to biomass conversion. Biomass Gasification, Pyrolysis, and Torrefaction 2024:1–26. https://doi.org/10.1016/B978-0-443-13784-6.00015-9.

[8] Sun Y, Cheng J. Hydrolysis of lignocellulosic materials for ethanol production: a review. Bioresour Technol 2002;83:1–11. https://doi.org/10.1016/S0960-8524(01)00212-7.

[9] Kiel JHA. Torrefaction for Biomass Co-Firing in Existing Coal-Fired Power Stations. 2005.

[10] Klass DL. Biomass for renewable energy, fuels, and chemicals. San Diego, CA: Academic Press; 1998.

[11] Atkins P, de Paula J, Keeler J. Physical Chemistry. 11th ed. Oxford: Oxford University Press; 2018.

[12] Potters G, Goethem D V., Schutte F. Promising biofuel resources: lignocellulose and algae 2010.

[13] Desch HE., Dinwoodie JM. Timber : structure, properties, conversion, and use 1996:306.

[14] Basu P. Gasification theory. Biomass Gasification, Pyrolysis and Torrefaction: Practical Design and Theory, 2018. https://doi.org/10.1016/B978-0-12-812992-0.00007-8.

[15] Kitani O, Hall CW. Biomass handbook 1989:963.

[16] Collazo J, Pazó JA, Granada E, Saavedra Á, Eguía P. Determination of the specific heat of biomass materials and the combustion energy of coke by DSC analysis. Energy 2012;45:746–52. https://doi.org/10.1016/J.ENERGY.2012.07.018.

[17] Sheng C, Azevedo JLT. Estimating the higher heating value of biomass fuels from basic analysis data. Biomass Bioenergy 2005;28:499–507. https://doi.org/10.1016/J.BIOMBIOE.2004.11.008.

[18] Grotkjær T, Dam-Johansen K, Jensen A, Glarborg P. An experimental study of biomass ignition. Fuel 2003;82:825–33.

[19] Miranda T, Esteban A, Rojas S, Montero I, Ruiz A. Combustion Analysis of Different Olive Residues. Int J Mol Sci 2008;9:512. https://doi.org/10.3390/IJMS9040512.

[20] Reed TB. Encyclopedia of biomass thermal conversion : the principles and technology of pyrolysis, gasification & combustion 2002.

[21] Shadangi KP, Sarangi PK, Behera AK. Characterization techniques of biomass: physico-chemical, elemental, and biological. Bioenergy Engineering: Fundamentals, Methods, Modelling, and Applications 2023:51–66. https://doi.org/10.1016/B978-0-323-98363-1.00022-3.

[22] Kamran M. Energy sources and technologies. Fundamentals of Smart Grid Systems 2023:23–69. https://doi.org/10.1016/B978-0-323-99560-3.00010-7.

[23] American Society for Testing and Materials (ASTM). Recording Standards or Basis for Coal Analysis, Coal Analysis, Kentucky Geological Survey, University of Kentucky 2013:515–7. https://www.uky.edu/KGS/coal/coal-analyses-recording-standards.php (accessed December 30, 2023).

[24] Daniel Ciolkosz. Characteristics of Biomass as a Heating Fuel. Pennsylvania State Universit 2010. https://extension.psu.edu/characteristics-of-biomass-as-a-heating-fuel (accessed December 30, 2023).

[25] Office of energy efficiency & renewable energy. Biomass Energy 2013. https://education.nationalgeographic.org/resource/biomass-energy/ (accessed December 31, 2023).

[26] Sam A, Barik D. Toxic Waste From Municipality. Energy from Toxic Organic Waste for Heat and Power Generation 2019:7–16. https://doi.org/10.1016/B978-0-08-102528-4.00002-X.

[27] Pishvaee MS, Mohseni S, Bairamzadeh S. Biofuel supply chain structures and activities. Biomass to Biofuel Supply Chain Design and Planning Under Uncertainty 2021:21–36. https://doi.org/10.1016/B978-0-12-820640-9.00002-7.

[28] Kumari K, Singh A, Marathe D, Pariyar P. Agricultural biomass as value chain developers in different sectors. Advanced Technology for the Conversion of Waste into Fuels and Chemicals: Volume 1: Biological Processes 2021:467–509. https://doi.org/10.1016/B978-0-12-823139-5.00014-9.

[29] Basu P, Kaushal P. Gasification theory. Biomass Gasification, Pyrolysis, and Torrefaction 2024:207–58. https://doi.org/10.1016/B978-0-443-13784-6.00008-1.

[30] Behrendt F, Neubauer Y, Oevermann M, Wilmes B, Zobel N. Direct liquefaction of biomass. Chem Eng Technol 2008;31:667–77. https://doi.org/10.1002/CEAT.200800077.

[31] Zheng Y, Liu C, Zhu J, Sang Y, Wang J, Zhao W, et al. Carbon Footprint Analysis for Biomass-Fueled Combined Heat and Power Station: A Case Study. Agriculture 2022, Vol 12, Page 1146 2022;12:1146. https://doi.org/10.3390/AGRICULTURE12081146.

[32] Termuehlen H, Emsperger W. Clean and efficient coal-fired power plants : development toward advanced technologies 2003.

[33] Held J. Gasification-Status and technology Rapport SGC Gasification Status and technology Rapport SGC 240 2012.

[34] Sjaak Van Loo JK. Introduction. Handbook of Biomass Combustion and Co-Firing 2008:7–30.

[35] Zhou Y, Swidler D, Searle S, Baldino C. Life-cycle greenhouse gas emissions of biomethane and hydrogen pathways in the european union. 2021.

[36] Mamvura TA, Danha G. Biomass torrefaction as an emerging technology to aid in energy production. Heliyon 2020;6:e03531. https://doi.org/10.1016/J.HELIYON.2020.E03531.

[37] AlNouss A, McKay G, Al-Ansari T. Superstructure Optimization for the Production of Fuels, Fertilizers and Power using Biomass Gasification. Computer Aided Chemical Engineering 2019;46:301–6. https://doi.org/10.1016/B978-0-12-818634-3.50051-5.

[38] Hamaidi BE, Boumeddane B, Benarous A, Vera D. Unlocking the potential of date palm waste for syngas and methanol production: Process simulation and optimization. Process Safety and Environmental Protection 2024;182:98–108. https://doi.org/10.1016/j.psep.2023.11.028.

[39] Molino A, Giordano G, Migliori M, Lauro V, Santarcangelo G, Marino T, et al. Process Innovation Via Supercritical Water Gasification to Improve the Conventional Plants Performance in Treating Highly Humid Biomass. Waste Biomass Valorization 2016;7:1289–95. https://doi.org/10.1007/S12649-016-9528-Y.

[40] Dutta PP, Pandey V, Das AR, Sen S, Baruah DC. Down Draft Gasification Modelling and Experimentation of Some Indigenous Biomass for Thermal Applications. Energy Procedia 2014;54:21–34. https://doi.org/10.1016/J.EGYPRO.2014.07.246.

[41] Mishra S, Upadhyay RK. Review on biomass gasification: Gasifiers, gasifying mediums, and operational parameters. Mater Sci Energy Technol 2021;4:329–40. https://doi.org/10.1016/J.MSET.2021.08.009.

[42] Trabelsi ABH, Ghrib A, Zaafouri K, Friaa A, Ouerghi A, Naoui S, et al. Hydrogen-Rich Syngas Production from Gasification and Pyrolysis of Solar Dried Sewage Sludge: Experimental and Modeling Investigations. Biomed Res Int 2017;2017. https://doi.org/10.1155/2017/7831470.

[43] Aguado R, Vera D, Jurado F, Beltrán G. An integrated gasification plant for electric power generation from wet biomass: toward a sustainable production in the olive oil industry. Biomass Convers Biorefin 2022. https://doi.org/10.1007/s13399-021-02231-0.

[44] Lam MK, Loy ACM, Yusup S, Lee KT. Biohydrogen Production From Algae. Biomass, Biofuels, Biochemicals: Biohydrogen, Second Edition 2019:219–45. https://doi.org/10.1016/B978-0-444-64203-5.00009-5.

[45] Liu S, Xing Y, Chen H, Tang P, Jiang J, Tang S, et al. Sustainable Reactors for Biomass Conversion Using Pyrolysis and Fermentation. Encyclopedia of Sustainable Technologies 2017:541–52. https://doi.org/10.1016/B978-0-12-409548-9.10245-3.

[46] Ahrenfeldt Jesper, Knoef Harrie, GasNet. Handbook biomass gasification 2005:378.

[47] Basu P. Production of synthetic fuels and chemicals from biomass. Biomass Gasification, Pyrolysis and Torrefaction: Practical Design and Theory 2018:415–43. https://doi.org/10.1016/B978-0-12-812992-0.00012-1.

[48] Lim MT, Alimuddin Z. Bubbling fluidized bed biomass gasification—Performance, process findings and energy analysis. Renew Energy 2008;33:2339–43. https://doi.org/10.1016/J.RENENE.2008.01.014.

[49] Guda VK, Steele PH, Penmetsa VK, Li Q. Fast Pyrolysis of Biomass: Recent Advances in Fast Pyrolysis Technology. Recent Advances in Thermochemical Conversion of Biomass 2015:177–211. https://doi.org/10.1016/B978-0-444-63289-0.00007-7.

[50] Higman C, van der Burgt M. Gasification Processes. Gasification 2008:91–191. https://doi.org/10.1016/B978-0-7506-8528-3.00005-5.

[51] Higman C, van der Burgt M. Applications. Gasification 2008:257–321. https://doi.org/10.1016/B978-0-7506-8528-3.00007-9.

[52] Zhang Z, Delcroix B, Rezazgui O, Mangin P. Simulation and techno-economic assessment of bio-methanol production from pine biomass, biochar and pyrolysis oil. Sustainable Energy Technologies and Assessments 2021;44:101002. https://doi.org/10.1016/J.SETA.2021.101002.

[53] Puig-Gamero M, Trapero JR, Pedregal DJ, Sánchez P, Sanchez-Silva L. Impact of the forecast price on economic results for methanol production from olive waste. Fuel 2021;295. https://doi.org/10.1016/j.fuel.2021.120631.

[54] Access to electricity – SDG7: Data and Projections – Analysis - IEA n.d. https://www.iea.org/reports/sdg7-data-and-projections/access-to-electricity (accessed December 22, 2024).

[55] Renewable Energy Agency I. Africa 2030: Roadmap for a Renewable Energy Future. 2015.

[56] You S, Ok YS, Chen SS, Tsang DCW, Kwon EE, Lee J, et al. A critical review on sustainable biochar system through gasification: Energy and environmental applications. Bioresour Technol 2017;246:242–53. https://doi.org/10.1016/J.BIORTECH.2017.06.177.

[57] Trabelsi ABH, Ghrib A, Zaafouri K, Friaa A, Ouerghi A, Naoui S, et al. Hydrogen-Rich Syngas Production from Gasification and Pyrolysis of Solar Dried Sewage Sludge: Experimental and Modeling Investigations. Biomed Res Int 2017;2017:7831470. https://doi.org/10.1155/2017/7831470.

[58] Allesina G, Pedrazzi S, Allegretti F, Morselli N, Puglia M, Santunione G, et al. Gasification of cotton crop residues for combined power and biochar production in Mozambique. Appl Therm Eng 2018;139:387–94. https://doi.org/10.1016/J.APPLTHERMALENG.2018.04.115.

[59] Abd El-Sattar H, Kamel S, Tawfik MA, Vera D, Jurado F. Modeling and Simulation of Corn Stover Gasifier and Micro-turbine for Power Generation. Waste Biomass Valorization 2019;10:3101–14. https://doi.org/10.1007/S12649-018-0284-Z/METRICS.

[60] Ozonoh M, Aniokete TC, Oboirien BO, Daramola MO. Techno-economic analysis of electricity and heat production by co-gasification of coal, biomass and waste tyre in South Africa. J Clean Prod 2018;201:192–206. https://doi.org/10.1016/J.JCLEPRO.2018.07.209.

[61] Arranz-Piera P, Kemausuor F, Darkwah L, Edjekumhene I, Cortés J, Velo E. Mini-grid electricity service based on local agricultural residues: Feasibility study in rural Ghana. Energy 2018;153:443–54. https://doi.org/10.1016/J.ENERGY.2018.04.058.

[62] Kushwah A, Reina TR, Short M. Modelling approaches for biomass gasifiers: A comprehensive overview. Science of The Total Environment 2022;834:155243. https://doi.org/10.1016/J.SCITOTENV.2022.155243.

[63] Baruah D, Baruah DC, Hazarika MK. Artificial neural network based modeling of biomass gasification in fixed bed downdraft gasifiers. Biomass Bioenergy 2017;98:264–71. https://doi.org/10.1016/J.BIOMBIOE.2017.01.029.

[64] Zeleznik FJ, Gordon S. Calculation Of Complex Chemical Equilibria. Ind Eng Chem 1968;60:27–57. https://doi.org/10.1021/IE50702A006/ASSET/IE50702A006.FP.PNG_V03.

[65] Altafini CR, Wander PR, Barreto RM. Prediction of the working parameters of a wood waste gasifier through an equilibrium model. Energy Convers Manag 2003;44:2763–77. https://doi.org/10.1016/S0196-8904(03)00025-6.

[66] Silva IP, Lima RMA, Silva GF, Ruzene DS, Silva DP. Thermodynamic equilibrium model based on stoichiometric method for biomass gasification: A review of model modifications. Renewable and Sustainable Energy Reviews 2019;114:109305. https://doi.org/10.1016/J.RSER.2019.109305.

[67] Gambarotta A, Morini M, Zubani A. A non-stoichiometric equilibrium model for the simulation of the biomass gasification process. Appl Energy 2018;227:119–27. https://doi.org/10.1016/J.APENERGY.2017.07.135.

[68] Kersten SRA. Biomass gasification in circulating fluidized beds 2002.

[69] Li XT, Grace JR, Lim CJ, Watkinson AP, Chen HP, Kim JR. Biomass gasification in a circulating fluidized bed. Biomass Bioenergy 2004;26:171–93. https://doi.org/10.1016/S0961-9534(03)00084-9.

[70] Petersen I, Werther J. Experimental investigation and modeling of gasification of sewage sludge in the circulating fluidized bed. Chemical Engineering and Processing: Process Intensification 2005;44:717–36. https://doi.org/10.1016/J.CEP.2004.09.001.

[71] Ravi MR, Kohli S. Thermodynamics and Kinetics of Gasification. Energy, Environment, and Sustainability 2018:37–62. https://doi.org/10.1007/978-981-10-7335-9_2.

[72] Kherbouche D, Benyoucef B. Production of hydrogen from pyrolysis of biomass: Influence of temperature, substrate and catalyst. Journal of Engineering and Applied Sciences 2011;6:91–5. https://doi.org/10.3923/jeasci.2011.91.95.

[73] Bradbury AGW, Sakai Y, Shafizadeh F. A kinetic model for pyrolysis of cellulose. J Appl Polym Sci 1979;23:3271–80. https://doi.org/10.1002/APP.1979.070231112.

[74] Sharma AK. Modeling and simulation of a downdraft biomass gasifier 1. Model development and validation. Energy Convers Manag 2011;52:1386–96. https://doi.org/10.1016/J.ENCONMAN.2010.10.001.

[75] Salem AM, Paul MC. An integrated kinetic model for downdraft gasifier based on a novel approach that optimises the reduction zone of gasifier. Biomass Bioenergy 2018;109:172–81. https://doi.org/10.1016/J.BIOMBIOE.2017.12.030.

[76] Giltrap DL, McKibbin R, Barnes GRG. A steady state model of gas-char reactions in a downdraft biomass gasifier. Solar Energy 2003;74:85–91. https://doi.org/10.1016/S0038-092X(03)00091-4.

[77] Wang Y, Kinoshita CM. Kinetic model of biomass gasification. Solar Energy 1993;51:19–25. https://doi.org/10.1016/0038-092X(93)90037-O.

[78] Di Blasi C. Modeling chemical and physical processes of wood and biomass pyrolysis. Prog Energy Combust Sci 2008;34:47–90. https://doi.org/10.1016/J.PECS.2006.12.001.

[79] Babu B V., Chaurasia AS. Pyrolysis of biomass: improved models for simultaneous kinetics and transport of heat, mass and momentum. Energy Convers Manag 2004;45:1297–327. https://doi.org/10.1016/J.ENCONMAN.2003.09.013.

[80] Syred N. Development of fragmentation models for solid fuel combustion and gasification as subroutines for inclusion in CFD codes. Fuel 2007.

[81] Wang Y, Yan L. CFD Studies on Biomass Thermochemical Conversion. International Journal of Molecular Sciences 2008, Vol 9, Pages 1108-1130 2008;9:1108–30. https://doi.org/10.3390/IJMS9061108.

[82] Oevermann M, Gerber S, Behrendt F. Euler–Lagrange/DEM simulation of wood gasification in a bubbling fluidized bed reactor. Particuology 2009;7:307–16. https://doi.org/10.1016/J.PARTIC.2009.04.004.

[83] Miao Q, Zhu J, Barghi S, Wu C, Yin X, Zhou Z. Modeling biomass gasification in circulating fluidized beds. Renew Energy 2013;50:655–61. https://doi.org/10.1016/J.RENENE.2012.08.020.

[84] Norton T, Sun DW, Grant J, Fallon R, Dodd V. Applications of computational fluid dynamics (CFD) in the modelling and design of ventilation systems in the agricultural industry: A review. Bioresour Technol 2007;98:2386–414. https://doi.org/10.1016/J.BIORTECH.2006.11.025.

[85] Xia B, Sun DW. Applications of computational fluid dynamics (cfd) in the food industry: a review. Comput Electron Agric 2002;34:5–24. https://doi.org/10.1016/S0168-1699(01)00177-6.

[86] Salam PA, Bhattacharya SC. A comparative hydrodynamic study of two types of spouted bed reactor designs. Chem Eng Sci 2006;61:1946–57. https://doi.org/10.1016/J.CES.2005.10.044.

[87] Guangul FM, Sulaiman SA, Ramli A. Temperature profile and producer gas composition of high temperature air gasification of oil palm fronds. IOP Conf Ser Earth Environ Sci, vol. 16, Institute of Physics Publishing; 2013. https://doi.org/10.1088/1755-1315/16/1/012067.

[88] Xiao G, Ni M jiang, Chi Y, Jin B sheng, Xiao R, Zhong Z ping, et al. Gasification characteristics of MSW and an ANN prediction model. Waste Management 2009;29:240–4. https://doi.org/10.1016/J.WASMAN.2008.02.022.

[89] Kalogirou SA. Artificial neural networks in renewable energy systems applications: a review. Renewable and Sustainable Energy Reviews 2001;5:373–401. https://doi.org/10.1016/S1364-0321(01)00006-5.

[90] Guo B, Li D, Cheng C, Lü ZA, Shen Y. Simulation of biomass gasification with a hybrid neural network model. Bioresour Technol 2001;76:77–83. https://doi.org/10.1016/S0960-8524(00)00106-1.

[91] Puig-Arnavat M, Hernández JA, Bruno JC, Coronas A. Artificial neural network models for biomass gasification in fluidized bed gasifiers. Biomass Bioenergy 2013;49:279–89. https://doi.org/10.1016/j.biombioe.2012.12.012.

[92] Hajek M, Judd MR. Use of neural networks in modelling the interactions between gas analysers at coal gasifiers. Fuel 1995;74:1347–51. https://doi.org/10.1016/0016-2361(95)00082-G.

[93] Zainal ZA, Ali R, Lean CH, Seetharamu KN. Prediction of performance of a downdraft gasifier using equilibrium modeling for different biomass materials. Energy Convers Manag 2001;42:1499–515. https://doi.org/10.1016/S0196-8904(00)00078-9.

[94] Melgar A, Pérez JF, Laget H, Horillo A. Thermochemical equilibrium modelling of a gasifying process. Energy Convers Manag 2007;48:59–67. https://doi.org/10.1016/J.ENCONMAN.2006.05.004.

[95] Sharma AK. Equilibrium modeling of global reduction reactions for a downdraft (biomass) gasifier. Energy Convers Manag 2008;49:832–42. https://doi.org/10.1016/J.ENCONMAN.2007.06.025.

[96] Jayah TH, Aye L, Fuller RJ, Stewart DF. Computer simulation of a downdraft wood gasifier for tea drying. Biomass Bioenergy 2003;25:459–69. https://doi.org/10.1016/S0961-9534(03)00037-0.

[97] Prins MJ, Ptasinski KJ, Janssen FJJG. Thermodynamics of gas-char reactions: first and second law analysis. Chem Eng Sci 2003;58:1003–11. https://doi.org/10.1016/S0009-2509(02)00641-3.

[98] Fortunato B, Brunetti G, Camporeale SM, Torresi M, Fornarelli F. Thermodynamic model of a downdraft gasifier. Energy Convers Manag 2017;140:281–94. https://doi.org/10.1016/J.ENCONMAN.2017.02.061.

[99] Patra TK, Sheth PN. Biomass gasification models for downdraft gasifier: A state-of-the-art review. Renewable and Sustainable Energy Reviews 2015;50:583–93. https://doi.org/10.1016/J.RSER.2015.05.012.

[100] Dejtrakulwong C, Patumsawad S. Four Zones Modeling of the Downdraft Biomass Gasification Process: Effects of Moisture Content and Air to Fuel Ratio. Energy Procedia 2014;52:142–9. https://doi.org/10.1016/J.EGYPRO.2014.07.064.

[101] Awais M, Li W, Arshad A, Haydar Z, Yaqoob N, Hussain S. Evaluating removal of tar contents in syngas produced from downdraft biomass gasification system. Int J Green Energy 2018;15:724–31. https://doi.org/10.1080/15435075.2018.1525557.

[102] Sait HH, Hussain A, Salema AA, Ani FN. Pyrolysis and combustion kinetics of date palm biomass using thermogravimetric analysis. Bioresour Technol 2012;118:382–9. https://doi.org/10.1016/j.biortech.2012.04.081.

[103] Bensidhom G, Ben Hassen-Trabelsi A, Alper K, Sghairoun M, Zaafouri K, Trabelsi I. Pyrolysis of Date palm waste in a fixed-bed reactor: Characterization of pyrolytic products. Bioresour Technol 2018;247:363–9. https://doi.org/10.1016/j.biortech.2017.09.066.

[104] Bassyouni M, Ul Hasan SW, Abdel-Aziz MH, Abdel-Hamid SMS, Naveed S, Hussain A, et al. Date palm waste gasification in downdraft gasifier and simulation using ASPEN HYSYS. Energy Convers Manag 2014;88:693–9. https://doi.org/10.1016/j.enconman.2014.08.061.

[105] AlNouss A, Mckay G, Al-Ansari T. Optimum Utilization of Biomass for the Production of Power and Fuels using Gasification. Computer Aided Chemical Engineering, vol. 43, Elsevier B.V.; 2018, p. 1481–6. https://doi.org/10.1016/B978-0-444-64235-6.50258-8.

[106] Sulaiman SA, Naz MY, Inayat M, Shukrullah S, Ghaffar A. Thermochemical Characteristics and Gasification of Date Palm Fronds for Energy Production. Theoretical Foundations of Chemical Engineering 2019;53:1083–93. https://doi.org/10.1134/S0040579519060113.

[107] Kabli MR, Ali AM, Inayat M, Zahrani AA, Shahzad K, Shahbaz M, et al. H2-rich syngas production from air gasification of date palm waste: an experimental and modeling investigation. Biomass Convers Biorefin 2022. https://doi.org/10.1007/s13399-022-02375-7.

[108] Martis R, Al-Othman A, Tawalbeh M, Alkasrawi M. Energy and economic analysis of date palm biomass feedstock for biofuel production in UAE: Pyrolysis, gasification and fermentation. Energies (Basel) 2020;13. https://doi.org/10.3390/en13225877.

[109] Yaghoubi E, Xiong Q, Doranehgard MH, Yeganeh MM, Shahriari G, Bidabadi M. The effect of different operational parameters on hydrogen rich syngas production from biomass gasification in a dual fluidized bed gasifier. Chemical Engineering and Processing - Process Intensification 2018;126:210–21. https://doi.org/10.1016/j.cep.2018.03.005.

[110] Inayat M, Sulaiman SA, Kurnia JC, Shahbaz M. Effect of various blended fuels on syngas quality and performance in catalytic co-gasification: A review. Renewable and Sustainable Energy Reviews 2019;105:252–67. https://doi.org/10.1016/j.rser.2019.01.059.

[111] Bertau M, Offermanns H, Plass L, Schmidt F, Wernicke H-J. Methanol: The Basic Chemical and Energy Feedstock of the Future. n.d.

[112] Ogden JM, Steinbugler MM, Kreutz TG. A comparison of hydrogen, methanol and gasoline as fuels for fuel cell vehicles: implications for vehicle design and infrastructure development. J Power Sources 1999;79:143–68. https://doi.org/10.1016/S0378-7753(99)00057-9.

[113] Giuliano A, Catizzone E, Freda C, Cornacchia G. Valorization of OFMSW digestate-derived syngas toward methanol, hydrogen, or electricity: Process simulation and carbon footprint calculation. Processes 2020;8. https://doi.org/10.3390/PR8050526.

[114] Zhang Y, Xiao J, Shen L. Simulation of methanol production from biomass gasification in interconnected fluidized beds. Ind Eng Chem Res 2009;48:5351–9. https://doi.org/10.1021/ie801983z.

[115] Recioui B, Mokhbi Y, Ghedamsi R, Settou N, Soualeh M. Assessment of biomass's potential in Algeria: energetic valorization and CO2 emissions mitigation 2024. https://doi.org/10.48047/AFJBS.6.14.2024.9077-9089.

[116] La production abondante de blé dur a permis d'assurer 1,2 milliard de dollars au profit du Trésor n.d. https://www.aps.dz/economie/172419-la-production-abondante-de-ble-dur-a-permis-d-assurer-1-2-milliard-de-dollars-au-profit-du-tresor (accessed December 24, 2024).

[117] Nabila Hales EU. Grain and Feed Update. Algiers: 2024.

[118] Merzaia AB. Dix sept wilayas productrices de datte , une richesse inépuisable pour l'Algérie. Algiers : 2014.

[119] Mallaki M, Fatehi R. Design of a biomass power plant for burning date palm waste to cogenerate electricity and distilled water. Renew Energy 2014;63:286–91. https://doi.org/10.1016/J.RENENE.2013.09.036.

[120] Bouguedoura N, Bennaceur M, Babahani S, Benziouche SE. Date palm status and perspective in Algeria. Date Palm Genetic Resources and Utilization: Volume 1: Africa and the Americas, Springer Netherlands; 2015, p. 125–68. https://doi.org/10.1007/978-94-017-9694-1_4.

[121] Elias A, Boumeddane B, Vera D, Jurado F. Gasification of olive mill solid wastes for cogeneration applications in Tizi Ouzou region: thermo-economic assessment. International Journal of Sustainable Energy 2021;40:1002–26. https://doi.org/10.1080/14786451.2021.1891069.

[122] El-Sayed SA, Khairy M. Effect of heating rate on the chemical kinetics of different biomass pyrolysis materials. Biofuels 2015;6:157–70. https://doi.org/10.1080/17597269.2015.1065590.

[123] Chevanan N, Womac AR, Bitra VSP, Igathinathane C, Yang YT, Miu PI, et al. Bulk density and compaction behavior of knife mill chopped switchgrass, wheat straw, and corn stover. Bioresour Technol 2010;101:207–14. https://doi.org/10.1016/j.biortech.2009.07.083.

[124] European Committee for Standardization (CEN). EN ISO 18123:2015 – Solid biofuels: Determination of the content of volatile matter. Brussels: 2015.

[125] European Committee for Standardization (CEN). EN 15104:2011 – Solid biofuels: Determination of total content of carbon, hydrogen and nitrogen – Instrumental methods. Brussels: 2011.

[126] Ahmed AMA, Salmiaton A, Choong TSY, Wan Azlina WAKG. Review of kinetic and equilibrium concepts for biomass tar modeling by using Aspen Plus. Renewable and Sustainable Energy Reviews 2015;52:1623–44. https://doi.org/10.1016/J.RSER.2015.07.125.

[127] Shahbaz M, Yusup S, Inayat A, Ammar M, Patrick DO, Pratama A, et al. Syngas Production from Steam Gasification of Palm Kernel Shell with Subsequent CO2 Capture Using CaO Sorbent: An Aspen Plus Modeling. Energy and Fuels 2017;31:12350–7. https://doi.org/10.1021/acs.energyfuels.7b02670.

[128] Al Amoodi N, Kannan P, Al Shoaibi A, Srinivasakannan C. ASPEN PLUS SIMULATION OF POLYETHYLENE GASIFICATION UNDER EQUILIBRIUM CONDITIONS. Chem Eng Commun 2013;200:977–92. https://doi.org/10.1080/00986445.2012.715108.

[129] Puig-Gamero M, Argudo-Santamaria J, Valverde JL, Sánchez P, Sanchez-Silva L. Three integrated process simulation using aspen plus®: Pine gasification, syngas cleaning and methanol synthesis. Energy Convers Manag 2018;177:416–27. https://doi.org/10.1016/j.enconman.2018.09.088.

[130] Gutiérrez Ortiz FJ, Serrera A, Galera S, Ollero P. Methanol synthesis from syngas obtained by supercritical water reforming of glycerol. Fuel 2013;105:739–51. https://doi.org/10.1016/J.FUEL.2012.09.073.

[131] Pala LPR, Wang Q, Kolb G, Hessel V. Steam gasification of biomass with subsequent syngas adjustment using shift reaction for syngas production: An Aspen Plus model. Renew Energy 2017;101:484–92. https://doi.org/10.1016/J.RENENE.2016.08.069.

[132] Ali AM, Shahbaz M, Shahzad K, Inayat M, Naqvi S, Al-Zahrani AA, et al. Polygeneration syngas and power from date palm waste steam gasification through an Aspen Plus process modeling. Fuel 2023;332:126120. https://doi.org/10.1016/j.fuel.2022.126120.

[133] Trop P, Anicic B, Goricanec D. Production of methanol from a mixture of torrefied biomass and coal. Energy 2014;77:125–32. https://doi.org/10.1016/j.energy.2014.05.045.

[134] Inayat A, Shahbaz M, Khan Z, Inayat M, Mofijur M, Ahmed SF, et al. Heat integration modeling of hydrogen production from date seeds via steam gasification. Int J Hydrogen Energy 2021;46:30592–605. https://doi.org/10.1016/J.IJHYDENE.2021.02.060.

[135] Babiker ME, A. Aziz AR, Heikal M, Yusup S. Gasification of Date Palm (Phoenix dactylifera) Seeds, 2018, p. 65–79. https://doi.org/10.1007/978-981-10-7754-8_5.

[136] Zhang Z, Delcroix B, Rezazgui O, Mangin P. Simulation and techno-economic assessment of bio-methanol production from pine biomass, biochar and pyrolysis oil. Sustainable Energy Technologies and Assessments 2021;44. https://doi.org/10.1016/j.seta.2021.101002.

## Appendix

Table A1

| Stream no. | S1 | Biomasdr | Moisture | S7 | S9 | Ash | S10 | S11 | S12 | S14 | S15 | S16 | Water | Product |
|---|---|---|---|---|---|---|---|---|---|---|---|---|---|---|
| Temp (°C) | 25 | 100 | 100 | 100 | 800 | 800 | 120 | 250 | 220 | 50 | 50 | 50 | 50 | 50 |
| Pressure (bar) | 1 | 1 | 1 | 1 | 1 | 1 | 1 | 100 | 60 | 10 | 10 | 10 | 1 | 1 |
| Flowrates (kg/h) | | | | | | | | | | | | | | |
| Biomass | 1000 | | | | | | | | | | | | | |
| Dry biomass | | 952 | | | | | | | | | | | | |
| $H_2O$ | | | 48 | 852 | 549.00 | | 549.00 | 553.20 | 779.31 | 779.31 | 5.99 | 1.19 | 773.31 | |
| $H_2$ | | | | | 94.88 | | 94.88 | 98.43 | 17.78 | 17.78 | 17.78 | 3.55 | | |
| CO | | | | | 546.86 | | 609.49 | 621.89 | 62.18 | 62.18 | 61.97 | 12.39 | | |
| $CO_2$ | | | | | 609.49 | | 546.86 | 677.07 | 651.07 | 651.07 | 651.07 | 130.20 | | |
| $CH_4$ | | | | | 0.51 | | 0.51 | 0.637 | 0. 637 | 0. 637 | 0. 637 | 0.127 | | |
| $N_2$ | | | | | 3.43 | | 3.43 | 4.29 | 4.29 | 4.29 | 4.29 | 0.859 | | |
| ASH | | | | | 47.12 | 47.12 | | | | | | | | |
| $CH_3OH$ | | | | | | | | | 419 | 419 | | 419 | | 419 |